UNIVERSITÀ DEGLI STUDI DI SALERNO

UNIVERSITÀ DEGLI STUDI DI SALERNO
Dipartimento di Farmacia

PhD Program
in **Drug Discovery and Development**
XXXII Cycle—Academic Year 2019/2020

PhD Thesis in
Pharmacology and Pharmacotherapy

Is the inflammasome at the crosstalk between
COPD and lung cancer?

Candidate

Chiara Colarusso

Supervisors

Prof. *Aldo Pinto*

Prof. *Rosalinda Sorrentino*

PhD Program Coordinator: Prof. Dr. *Gianluca Sbardella*

To my beloved Dad

ABSTRACT

Background. Chronic obstructive pulmonary disease (COPD) is considered as a risk factor for lung cancer establishment. Epidemiological evidence indicate that patients with COPD have a 6.35-fold higher risk to develop lung cancer compared to the normal population.

Aim. Based on the notion that chronic inflammation is common to both COPD and lung cancer and that in our laboratory we found that the inflammasome is involved in lung carcinogenesis, we focused our attention on this multimeric complex, which role in both pathologies still counts many controversies in literature.

Therefore, the main goal of this PhD project was to evaluate whether the inflammasome was at the crosstalk between COPD and lung cancer. In particular, we focused our attention on air pollution and smoking as inflammasome inducers.

1st year results. The exposure of peripheral blood mononuclear cells (PBMCs) isolated from smokers to ultrafine particles (UFPs), which mimic small size air pollutants, led to an inflammatory process that was responsible for IL-1-like cytokines release and was associated to the activation of the canonical, caspase-1-dependent, NLRP3 inflammasome. This effect was not observed in non-smoker subjects, who instead released higher levels immunesuppressive IL-10 (Chapter 1). Instead, UFPs induced the release of IL-18 and IL-33 from exacerbated COPD-derived circulating cells in a NLRP3-/caspase-1- and caspase-8-independent manner (Chapter 2).

2nd year results. The exposure to UFPs *in vivo* led to a state of latent lung inflammation and bronchial dysfunction in mice; this effect was caspase-1-independent and associated to an immunesuppressive lung microenvironment, characterized by high levels of IL-10 (Chapter 3). Moreover, to understand the role of the inflammasome in COPD, we stimulated PBMCs with

NLRP3 or AIM2 inflammasome activators. The sole AIM2 inflammasome was functional in that its activation led to IL-1α-dependent TGF-β release via the canonical, caspase-1-dependent, and non-canonical, caspase-4-dependent, pathway from exacerbated COPD-derived PBMCs (Chapter 4).

3rd year results. To pursue the investigation on the inflammasome in the lung, we used a mouse model of smoking mice in the attempt to mimic COPD to be compared to a mouse model of carcinogen-induced lung cancer. The exposure to cigarette smoking increased the alveolar space, induced bronchial tone impairment and an immunesuppressive microenvironment, which were not reverted by caspase-1 inhibition. Interestingly, we found that the expression of IL-1α and AIM2 was increased both in smoke- and carcinogen-treated mice (Chapter 5).

Conclusions. Both smoking and air pollution can prompt towards lung immunesuppression and pulmonary inflammation in an IL-1-like manner, most likely via the AIM2 inflammasome activation. Therefore, although other studies are needed, we found that the common pathways between COPD and lung cancer stand in the activation of AIM2 and the ensuing IL-1α, as demonstrated by preclinical models and human lung cancer samples.

These results improve the knowledge on the inflammasome biology in COPD and lung cancer and suggest a potential pro-carcinogenic role of IL-1α and AIM2 in COPD.

TABLE OF CONTENTS

INTRODUCTION

Chronic Obstructive Pulmonary Disease (COPD) is currently the fourth-leading causes of death worldwide after cancer, heart disease and stroke, and it is estimated to become the third leading cause of death in the world by 2030 as predicted by World Health Organization (who.it). COPD is a devastating disease that causes progressive and irreversible decline of lung function (Sugimoto *et al*., 2016) and it is characterized by cough, shortness of breath, mucus hypersecretion, chronic bronchitis, airway remodelling, emphysema and airway limitation due to airway and alveolar abnormalities (Colarusso *et al*., 2017). COPD patients are highly susceptible to exacerbation episodes which further promote lung function decline and consequent deterioration of the quality of life. As reported by Global Iniziative for Chronic Obstructive Lung Disease (GOLD), nowadays the current pharmacological therapy is not able to modify the progressive decreased pulmonary functions, rather, it can only control the symptoms, reduce the frequency and severity of exacerbation episodes (goldcopd.org/wp-content/uploads/2018/11/GOLD-2019-POCKET-GUIDE-FINAL_WMS.pdf). The actual therapy for COPD patients refers to the usage of bronchodilators, especially long-acting beta agonists (LABAs), and long-acting muscarinic antagonists (LAMAs), alone or in association with inhaled corticosteroids (ICS), which improve lung function but are not able to avoid exacerbation episodes that lend the COPD patient to the clinical decline. Therefore, there is an urgent unmet clinical need to identify novel therapeutic strategies and molecular/cellular targets to improve clinical outcomes and to revert and/or block long-term deterioration of pulmonary function. The identification of new therapeutic approaches is pivotal because COPD contributes significantly to chronic morbidity and mortality, indeed The Global Burden of Disease Study reports that in 2015, 3.2 million of people died of COPD worldwide, and that the prevalence of

COPD increased by 44.2% in the last 15 years, accounting for 251 million of cases globally (GBD 2015 Chronic Respiratory Disease Collaborators, 2017). However, as discussed in the GOLD, it is very difficult to make an accurate estimation about the prevalence and mortality of COPD due to the often undiagnosed/misdiagnosed pathology and to poor survey methods and diagnostic criteria (Vestblo *et al*., 2013). The actual diagnostic tools are based on spirometry which is performed to patients who present dyspnea, chronic cough or sputum production. Spirometry can confirm airflow limitation (goldcopd.org/wp-content/uploads/2018/11/GOLD-2019-POCKET-GUIDE-FINAL_WMS.pdf) and is able to measure the forced vital capacity (FVC), forced expiratory volume in 1 second (FEV1) and the ratio FEV1/FVC, values that are compared to standard values representing healthy airflow (Vestblo *et al*., 2013). Based on this concept, COPD patients are stratified according to the ratio FEV1/FVC as reported in Table 1. According to the spirometry values COPD severity is classified as mild when the FEV1 is around 80%, as moderate when FEV1 is between 50-80%, severe when FEV1 is between 30-50% and very severe when FEV1 is less than 30% (Vestblo *et al*., 2013).

Table 1. *Classification of COPD severity based on spirometry values that record airflow limitation/obstruction.*

COPD Stage	COPD Severity	FEV1
GOLD 1	Mild	≥ 80%
GOLD 2	Moderate	≤ 50% < 80%
GOLD 3	Severe	≤ 30% < 50%
GOLD 4	Very Severe	< 30%; < 50%

Besides spirometry, computed tomographic (CT) of the chest is an imaging clinical tool which has revolutionized COPD diagnosis, in that it is possible to define COPD phenotype. Chest CT detects and quantifies the emphysema phenotype defined as *multiorgan loss of tissue*

(MOLT), which is frequently associated to the loss of mesenchymal tissue and to airway luminal narrowing and wall thickening associated with cough, phlegm production or discoloration, bronchitis and exacerbation of COPD (Celli & Wedzicha, 2019).

The development of COPD is caused by long-term inhalation of noxious particles or gas, especially cigarette smoke (CS) (Lee *et al*., 2016). Although CS is still the highest risk factor for the onset of COPD, only 15-20% of smokers develop COPD, suggesting that several other factors may contribute to the development of this disease, including genetic and environmental factors (indoor and outdoor air pollution, smoke from biomass fuels, occupational particulate, ozone, and second-hand smoke) (Eisner *et al*., 2010). In support, inhalation of toxic pollutants from environment contributes to COPD symptoms onset and can cause exacerbation episodes (Perez-Padilla *et al*., 2010). In 2014, Song *et al*., reported that air pollution contributes to the increasing burdens of COPD; 34% of COPD deaths are attributable to air pollution, particularly among non-smoker COPD patients exposed to indoor air pollution from biomass combustion and second-hand tobacco smoke as well as to occupational and outdoor pollutants (Xia *et al*., 2016). An explanation to the correlation between environmental pollution and the incidence/mortality among COPD patients could be due to the fact that a prolonged/constant exposure to toxic environmental stimuli can lead to chronic latent inflammation which involves both innate and adaptive immunity cells, that in association with structural cells, can trigger the release of cytokines and chemokines resulting in the recruitment of others inflammatory cells (monocytes, neutrophils and lymphocytes) into the lungs, further enhancing the inflammatory burden, which in the end can ensue pulmonary dysfunction (Colarusso *et al*., 2017). The state of inflammation in the lungs of COPD patients can affect not only airway structural cells but also circulating cells, increasing the susceptibility of infections (Perez-Padilla *et al*., 2014) and other comorbidities such as heart, gut and skeletal muscle diseases (Colarusso *et al*., 2017).

To date, tobacco smoke and air pollution represent the main risk factors not only for COPD, but also for lung cancer establishment (who.int/gard/publications/Risk%20factors.pdf). Every

year tobacco kills 8 million of people, among which 1 million of deaths among COPD patients and 0.85 million of subjects affected by lung cancer (U.S. Department of Health and Human Services, 2014), data that reflect the impact of both CS and environmental pollution as risk factors for either diseases. It is well known that cigarette smoking alters the physiological cellular oxidative state, the epigenetic and genomic signature (Talikka *et al*., 2012). Similarly, air pollution can lead to pro-oxidant status and epigenetic alterations (Li *et al*., 2017), which may underlie lung cancer establishment. It was demonstrated a positive correlation between the exposure to outdoor air pollutants, specifically particular matter (PM) and nitrogen dioxide (NO_2), and lung adenocarcinoma incidence (Jiang *et al*., 2016). In support, in October 2013, the International Agency for Research on Cancer (IARC) classified outdoor air pollution and PM as carcinogenic to humans (IARC Group 1) (Loomis *et al*., 2013).

Lung cancer is the most common solid tumor, accounting for an estimated 2.09 million of cases in 2018 and the leading cause of cancer-related death worldwide (cancer.org/cancer/non-small-cell-lung-cancer/about/key-statistics.html). Lung cancers are broadly classified into 3 major types: non-small cell lung cancer (NSCLC), small cell lung cancer (SCLC) and lung carcinoid tumor. In particular, NSCLC is the most frequent type of lung cancer (about 85% of cases) classified into three major histopathological subtypes: squamous cell carcinoma, adenocarcinoma and large cell carcinoma; SCLC and lung carcinoid tumor, that represent, respectively, about 10-15% and fewer than 5% cases of lung cancer. Although many previous studies have investigated the role of COPD in the development and prognosis of lung cancer, the conflicting results have not been able to establish a defined crosstalk between the two pathologies. Nevertheless, some burgeoning areas of research suggested the incorporation of COPD into lung cancer screening criteria, which, however, it still remains a forum of open discussion. Therefore, the link between COPD and lung cancer is still heated hot-topic, object of debated and compulsory additional investigation.

Crosstalk between COPD and lung cancer. COPD and lung cancer may represent two sides

of the same coin although they are characterized by different pathological changes (Punturieri

et al., 2009). The relationship between COPD and lung cancer has been studied since 1986

when Skillrud et colleagues demonstrated that lung cancer incidence increased in individuals

with COPD and was correlated to decrease in respiratory airflow and chronic inflammation in

these patients (Skillrud *et al*., 1986). Since then, a huge number of epidemiological studies were

performed to this purpose. Recently a meta-analysis showed that the prevalence of lung cancer

in COPD is greater than in other patient population (Butler *et al.,* 2019), and that lung cancer is

a leading cause of morbidity and mortality among patients with a confirmed diagnosis of COPD

(Zanarron *et al*., 2019). In support, COPD patients are 6.35 times more likely to develop lung

cancer compared to the normal population (Figure 1) (Butler *et al*., 2019).

Study or Subgroup	COPD Events	Total	Control Events	Total	Weight	Odds Ratio M-H, Random, 95% CI
Cazzola 2010	285	15018	1305	326311	18.6%	4.82 [4.23, 5.48]
Greulich 2017	2663	146141	317	146141	18.6%	8.54 [7.60, 9.59]
Jo 2015	2	744	1	3313	3.2%	8.93 [0.81, 98.58]
Lopez Varela 2013	8	759	5	4555	9.1%	9.69 [3.16, 29.71]
Masuda 2017	13	920	24	11785	13.5%	7.02 [3.56, 13.84]
Nishida 2017	354	2309	573	9589	18.5%	2.85 [2.47, 3.28]
Stallberg 2018	428	17479	213	84514	18.4%	9.93 [8.42, 11.72]
Total (95% CI)		183370		586208	100.0%	6.35 [3.98, 10.15]
Total events	3753		2438			

Heterogeneity: Tau² = 0.30; Chi² = 198.95, df = 6 (P < 0.00001); I² = 97%
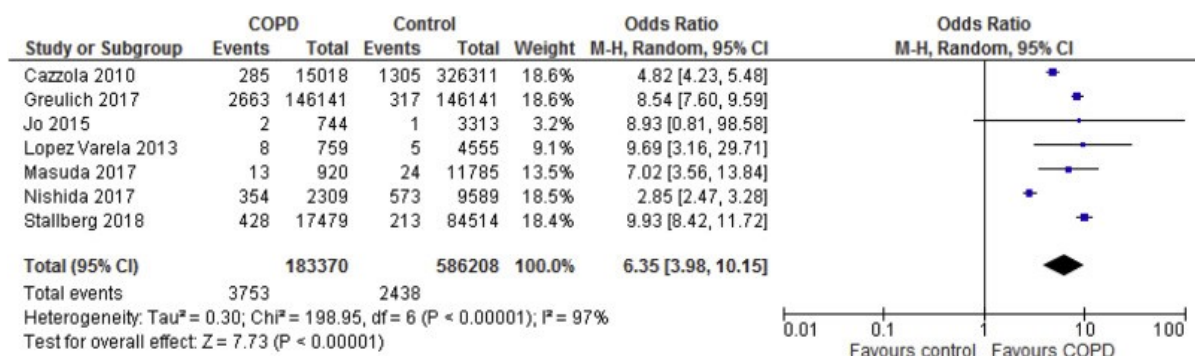Test for overall effect: Z = 7.73 (P < 0.00001)

Figure 1. *Pooled estimates of odds ratio for lung cancer in COPD and normal population*.
Odds ratios were calculated using Cochran-Mantel-Haenszel method and random effects model. The odds ratio for lung cancer in COPD was determined to be 6.35 (95% CI: 3.98–10.15, p < 0.0001) (Butler *et al*., 2019).

Indeed, COPD diagnosis, regardless of patients' smoking history, increases the risk of lung cancer up to 4.5-fold (Punturieri *et al*., 2009). In this regard, the prevalence of COPD in lung cancer patients varies from 40 to 70%, (Young *et al*., 2009). Noteworthy, Powell *et al*., (2013) demonstrated that COPD diagnosis may be timely relevant in that it is considered a lung cancer risk factor, thus allowing earlier lung cancer diagnosis. Indeed, the evaluated odd ratio of COPD patients diagnosed of lung cancer within 6 months were 11-fold higher than those lung cancer patients without COPD, and 2-fold higher in patients who received COPD diagnosis 10 years before lung cancer diagnosis. Thus, these data highlight the clinical relevance of an early diagnosis for both COPD and lung cancer. Recently it was found that COPD has an impact on lung cancer prognosis (Wang *et al*., 2018). The authors demonstrated that the 3-/5-year overall survival (OS) rates of lung cancer patients with COPD were 73.0%/65.2%, and were 79.5%/73.3% in lung cancer patients without COPD, indicating that COPD, as well as COPD severity, were significantly associated with worse OS of lung cancers.

Several studies have also pointed at the risk to develop lung cancer according to the severity of COPD. However, the results are still controversial. De Torres *et al*., (2011) demonstrated that lung cancer incidence was lower in patients with worse severity of airflow obstruction (GOLD Stage III and IV). In sharp contrast, previously Mannino *et al*., (2003) demonstrated a positive correlation between the degree of airflow obstruction and lung cancer incidence, in that patients with mild COPD and moderate to severe COPD had, respectively, a relatively and a significantly higher risk of lung cancer incidence. Afterwards, Wasswa-Kintu *et al*., (2005) and Calabrò *et al*., (2010) demonstrated that the risk of lung cancer increased with decreasing FEV1 and that even a relatively modest reduction in FEV1 was a significant predictor of lung cancer. In support to these latter independent studies, very recently Carr *et al*., (2018) found that the degree of COPD severity, including airflow obstruction, visual emphysema, and respiratory exacerbations, is independently predictive of lung cancer. In this nested case-control study, which involved both smoker subjects with and without lung cancer, and with and without

COPD, the authors also found that respiratory exacerbations are associated with SCLC histology. In a large prospective study, it was demonstrated that, even in non-smokers, lung cancer risk is associated with non-malignant pulmonary conditions, especially emphysema (Turner *et al*., 2007). Moreover, lung cancer mortality was also associated with the two COPD phenotypes, that are emphysema and chronic bronchitis. In addition, a recent case-control study highlighted that COPD is an independent risk factor for all histological subtypes except for carcinoid tumors; in particular, the risk for SCLC was higher, followed by large-cell neuroendocrine carcinoma, squamous cell carcinoma, large cell-carcinoma, and adenocarcinoma (Wang *et al*., 2018b). The comparison between non-COPD and COPD patients with emphysema-predominant or non-emphysema-predominant phenotype were independently at risk of cancer. However, patients with emphysema-predominant phenotype of COPD had higher risk of squamous cell carcinoma and small-cell lung carcinoma (Wang *et al*., 2018b). Thus, the crosstalk between COPD phenotypes and the risk of specific histological subtypes of lung cancer is still under debate.

A growing number of evidence suggest that several mechanisms may link COPD and lung cancer, among which DNA damage caused by aging and/or telomere shortening, familial predisposition, genetic and epigenetic alterations, epithelial to mesenchymal transition (EMT), chronic inflammation and oxidative stress (Duhram & Adcock, 2015). Chronic airway inflammation is one of the main features of COPD (Colarusso *et al*., 2017) and represents meanwhile the seventh hallmark of cancer (Colotta *et al*., 2009). Studies on respiratory inflammation and pulmonary carcinogenesis have shown a high correlation between pulmonary carcinogenesis and the exposure to various inhalable toxic pollutants, as airborne PM and CS. Both PM and CS are able to increase epithelial inflammation and lung cancer risk due to their high carcinogenic potential leading to oxidative stress and increased production of mediators of pulmonary inflammation (Valavanidis *et al*., 2013). As previously reported, lung inflammation in COPD involves many types of inflammatory and immune cells which, together

with structural cells, release inflammatory mediators in the airways in response to the toxic particles (CS and air pollutants) into the respiratory tract resulting in structural damage and functional impairment (Colarusso *et al*., 2017). A pivotal role in this context is played by lung macrophages which orchestrate COPD-associated inflammation through the release of pro-inflammatory cytokines, chemokines that attract neutrophils, monocytes and T cells, and proteases, such as matrix metalloproteinase 9 (MMP9) (Barnes, 2008). Among cells in the tumor microenvironment, macrophages highly populate lung cancer tumor mass and their dominant M2 phenotype is correlated with a minor survival (Quatromoni & Eruslanov, 2012). Based on the concept that tumor-associated macrophages (TAMs) are M2-like cells, which facilitate immunesuppression leading to tumor progression (Terlizzi *et al*., 2016), to the concept that M2 macrophages are predominant in patients with mild to moderate COPD (Ma *et al*., 2010), it is likely to speculate that macrophage polarization in COPD could play a pro-tumorigenic role, favoring the onset of lung cancer.

Inflammasome in COPD and lung cancer. The impact of chronic inflammation in both diseases is further proved by the detection of pro-inflammatory cytokines and immune infiltrates in samples collected from COPD and lung cancer patients. IL-1 like cytokines are highly present in broncho-alveolar lavage fluid (BAL), sputum and lung tissue of COPD patients (Colarusso *et al*., 2017), and IL-1β and IL-18 are detected in the plasma and tissues of lung cancer patients (McLoed *et al*., 2016). It is well-known that the multiprotein complex inflammasome is responsible of IL-1-like cytokines (i.e. IL-1α, IL-1β, IL-18 and IL-33) release (Terlizzi *et al*., 2014). The inflammasome comprises the assembly of NLRs (NOD-like receptors) or HIN200 family receptors, such as absent in melanoma 2 (AIM2), able to bind the adaptor apoptosis-associated speck-like protein (ASC) that acts as a 'zipper' and induces the auto-cleavage of pro-caspase-1, that in its active form facilitates the activation and then release of IL-1-like cytokines. To date, different types of inflammasome have been identified both in humans and in mice, but the best characterized is the inflammasome NLRP3, a NLRs which

contains a C-terminal leucine-rich repeat (LRR) domain, a central NACHT domain (or NBD: nucleotide-binding domain), and an N-terminal pyrin domain (PYR). It is postulated that in mice the canonical activation of NLRP3 inflammasome requires two signals. The first signal involves the recognition of pathogen-associated molecular patterns (PAMPs) and damage-associated molecular patterns (DAMPs), by Toll-like receptor (TLR) 4 or TLR2, TNF-receptor (TNFR) and IL-1 receptor (IL-1R) that trigger NF-κB dependent gene expression. The second signal leads to the assembly of the components into the inflammasomes structure and provides the intracellular recognition of DAMPs or PAMPs by NLRs. However, differences between humans and mice exist regarding inflammasome activation. Dr. Hornung's laboratory (Gaindt *et al*., 2016) discovered that the sole addition of lipopolysaccharide (LPS) to human monocytes induce the inflammasome activation and the consequent release of IL-1β and IL-18 without cell death, as instead widely described in mice. The inflammasome plays a role in different forms of cancer including lung cancer (Moosavi *et al*., 2018) and is involved in various pulmonary diseases (Terlizzi *et al*., 2018). It is to point out that, although some evidence reports the biological relationship between inflammasomes and cancer, it remains controversial whether they play a pro- or anti-tumorigenic role. Indeed, on one side the activation of inflammasome sensors is largely beneficial in colitis-associated colorectal cancer, but on the other they lead to the development of fibrosarcoma, melanoma and gastric carcinoma (Terlizzi *et al*., 2014). In our laboratory we demonstrated that the inflammasome and its related cytokines play a role in lung tumour growth both in a mouse model of N-methyl-N-nitrosourea (NMU)-induced lung cancer and in human samples of NSCLC (Terlizzi *et al*., 2015; Terlizzi *et al*., 2016). We found that human lung tumour masses were highly populated by plasmacytoid dendritic cells (pDCs), able to produce high levels of IL-1α, which was strictly correlated to the activation of AIM2 inflammasome, suggesting its pro-carcinogenic role in lung cancer (Sorrentino *et al*., 2015b).

Air pollution and tobacco smoke, shared risk factors for COPD and lung cancer onset, are reported as inflammasome activators. Air pollution can trigger the inflammasome activation in

airway epithelia (Hirota *et al*., 2012). Although the precise mechanisms is still unclear, a recent study has reported that urban PM activates NLRP3/IL-1 receptor axis (Figure 2) involving IL-1β, C-C motif chemokine 20 (CCL-20) and granulocyte-macrophage colony-stimulating factor (GM-CSF) production which are linked to dendritic cell (DCs) activation and neutrophilia (Hirota *et al*., 2012).
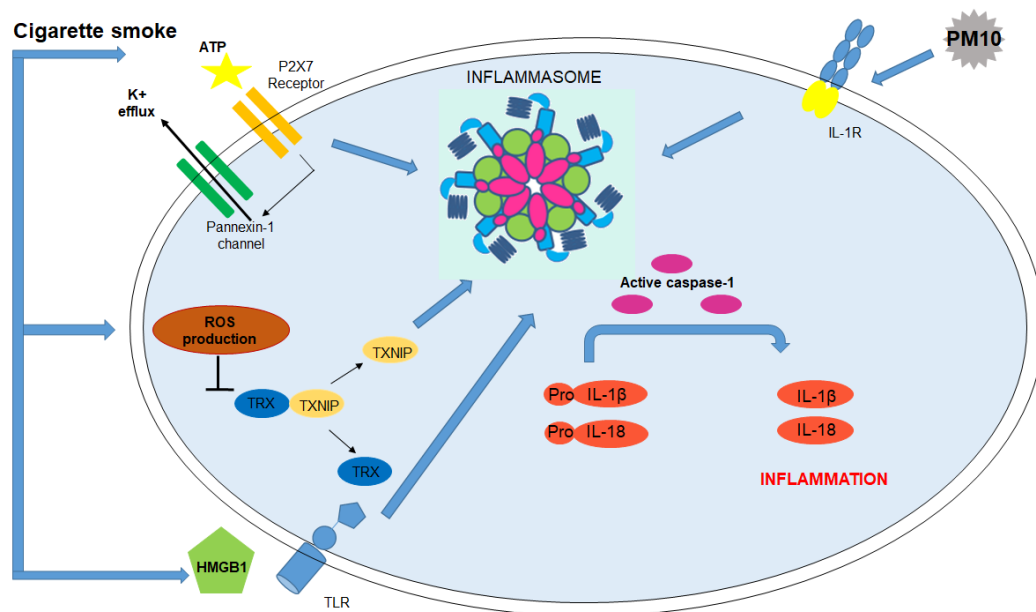
Figure 2. *Correlation between COPD and Inflammasome activation*.

The role of NLRP3 inflammasome in COPD is still unclear, however there are different possible activators of this complex which could contribute to its triggering in COPD establishment and progression. CS, major risk factor for COPD, can active the inflammasome by increasing ATP and/or ROS or by leading to HMGB1 secretion that, activating TLRs amplifies inflammasome-dependent response. Urban PM can active the inflammasome via NLRP3/IL-1receptor axis inducing inflammasome-dependent IL-1 like cytokine release.

Tobacco smoke can induce the activation of the inflammasome via oxidative stress induction (Colarusso *et al*., 2017), key feature in several molecular processes during the pathogenesis of COPD (Barnes, 2016) and lung cancer (Loke *et al*., 2014). Tobacco smoke, contains free radicals, including reactive nitrogen and oxygen species (RNOS), and reactive oxygen species (ROS), able to damage airways and to induce the release of pro-inflammatory cytokines triggering airway destruction, air trapping and lung hyperinflation (Duhram & Adcock, 2015). Although it is not still fully clear how ROS trigger NLRP3 activation, an early theory suggests that NADPH oxidase, the main source of bactericidal ROS in phagocytes, may be responsible for particle-induced inflammasome activation (Gross *et al*., 2011). The activation of the NLRP3 inflammasome can also be induced by an increase of mitochondrial ROS (mtROS) production due to mitochondrial alteration (Zhou *et al*., 2011). Moreover, it was found that inflammasome activators triggered ROS-dependent association of thioredoxin (TRX)-interacting protein (TXNIP), a protein that during oxidative stress conditions binds NLRP3 and leads to its activation (Figure 2) (Colarusso *et al*., 2017). The burden of ROS generated by CS and inflammatory cells drives many features of COPD (Figure 3).

Figure 3. *Oxidative stress in COPD.*

Both oxidants generated from inhaled oxidants (cigarette smoke and environmental pollution) and inflammatory cells in the lungs contribute to a burden of ROS, which drives many features of COPD.

In this context, the exposure to tobacco smoke augments ROS levels, which in turn trigger NLRP3 inflammasome activation. The correlation between CS and inflammasome activation can be explained in multiple wa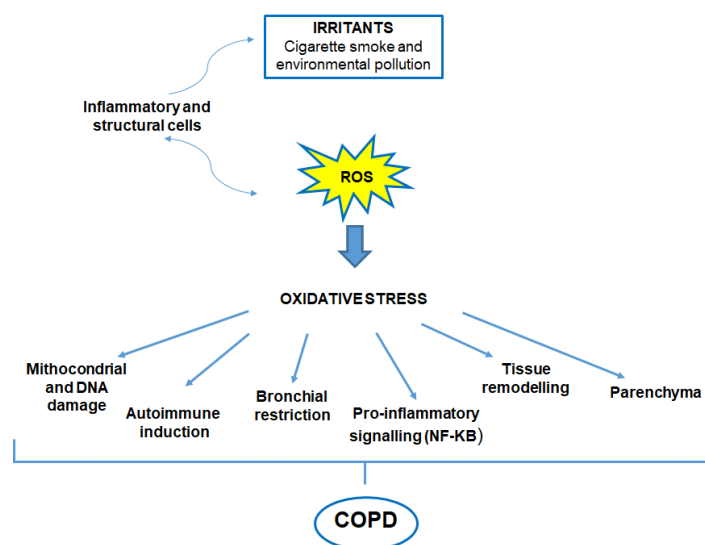ys: 1.CS increases the levels of ATP, which in turn, by acting as an endogenous danger signal, leads to NLRP3 activation via purino-receptor P2X7 binding, altering cytosolic calcium and potassium levels; 2. CS increases ROS levels which, directly or indirectly can activate the inflammasome; 3. CS augments ROS levels which are involved in NLRP3 inflammasome activation, and leads to the secretion of high mobility group box 1 protein (HMGB1) that amplifies inflammasome-dependent response via TLRs signalling (Figure 2) (Colarusso *et al*., 2017). The possible involvement of the inflammasome in COPD is supported by several *in vivo* studies demonstrated that the genetic absence of caspase-1 (Churg *et al*., 2009), the enzyme involved in the canonical activation, and NLRP3 (Heng & Painter 2018) reduces COPD-like features and leads to lower release of IL-1β/IL-18 in BAL samples in mice exposed to CS. Moreover, high levels of IL-1β were found in lungs of COPD patients after CS exposure (Kim *et al*., 2015), high levels of IL-18 were detected in sputum and peripheral blood of COPD patients (Wang *et al*., 2012), and increased levels of the adaptor protein ASC were found in sputum samples of COPD patients (Franklin *et al*., 2014). However, published data on human samples from COPD are controversial, probably due to technical issues and the nature of COPD-derived samples (derived from exacerbated or stable COPD patients); indeed, it was suggested that the inflammasome may be critical in COPD exacerbation, but not in stable condition (Di Stefano *et al*., 2014). In support to this latter study, stable COPD patients are treated with corticosteroids, which should be able to inhibit inflammasome components and effectors (Barnes, 2016), probably explaining the inefficacy of Canakinumab, an human antibody against IL-1β, and other drugs targeting inflammasome-related effectors in clinical trial on COPD patients (Colarusso *et al*., 2017). To note, most of literature data are exclusively focused on the role of NLRP3 inflammasome and its activation

in COPD pathogenesis, but little is reported about the involvement of other type of inflammasome receptors, such as AIM2, NLRP1 and NLRP6.

Whilst inflammasomes play crucial roles in the clearance of pathogens, the precise mechanisms underlying the inflammasome/s involvement in COPD and lung cancer development and progression is far from clear, so further studies are needed to elucidate the role of these complexes in these two diseases (Figure 4).
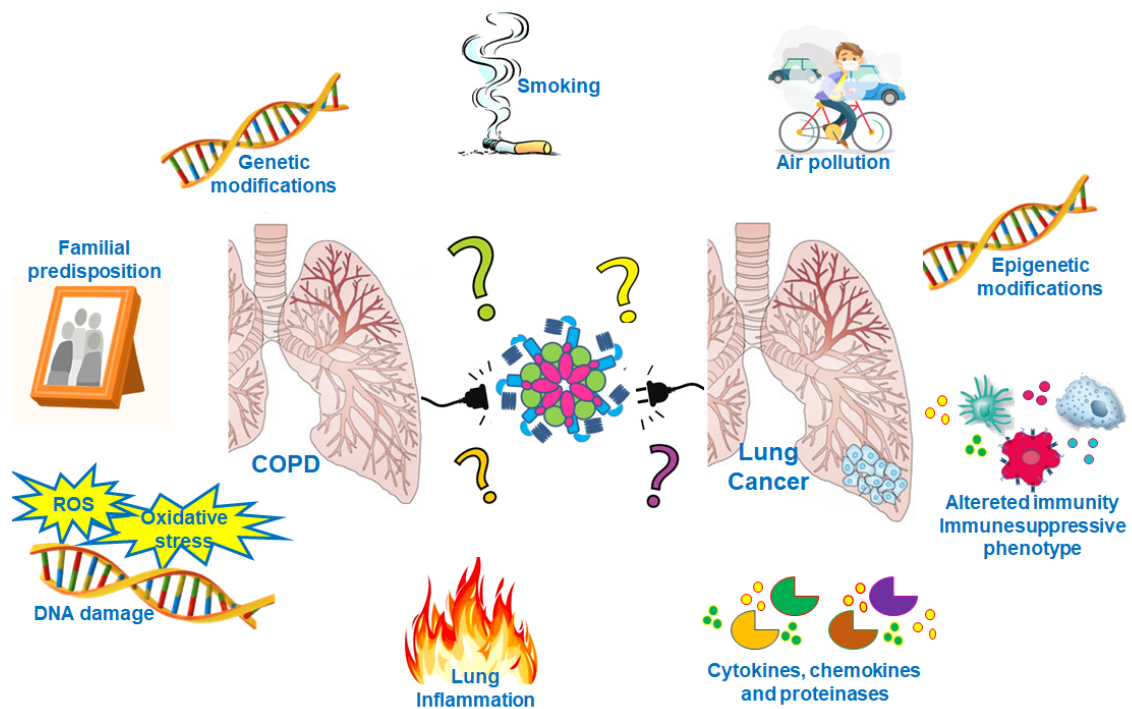
Figure 4. *Putative mechanisms at the interface between COPD and Lung Cancer.*

Smoke and exposure to air pollution are shared causes of COPD and lung cancer, and strongly associated to oxidative stress and chronic lung inflammation. Although familial predisposition is involved, both COPD and lung cancer are correlated to genetic and epigenetic alterations, DNA damage, and following recruitment of immunesuppressive immune cells and pro-inflammatory mediators (cytokines, chemokines, proteinases) leading to lung structural damage and functional impairment. Based on the concept that the inflammasome may play a critical role in COPD onset and lung cancer establishment, the activation of this multimeric complex may be at the crosstalk between COPD and lung carcinogenesis.

AIM OF THE PROJECT

Based on the fact that COPD could be a driving factor for lung cancer establishment, and that these two diseases share as common etiological factors CS and environmental pollutants, and as common trait lung-associated chronic inflammation, the aim of this project was to investigate the molecular mechanisms that could underlie the development of lung cancer in COPD patients. The pathway of this link could approach to novel therapy strategies. Therefore, we focused our attention on the inflammasome which, playing a role in both diseases, may be the link between inflammatory and immune responses at the basis of lung cancer establishment in COPD condition. For this aim our research plan was to:

1. Evaluate the molecular and cellular mechanism/s that promote the inflammasome activation by analyzing the release of pro- and anti-inflammatory cytokines release by using human samples from healthy subjects (non-smoker and smoker) and COPD patients exposed to particles mimicking air pollution, and a mouse model of PM exposure to analyse lung cellular infiltrates;

2. Study the role and the involvement of the inflammasome in the pathogenesis of COPD in unstable/exacerbated and stable COPD patients compared to healthy non- and smoker subjects, by stimulating isolated mononuclear cells by using well-known inflammasome activators;

3. Define the relationship between COPD and lung cancer evaluating the inflammasome involvement in lung carcinogenesis by using a mouse model of CS and carcinogen exposure.

To pursue these goals, we elaborated this PhD research described in five chapters.

CHAPTER 1

Smokers-derived peripheral blood mononuclear cells (PBMCs) released IL-1-like cytokines under combustion-generated ultrafine particles (UFPs) exposure in a NLRP3-/caspase-1-dependent manner.

1.1 Introduction

A strong correlation was highlighted between air pollution exposure and the onset of respiratory disorders (www.who.int/news-room/fact-sheets/detail/ambient-(outdoor)-air-quality-and-health). One of the main sources of toxic environmental particles are the anthropogenic activities such as combustion (e.g., power generation, land traffic), industrial processes, dust and biomass burning (Xia *et al*., 2016). Recently it was demonstrated that particles obtained during combustion process of modern engines (as diesel) consist of ultrafine particles (UFPs), often referred as Soot. These latter particles are sub-100 nm in diameter, so that, they can move deep through the airways until the alveolar regions, affecting the immune system with ensuing respiratory disorders (Terzano *et al*., 2010). Short-term exposure to UFPs can promote exacerbation episodes in respiratory diseases (bronchitis, asthma), whereas long-term exposure to high levels of UFPs can increase the risk of chronic respiratory diseases (COPD) and lung cancer onset (Lodovici & Bigagli, 2011). Several studies demonstrated that exposure to Soot particles has remarkable effects on the immune system (Provoost *et al*., 2010; Shaw *et al*., 2016). Indeed, it was found that exposure to Soot particles causes changes in lymphocyte homeostasis and immune responses (Pierdominici *et al*., 2014). However, the exact mechanism by which combustion-derived particles cause the alteration of immune cells

function, which in turn may trigger inflammatory processes, is still unknown. It was reported that the mechanism by which air pollution induces detrimental health effects involves an inflammation-related cascade and oxidation stress both in lung, vascular, and heart tissue (Lodovici & Bigagli, 2011). In support to the hypothesis that link oxidative stress to diseases induced by combustion-derived particles, it was demonstrated that exposure to diesel exhaust particles (DEP), which is the major source of environmental UFPs, increased the production of ROS responsible for lipid peroxidation and oxidative DNA damage, and likely to cell death processes (i.e. apoptosis and necrosis) (Vesterdal *et al*., 2014). In this context, the role of mitochondria may play a crucial role. Mitochondrial membrane depolarization alteration induces mitochondrial ROS (mtROS) release, which has recently been described as potential inducers of the NLRP3 inflammasome, whose activation may contribute to specific immune changes, such as induction of pro-inflammatory cytokines production and cell death (Li *et al*., 2003). The inflammasome is a cytosolic multimeric complex that plays a pivotal role in innate immunity by participating to the production of pro-inflammatory cytokines via pro-caspase-1 cleavage. (Terlizzi *et al*., 2014; Colarusso *et al*., 2017). The activation of the inflammasome leads to the release of IL-1-like cytokines, which are responsible for early inflammation and can result in long-term chronic inflammation (Terlizzi *et al*., 2014).

In this Chapter, we describe that human peripheral blood mononuclear cells (PBMCs) derived from healthy smokers are more susceptible to Soot-induced IL-1-dependent inflammation via the activation of NLRP3 inflammasome that leads to caspase-1 activation with the ensuing release of IL-1α, IL-18 and IL-33. Instead, PBMCs isolated from non-smoker individuals showed higher release of the immunesuppressive cytokine IL-10 after the addition of Soot particles. In contrast, PBMCs from smokers released less pronounced IL-10 levels. The results obtained from smokers-derived PBMCs imply that both smoking and air pollution can prompt toward pulmonary inflammation in an IL-1-like manner.

1.2 Materials and Methods

1.2.1 Human Samples

Peripheral blood samples from healthy volunteers (smokers and non-smokers), recruited at the "Monaldi-Azienda Ospedaliera (AORN)-Ospedale dei Colli" Hospital in Naples, Italy, were collected after patient's informed consent. All experimental protocols were approved by the Review Board of "Monaldi-AORN-Ospedale dei Colli" Hospital (approval number 1254/2014). Human samples were obtained according to the guidelines and regulations provided and accepted by the Review Board of the "Monaldi-AORN-Ospedale dei Colli" Hospital. The healthy volunteers were 50±10 years old. All subjects had no history of allergic diseases or chronic respiratory conditions. Blood was collected and used within 24 hours in order to isolate mononuclear cells.

1.2.2 Isolation of human PBMCs

PBMCs were isolated according to Ficoll's protocol. Briefly, blood (5 mL) was mixed with cell medium (5 mL) supplemented with sole antibiotics and gently layered on the top of Ficoll medium. Then, it was centrifuged at 1125 g for 20 minutes. PBMCs layer, in the interphase between Ficoll solution and medium, were collected, diluted with cell medium and centrifuged at 753 g to remove the remaining Ficoll solution. Platelets were separated by centrifugation at 149 g for 10 min and PBMCs were collected.

1.2.3 Cell Culture

Macrophagic cells, J774.1, and collected PBMCs were cultured in Roswell Park Memorial Institute (RPMI) 1640 supplemented with 10% heat-inactivated fetal bovine serum (FBS), 100 units/mL penicillin, 100 units/mL streptomycin and 2 mM L-glutamine. In order to mimic the effect of environmental pollution from combustion processes, J774.1 cells and isolated PBMCs were treated with Soot particles (1 pg/mL up to 5 ng/mL; Soot particles preparation is

described in paragraph 1.2.4), and with the NLRP3 inflammasome activators: LPS (0.1 µg/mL), and/or ATP (0.5 mM) according to the two-signal model (Terlizzi *et al*., 2014). Moreover, isolated PBMCs were treated with Ac-YVAD-cmk (YVAD, 1 µg/mL), a caspase-1 inhibitor (Sorrentino *et al*., 2015b), M6690 (M66,10 µM), a calpain I/II inhibitor, and/or Glybenclamide (Gly, 1 µM), a pharmacological inhibitor of NLRP3 (Sorrentino *et al*., 2015b). Concentrations of the above treatments were chosen according to published data (Sorrentino *et al*., 2015b; Terlizzi *et al*., 2015; Terlizzi *et al*., 2016; Terlizzi *et al*., 2018).

1.2.4 Preparation of Soot particles

Soot particles were prepared by Professor D'Anna's group, at the Department of Chemical, Materials and Industrial Production Engineering of the University Federico II of Naples, by collection at the exhaust of an atmospheric pressure acetylene/air premixed flame operated in fuel-rich conditions (equivalence ratios greater than 3). McKenna burner was used to create the flame which was stabilized on the burner by a metal plate located approximately 3 cm from the burner outlet. After some hours of combustion process, Soot particles deposited on the metal plate were removed by mechanical ablation and collected as a powder. Structural analysis of the carbon-network constituting the Soot particles were carried out by Ultraviolet-visible (UV-vis) and infrared spectroscopy and Raman spectroscopy. Soot particles appeared as a small (< 2 nm) network of aromatic structures with few peripheral H-atoms. Elemental analysis confirmed the low presence of H atoms in the Soot particles, as the amount of C was approximately 96%, in mass, of the total material, and H was approximately 2.5–2.8%, with the rest being trace compounds. Soot particles were made up of spherical particles with sizes on the order of 20–30 nm and larger, chain-like, Soot agglomerates with sizes up to a few hundred nanometers. Soot particles were dispersed in bidistilled water to obtain a suspension with a concentration of 5 ppm (5 µg/mL), which was later sonicated to avoid particle disaggregation and prevent further agglomeration. In order to obtain a stable suspension, we

decided to add 10% dimethyl sulfoxide (DMSO) to the suspension and, after sonication, we did not observe any deposits after 72 hours. The mean sizes of the suspended particles ranged from 80 to 120 nm, and the mass concentration was determined assuming a Soot density of 1.8 g/cm^3. Soot particles solution used for PBMCs treatment were obtained by serial dilution in RPMI.

1.2.5 Cytokine measurements

IL-1α, IL-1β, IL-18, IL-33, IL-10, TNF-α and IL-6 release was measured in cell-free supernatants from J774.1 and PBMCs after 5 and 24 hours of treatment. The assays were performed using commercially available enzyme-linked immunosorbent assay (ELISA) kits (eBioscience, CA, USA).

1.2.6 MTT assay

To assess cell viability, 3-(4,5-dimethylthiazol-2-yl)-2,5-diphenyltetrazolium bromide (MTT) was added to medium-free cells post treatment. DMSO was used to dissolve the purple formazan crystals. The formazan concentration was determined by measuring the optical density. The data are presented as absorbance (550 nm) vs treatment.

1.2.7 Statistical Analysis

Data are reported as violin plots indicating the median ± interquartile range or as mean ± SEM. Statistical differences were assessed with ONE-way analysis of variance (ANOVA) followed by Bonferroni's multiple comparison post-test. p values less than 0.05 were considered significant.

1.3 Results

1.3.1 Ultrafine Soot particles induced the release of IL-1-like cytokines in murine macrophages in a concentration-dependent manner.

To study the potential pro-inflammatory activity of Soot particles, we preliminarily used murine macrophage cell line J774.1, because these cells have been widely used as a model for studying pro- and anti-inflammatory activity of compounds (Justo *et al*., 2015). J774.1 cells were treated with laboratory-made Soot particles in a concentration-dependent manner starting from 1 pg/mL and increasing up until to 5 ng/mL, and in medium we evaluated the release of IL-1-like cytokines, such as IL-1α, IL-1β, IL-18 and IL-33. We found that, after 5 hours of treatment, Soot particles were able to statistically increase the release of IL-1α (Figure 5A, red violin plots), IL-1β (Figure 5B, red violin plots) and IL-33 (Figure 5C, red violin plots), but not IL-18 (data not shown). Most importantly, it is to underlie that the sub-maximal effect in terms of IL-1α (Figure 5A), IL-1β (Figure 5B) and IL-33 (Figure 5C) was reached at low concentrations (5, 10, 50 and 100 pg/mL) rather than higher concentrations (500, 1000 and 5000 pg/mL). Moreover, we observed that Soot-treated J774.1 cells were able to release a similar or a higher amount of pro-inflammatory cytokines than those observed for positive controls (LPS±ATP; Figure 5, white violin plots).
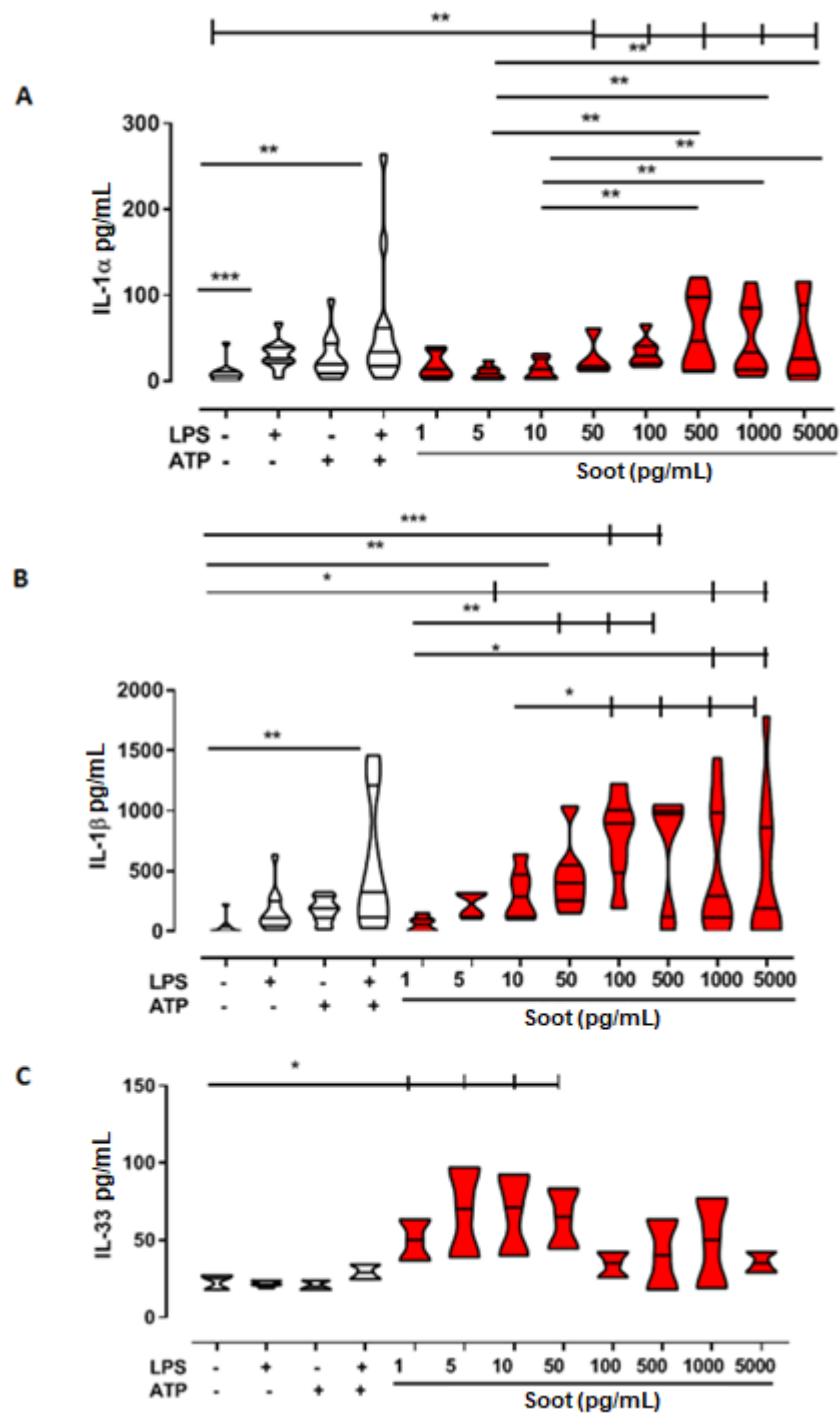
Figure 5. *Soot particles led to the release of IL-1-like cytokines by murine macrophages*.

J774.1 cells were exposed to Soot particles in a concentration-dependent manner (1 pg/mL–5 ng/mL) for 5 hours. LPS (0.1 µg/mL) and/or ATP (0.5 mM) was used as a positive control. The administration of Soot particles to macrophages induced the release of IL-1α **(A,** red violin plots**)**, IL-1β **(B**, red violin plots**)** and IL-33 **(C**, red violin plots**)**. Data are presented as violin plots showing median ± interquartile range (n = 12). Statistically significant differences are determined by ONE-way ANOVA followed by Bonferroni's multiple comparison post-test. *, ** and ***, indicate p < 0.05, p < 0.01 and p < 0.001 respectively.

To better understand the pro-inflammatory effect of Soot particles, we then analyzed the release of IL-6 and TNF-α after 24 hours of treatment. Soot particles were not able to induce the release of IL-6 (Figure 6A, black bars) and TNF-α (Figure 6B, black bars) at our working concentrations, suggesting that the nature and the size of Soot particles did not play a pivotal role at this level.
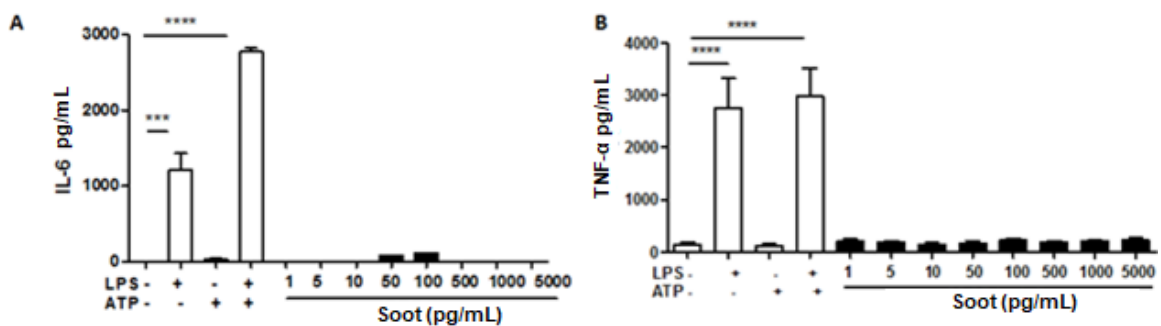
Figure 6. *The addition of Soot particles for 24 hours did not induce the release of IL-6 and TNF-α by murine macrophages.*

J774.1 cells were treated with Soot particles in a concentration dependent manner (1 pg/mL-5 ng/mL) for 24 hours. LPS (0.1 µg/mL) and or ATP (0.5 mM) were used as positive control. The addition of Soot particles onto J774.1 cells did not lead to IL-6 (**A,** black bars) and TNF-α (**B,** black bars) release. Data represent means ± SEM (n = 12). Statistically significant differences are denoted by *** and **** indicating $p<0.001$ and $p<0.0001$, respectively, as determined by ONE-way ANOVA followed by Bonferroni's multiple comparison post-test.

To rule out the possibility that the observed effects were due to cytotoxicity of Soot particles, we evaluated the cell viability. The MTT assay showed that cell viability was not affected by UFPs at both 5 hours (Figure 7A) and 24 hours (Figure 7B). In addition, to exclude any interference of Soot particles to absorb at 550 nm, we also performed the MTT assay in a cell-free medium after the addition of the sole Soot particles at the concentration of 1 pg/mL−5 ng/mL. Soot particles did not alter the absorbance of the MTT assay compared to the sole medium without particles (Figure 7C).

These preliminary data, taken all together, indicate that in J774.1 cells, Soot particles induce early inflammation via the release of IL-1-like cytokines without affecting cell viability.
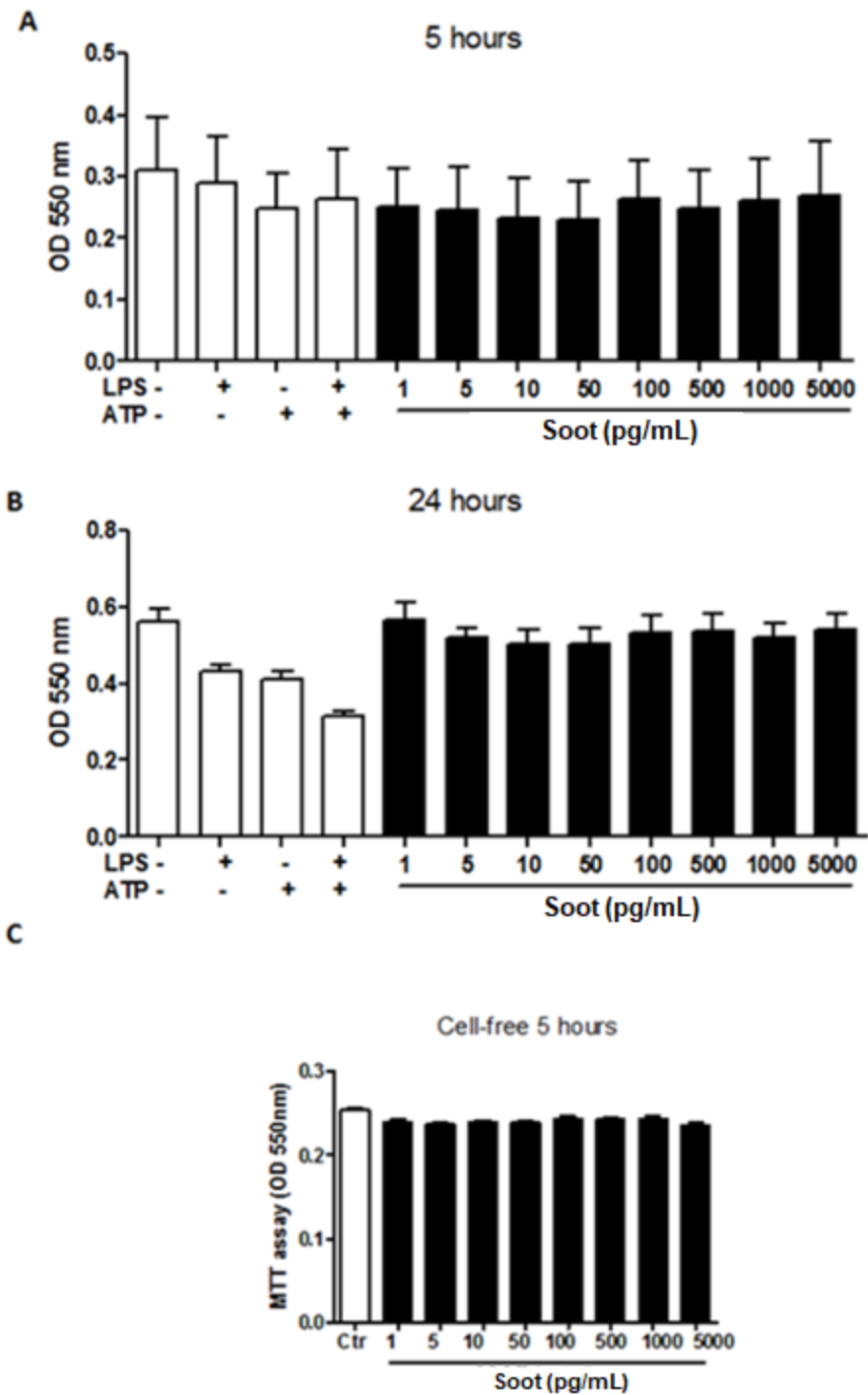
Figure 7. *The treatment with Soot particles did not induce murine macrophages cell death.*

J774.1 cells were exposed to Soot particles in a concentration dependent manner (1 pg/mL-5 ng/mL) for 5 (**A**) and 24 hours (**B**). LPS (0.1 µg/mL) and or ATP (0.5 mM) were used as positive control. The administration of Soot particles onto J774.1 cells did not lead to cell death at both time points considered. Moreover, Soot particles did not alter the absorbance of the MTT assay in a cell-free medium at 550 nm compared to the absorbance of the sole medium (**C**). Data represent means ± SEM (n = 12).

1.3.2 Ultrafine Soot particles led to a concentration-dependent release of IL-1-like cytokines from healthy smokers-derived PBMCs.

Based on the results reported in the previous paragraph, we wondered whether the same effect could be observed in human primary cells. To this purpose, PBMCs were isolated from healthy non-smoker and smoker volunteers, and exposed to combustion-generated Soot particles. We observed that Soot particles treatment (1 pg/mL–5 ng/mL) did not induce IL-1α (Figure 8A, white violin plots), IL-33 (Figure 8B, white violin plots) and IL-18 (Figure 8C, white violin plots) release from PBMCs obtained from healthy non-smokers after 5 hours of treatment. In sharp contrast, the exposure to Soot particles significantly increased the release of IL-1α, IL-33 and IL-18 (Figure 8A, 8B and 8C, respectively, dotted violin plots) from healthy smokers-derived PBMCs. Similarly to what we observed for J744.1 cells, Soot-induced IL-1-like cytokines secretion was comparable or higher than the cytokines release of the positive control (LPS±ATP; Figure 8).

To try to understand the different response to Soot particles in non-smokers and smokers, we evaluated the release of IL-10, an immunesuppressive cytokine (Mittal *et al*., 2015). We observed that the release of IL-10 was significantly increased both in non-smokers- (Figure 9A) and smokers-derived PBMCs (Figure 9B). However, it is important to note that Soot-induced IL-10 reached higher levels for PBMCs obtained from non-smokers (Figure 9C, white violin plots) than PBMCs from smokers (Figure 9C, dotted violin plots).

These results imply that healthy smokers are more susceptible to Soot-induced IL-1-dependent inflammation than non-smokers, in that these latter show an immunesuppressive response to UFP.
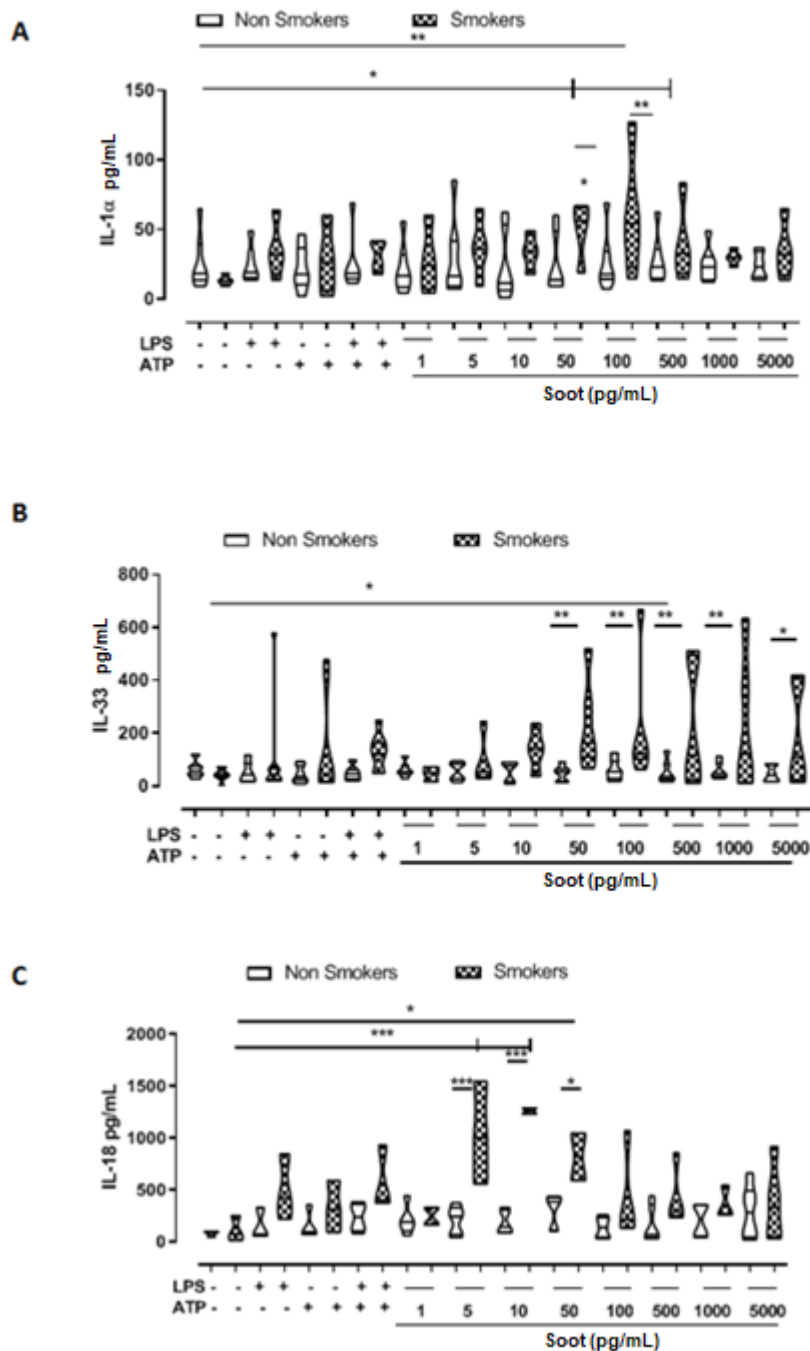
Figure 8. *Healthy smokers-derived PBMCs were more susceptible to Soot particles-induced IL-1-like cytokines release.*

Healthy non-smokers- (white violin plots) and smokers-derived PBMCs (dotted violin plots) were treated with Soot particles for 5 hours. LPS (0.1 μg/mL) and/or ATP (0.5 mM) were used as positive control. The addition of Soot (1 pg/mL–5 ng/mL) did not trigger the release of IL-1α (**A**) and IL-33 (**B**) from non-smokers-derived PBMCs. However, Soot slightly increased IL-18 release (50 pg/mL) (**C**). In sharp contrast, the administration of Soot to smokers-derived PBMCs significantly increased the release of IL-1α (**A**), IL-33 (**B**) and IL-18 (**C**). Data are presented as violin plots showing median ± interquartile range (n = 5). Statistically significant differences are determined by ONE-way ANOVA followed by Bonferroni's multiple comparison post-test. *, ** and *** represent $p < 0.05$, $p < 0.01$ and $p < 0.001$, respectively.
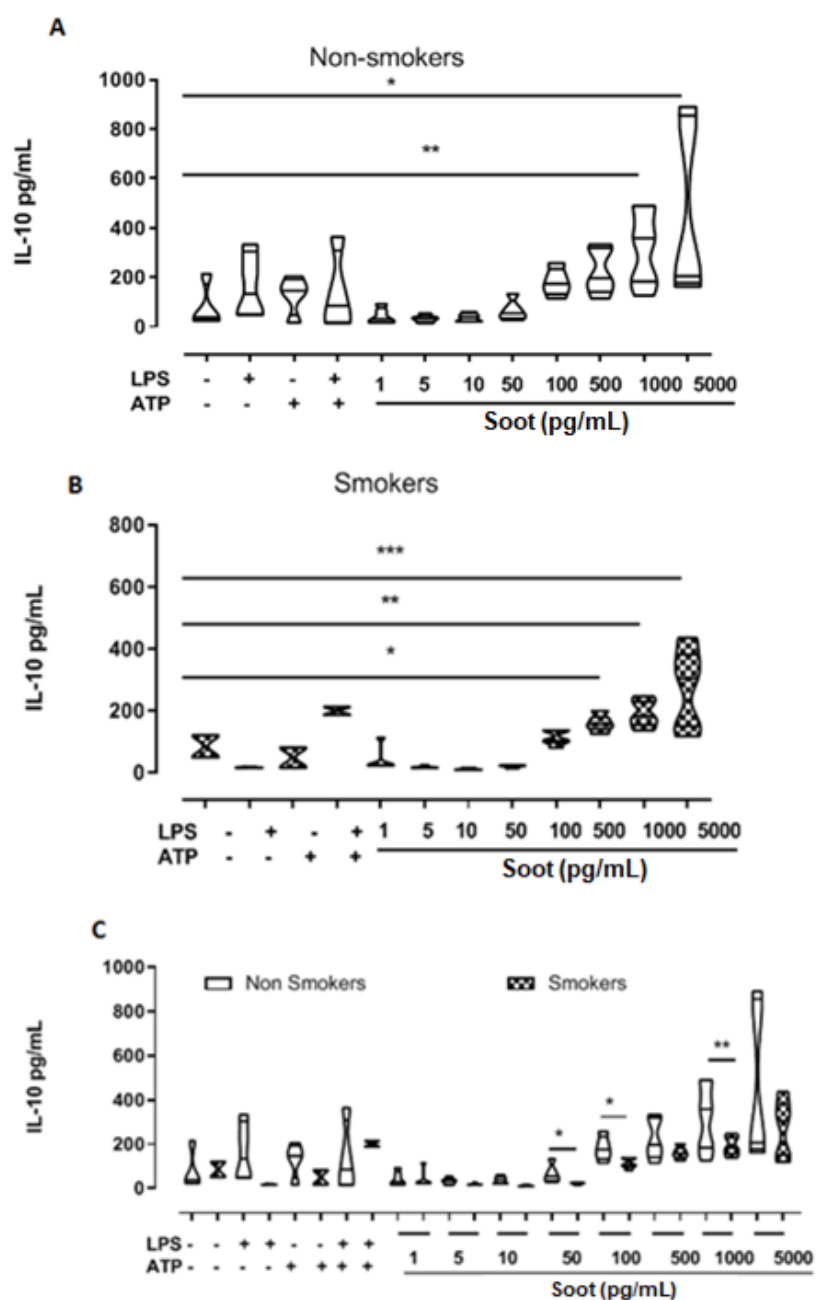
Figure 9. *The administration of Soot particles led to the release of IL-10 from non-smokers and smokers-derived PBMCs*.

Healthy non-smokers- (white violin plots) and smokers-derived PBMCs (dotted violin plots) were treated with combustion-derived Soot particles for 5 hours. LPS (0.1 µg/mL) and/or ATP (0.5 mM) were used as positive control. Soot particles (1 pg/mL–5 ng/mL) exposure significantly increased the release of IL-10 from non-smokers-derived-PBMCs (**A**). Similarly, PBMCs obtained from smoker subjects released IL-10 after Soot particles treatment, but to a lower extent (**B**). Comparison of Soot particles-induced IL-10 levels between non-smokers (white violin plots) and smokers (dotted violin plots) are represented (**C**). Data are presented as violin plots showing median ± interquartile range (n = 5). Statistically significant differences are determined by ONE-way ANOVA followed by Bonferroni's multiple comparison post-test. *, ** and *** represent p < 0.05, p < 0.01 and p < 0.001, respectively.

1.3.3 The release of IL-1-like cytokines from smokers-derived PBMCs after Soot particles treatment was NLRP3-/caspase-1-dependent.

The cytokines of IL-1-family play a significant role in inflammatory processes and their secretion is strictly dependent on the multimeric inflammasome complex (Terlizzi *et al*., 2014). To understand the molecular mechanism underlying the release of IL-1α, IL-18 and IL-33 cytokines after Soot particles exposure, we went on by using well-known pharmacological inhibitors to evaluate the possible involvement of the inflammasome in this context.

PBMCs isolated from smoker subjects were co-treated with Soot particles and Ac-YVAD-cmk (YVAD, 1 µg/mL), a caspase-1 inhibitor (Sorrentino *et al*., 2015b, Terlizzi *et al*., 2016; Terlizzi *et al*., 2018). The pharmacological inhibition of caspase-1 significantly decreased the release of IL-1α, IL-18 and IL-33 (Figure 10A, 10B and 10C, green violin plots, respectively). However, we observed that PBMCs exposed to Soot particles at the concentration of 100 pg/mL, in presence of caspase-1 inhibition still induced release of IL-1α (Figure 10A, green violin plots); this effect could imply that another mechanism, probably, was involved.
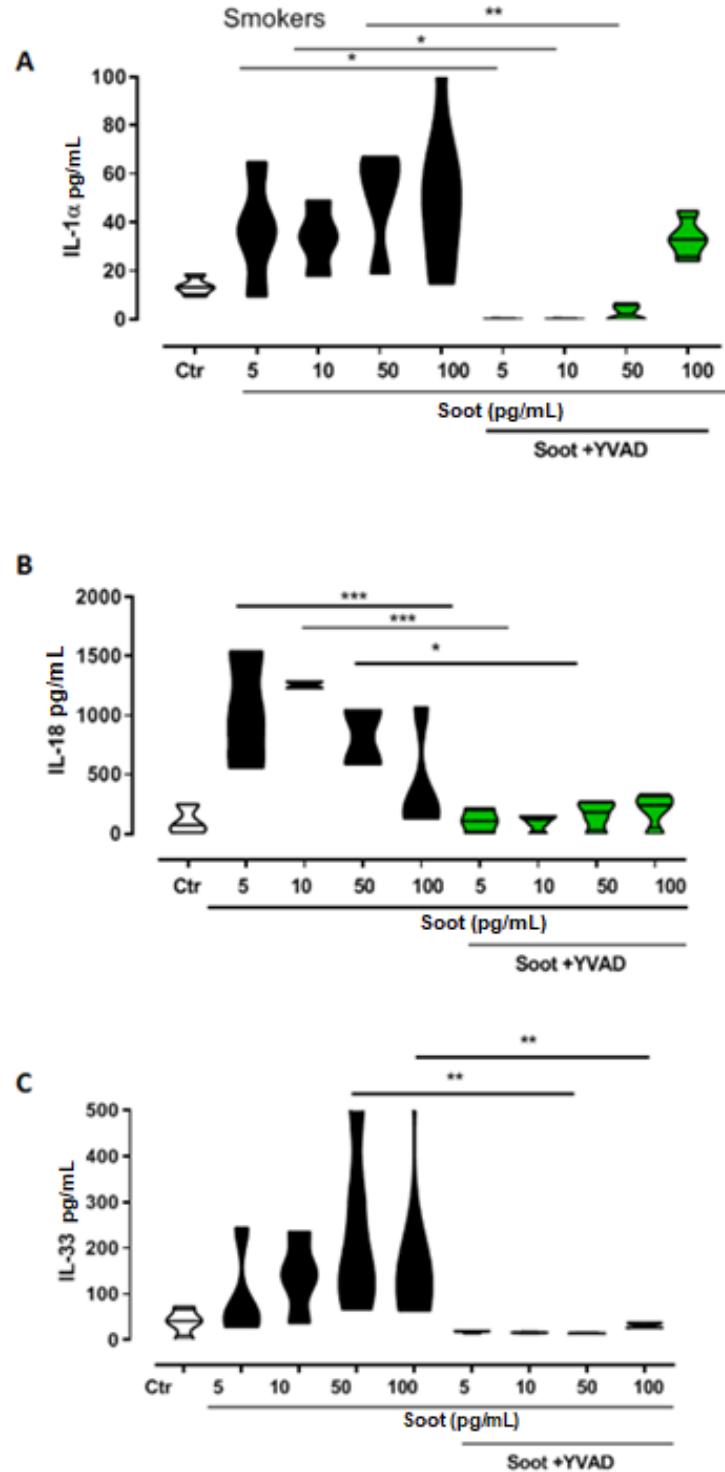
Figure 10. *Soot particles induced the release of IL-1-like cytokines from healthy smokers-derived PBMCs in a caspase-1-dependent manner.*

PBMCs isolated from smokers were treated for 5 hours with Soot particles (5-10-50-100 pg/mL) in the presence or absence of Ac-YVAD-cmk (YVAD, 1 μg/mL), a caspase-1 inhibitor (green and black violin plots, respectively). The inhibition of caspase-1 significantly reduced the release of IL-1α (**A**), IL-18 (**B**) and IL-33 (**C**) from treated PBMCs. Data are presented as violin plots showing median ± interquartile range (n = 5). Statistically significant differences are determined by ONE-way ANOVA followed by Bonferroni's multiple comparison post-test. *, ** and *** represent $p < 0.05$, $p < 0.01$ and $p < 0.001$, respectively.

Because Gross *et al*, (2012) showed that IL-1α processing is also associated to calcium-dependent calpain protease activity, to evaluate whether this pathway could be involved, we inhibited the calpain system by means of M6690 (M66, 10 µM), a calpain I/II inhibitor (Sorrentino *et al*., 2015b). The addition of M66 completely abrogated the release of IL-1α (Figure 11) from smokers-derived PBMCs after Soot particles treatment, even at higher concentrations (50–100 pg/mL).
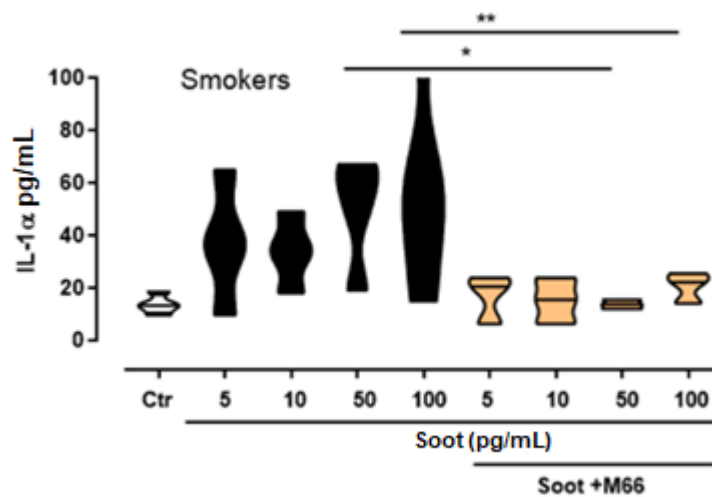
Figure 11. *Soot particles induced the release of IL-1α from healthy smokers-derived PBMCs in a calpain-dependent manner.*

PBMCs obtained from smokers were treated for 5 hours with Soot particles (5-10-50-100 pg/mL) in the presence or absence of M6690 (M66, 10 µM), a calpain I/II inhibitor (orange and black violin plots, respectively). The inhibition of calpain I/II significantly reduced the release of IL-1α from treated PBMCs. Data are presented as violin plots showing median ± interquartile range (n = 5). Statistically significant differences are determined by ONE-way ANOVA followed by Bonferroni's multiple comparison post-test. * and ** represent $p < 0.05$ and $p < 0.01$, respectively.

Because the inflammasome complex comprises the NLRP3 receptor which can bind ASC leading to the recruitment and activation/autocleavage of caspase-1 (Terlizzi *et al*., 2014), we examined the involvement of NLRP3 inflammasome. To this purpose, PBMCs from smokers were treated with Soot particles in the presence of Glybenclamide (Gly, 1 μM), a well-known inhibitor of the NLRP3 inflammasome (Sorrentino *et al*., 2015b). The inhibition of NLRP3 significantly reduced the release of IL-1α, IL-18 and IL-33 (Figure 12A, 12B and 12C, blue violin plots, respectively). Similarly to what we observed in Figure 10A, the release of IL-1α after Soot particles exposure at the concentration of 100 pg/mL was not completely reduced when NLRP3 was inhibited (Figure 12A), suggesting that most likely the activation of calpain I/II was primarily involved in IL-1α release after Soot particles exposure (Figure 11).

All together these data imply that healthy smoker subjects are more susceptible to the effect of UFP obtained from combustion process and mimicking air pollution. Particularly, Soot-induced IL-1-like cytokines release from smokers-derived PBMCs is NLRP3-/caspase-1-dependent inflammasome.
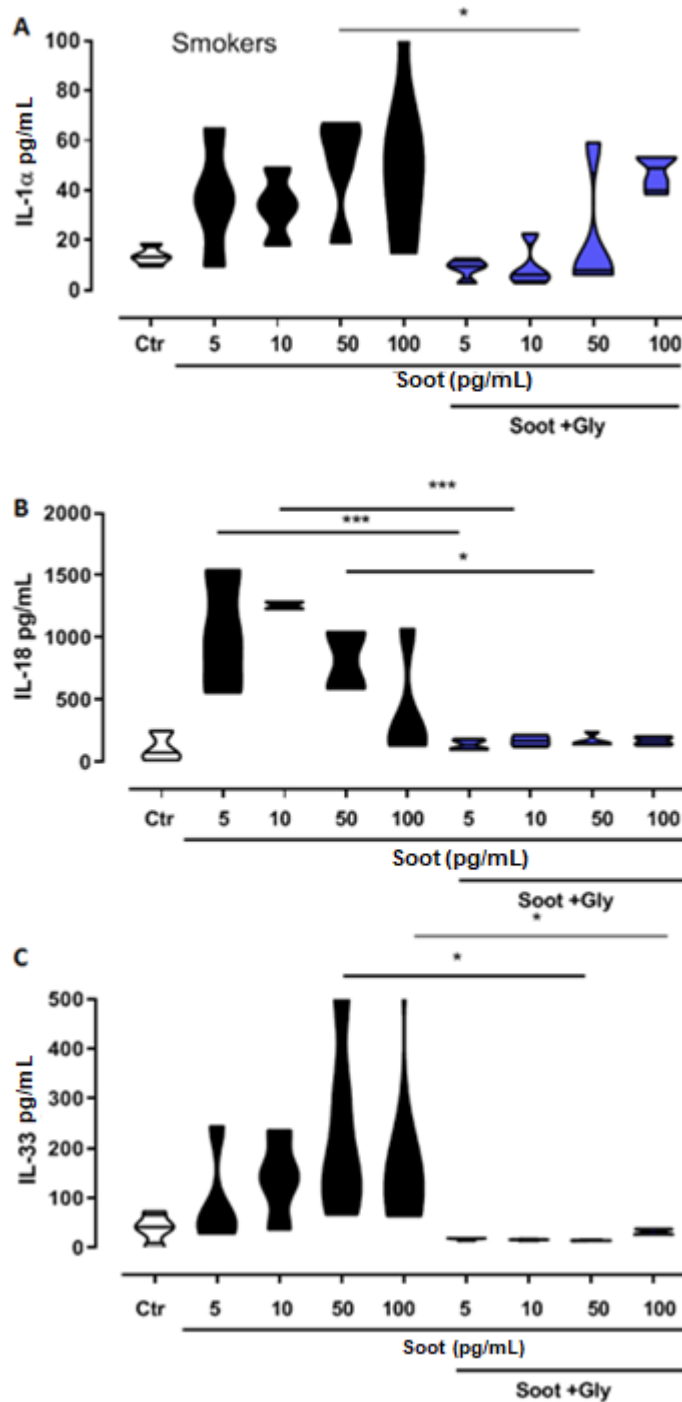
Figure 12. *NLRP3 was involved in Soot particles-induced IL-1-like cytokines release from healthy smokers-derived PBMCs*.

PBMCs isolated from smokers were treated for 5 hours with Soot particles (5-10-50-100 pg/mL) in the presence or absence of Glybenclamide (Gly, 1 μM), an NLRP3 inhibitor (blue and black violin plots, respectively). The inhibition of NLRP3 by means of Gly significantly reduced the release of IL-1α (**A**), IL-18 (**B**) and IL-33 (**C**) from treated PBMCs. Data are presented as violin plots showing median ± interquartile range (n = 5). Statistically significant differences are determined by ONE-way ANOVA followed by Bonferroni's multiple comparison post-test. * and *** represent p < 0.05 and p < 0.001, respectively.

1.4 Conclusions

Combustion processes typical of modern engines have been recognized as potential source of harmful particles for the health, especially in the airway where they can promote chronic inflammatory lung diseases (Donaldson *et al*., 2005). In this study, we found that human PBMCs isolated from healthy smokers were more susceptible to ultrafine Soot particles in terms of IL-1-dependent inflammation. It is important to underlie that this effect was observed when PBMCs were exposed to very low concentrations of Soot particles; indeed, we used particles concentrations on the order of pg/mL compared to what has already been reported in literature which has described the pro-inflammatory and cytotoxic activities of DEP/air pollution-derived particles at concentrations of μg/mL (Provoost *et al*., 2010; Totlandsdal *et al*., 2010). Particularly, we demonstrated that Soot-induced IL-1-like cytokines release was associated to the activation of the canonical, caspase-1-dependent, NLRP3 inflammasome. The crosstalk between noxious particles in the air derived from combustion processes and the activation of the inflammasome was found also by Li *et al*., (2016). The authors found that the exposure to biomass fuel smoke led to the release of DAMPs and the following activation of NLRP3 inflammasome and caspase-1 (Li *et al*., 2016). Moreover, our results are supported by a study reporting the ability of fine PM (10 nm in diameter) to trigger in THP-1 cells the release of IL-1β in a NLRP3 inflammasome-dependent manner via TLR2 and TLR4 (Bengalli *et al*., 2013). It is very important to note that Soot particles-induced IL-1-dependent inflammation was observed solely in PBMCs from smokers and not those from non-smokers, which instead showed immunesuppressive behavior. Although we observed the release of IL-10 under Soot treatment from both groups, the levels of this cytokine reached higher values in non-smoker-derived PBMCs.

It is well-known that the release of IL-1-like cytokines is involved in immune response and can promote the activation of NF-κB, which play a critical role in inflammatory processes (Hoesel & Schimid, 2013). In support of this, Barton *et al*., (2014) demonstrated that diesel PM

triggered NF-κB activation and ensuing inflammation in primary alveolar macrophages. According to the sterile inflammation theory, sterile and noninfectious exogenous insults can induce chronic inflammation (Terlizzi *et al*., 2014), therefore it is possible to speculate that the immune system recognizes combustion-derived particles and other noxious pollutants in the air as dangerous stimuli which may be sensed by the inflammasome and lead to inflammation (Gross *et al*., 2011). Because inflammation plays a key role in cancer establishment and air pollution was defined by IARC as cancer-causing agent (Loomis *et al*., 2013), based on the results reported in this study we can speculate that smokers, a high-risk population, exposed to ultrafine Soot particles may be more susceptible to the inflammatory processes involved into lung cancer development than non-smokers. Although we did not evaluate whether Soot particles were able to induce cell transformation in that this study was carried out using human PBMCs, we demonstrated that combustion-derived particles had an impact on immune cells in term of IL-1-like cytokines release. Immune system plays a pivotal role in cancer immune escape in that the immune cells in tumor context were tolerogenic and therefore incapable of recognizing transformed cells as non-self (Zitvogel *et al*., 2006). It is known that tumor cell escape can occur through many different mechanisms including the development of an immunesuppressive tumor microenvironment (Mittal *et al*., 2014). Our results about the release of IL-10 in response to combustion-derived particles exposure may confirm the hypothesis about the role of Soot particles-induced IL-1-like cytokines favoring the establishment of a pro-tumor environment. Indeed, in cancer context IL-10, an immunesuppressive cytokine, regulates the switch of macrophages to M2 phenotype which is correlated to cancer progression (Nam *et al*., 2014). Moreover, in our previous study, we found that pDCs derived from cancerous lesions of patients with lung cancer were able to release IL-1α, rendering pDCs tolerogenic (Sorrentino *et al*., 2015b). Here we found that, PBMCs from smokers, a population well known to be at high risk of lung cancer, released higher levels of IL-1α than PBMCs from non-smokers. These

data imply that the release of both IL-10 and IL-1α may promote lung carcinogenesis via cell transformation.

In conclusion, our study demonstrated that combustion-derived particles (size 80-120 nm) trigger the release of IL-1-like cytokines from smokers via the canonical inflammasome pathway, although IL-1α release appears to be primarily dependent on the activation of calpain I/II.

CHAPTER 2

Combustion-generated UFPs induced the release of IL-1-like cytokines from unstable/exacerbated COPD-derived PBMCs in a NLRP3-/caspase-1- and caspase-8-independent manner.

2.1 Introduction

Air pollution represents another risk factor for COPD exacerbation (Colarusso *et al*., 2017). Although cigarette smoke (CS) has been widely described as the main risk factor, only 15-20% of smokers develop COPD, suggesting that genetic predisposition and environmental factors may play an eligible role in the onset of the pathology (Duhram & Adcock, 2015). Chronic lung inflammation in COPD patients reflects the site of deposition of irritants from CS and noxious particles from air pollution (Perez-Padilla, *et al*., 2010), which affect airway structural cells and circulating cells and increase the susceptibility to infections (Colarusso *et al*., 2017). Over recent years, a strong correlation between respiratory disorders and air pollution exposure was highlighted (who.int/news-room/fact-sheets/detail/ambient-(outdoor)-air-quality-and-health). As already reported, combustion-derived particles consist of ultrafine particles (UFPs) which can contribute to the onset of lung disorders due to their deposition in the respiratory tract (Valavanidis *et al*., 2013). The ability of noxious air pollutants to cause adverse health effects is also dependent on their chemical composition (Donaldson *et al*., 2001). The composition of combustion-generated particles usually depends on the type of fuel, burn conditions and atmospheric conditions, all factors that influence the particle numbers and size distribution of the UFPs emitted (Xia *et al*., 2016). Although the impact of UFPs on human health is still not clear, it was reported that UFPs are more toxic than their larger counterparts (Donaldson *et al*.,

2001). Indeed, due to their small size (< 100 nm diameter), UFPs may penetrate deep into the alveolar region and deposit at high percentages, promoting pro-inflammatory processes. In Chapter 1 we demonstrated that Soot particles (80-120 nm diameter) generated from combustion processes were able to induce the release of pro-inflammatory cytokines in an inflammasome-dependent manner from smokers-derived PBMCs (De Falco *et al*., 2017b). Therefore, we carried on our study to understand whether the activation of the NLRP3 inflammasome occurred in COPD, as well. Indeed, emerging evidence suggested that NLRP3 inflammasome could be involved in COPD pathogenesis (Colarusso *et al*., 2017) in that its genetic ablation and pharmacological inhibition prevented the release of inflammasome-dependent cytokines, such as IL-1α, IL-1β, IL-33, IL-18 in an *in vivo* mouse model of COPD (Hirota *et al*., 2012). To date, IL-1-like cytokines have been highly detected in biological fluids and lung tissues of COPD patients (De Nardo *et al*., 2014). Nevertheless, the role of the inflammasome in COPD is still controversial. While some authors reported IL-1β as involved in the typical chronic inflammation, many clinical trials targeting IL-1β (clinicaltrials.gov/ct2/show/NCT00581945; Rogliani *et al*., 2015; Calverley *et al*., 2015) failed to prove beneficial effects in COPD patients. Therefore, in this Chapter we analyze the impact of particles obtained from combustion processes (2-40 nm diameter) and mimicking environment pollutants on PBMCs isolated from exacerbated to be compared to stable COPD patients and healthy non-smoker and smoker subjects.

2.2 Materials and Methods

2.2.1 Human Samples

To evaluate the contribution of air pollution and the role of CS on the pro-inflammatory mechanisms associated with COPD, peripheral blood samples from hospitalized patients affected by COPD and healthy subjects were collected at "Monaldi-AORN-Ospedale dei Colli" Hospital in Naples, Italy, after informed consent. Human samples were obtained according to the guidelines and regulations provided and accepted by the Ethical Committee of the Hospital (approval number 1254/2014). Based on their medical history, COPD patients, all former or current smokers, were divided into two groups: unstable/exacerbated (blood was collected during exacerbation phase of the disease, that is when patients were hospitalized due to their low/altered pulmonary function) and stable (blood was collected 3-5 days after exacerbation event during which patients had received intravenous administration of corticosteroids and had stable respiratory functionality) COPD patients. Based on their smoking habits, healthy subjects (non-COPD patients) were divided into two groups: non-smokers and smokers. All subjects involved in this study were 60 ± 10 (mean $\pm$ S.E.M.) years of age and had no history of allergic diseases. Blood was used within 24 hours after collection in order to isolate mononuclear cells.

2.2.2 Isolation of human PBMCs

PBMCs were isolated according to Ficoll's protocol as already reported in Materials and Methods section of the Chapter 1 (paragraph 1.2.2). Collected PBMCs were plated and treated at different time points (1, 3, or 5 hours) with different UFPs (particles characteristics are reported in paragraph 2.2.3) in order to mimic the effect of environmental pollution from biofuel combustion. We used UFPs at the concentration of 50 and 100 pg/mL, according to our preliminary data on concentration-dependent (1 pg/mL up to 5 ng/mL) treatment. Moreover, in order to evaluate the possible involvement of the inflammasome complex into the release of pro-inflammatory cytokines after UFPs treatment, PBMCs were treated in presence or not of

UFPs with the following substances: Ac-YVAD-cmk (YVAD, 1 µg/mL) , a pharmacological inhibitor of caspase-1 (Sorrentino *et al*., 2015b), Glybenclamide (Gly, 1 µM), a pharmacological inhibitor of NLRP3 (Sorrentino *et al*., 2015b), and/or Z-IETD-FMK (IE, 0.5 µg/mL) a pharmacological inhibitor of caspase-8 (Terlizzi *et al*., 2015), enzyme involved in the non-canonical inflammasome-dependent pathway.

2.2.3 Preparation of UFPs samples

UFPs were generated by Professor D'Anna's group, at the Department of Chemical, Materials and Industrial Production Engineering of the University Federico II of Naples. Four different kinds of UFPs were collected and reported as Soot-E, Soot-E/DMF, NOC-E and NOC-ED. These particles were obtained during combustion condition typical of modern engines after burning either a fossil fuel (ethylene, for Soot-E and NOC-E) and a mixture of biofuels (ethylene and dimethylfuran, for Soot-E/DMF and NOC-ED). Based on chemical differences, area and size, particles were divided in two groups: Soot particles and NOC particles. NOC (nano organic carbon) particles were mostly constituted of organic carbon (D'Anna, 2009) and had a size of sub-10 nm (around 2-5 nm diameter). They were stacks of few aromatic molecules, which had high-molecular mass and were constituted by four to six fused benzene rings with a dimension of about 1.2 nm connected by chain-like bridge (van der Waals interactions). Soot particles were more graphitic carbon structures (D'Anna, 2009); they had sizes ranging from 20–40 nm, typical of the primary Soot particles, to 100–200 nm typical of the chain-like aggregates of the primary particles appeared as a network of aromatic structures with few peripheral H atoms. Elemental analysis confirmed the low presence of H atoms in the Soot particles, as the amount of C was approximately 95–98%, in mass, of the total material, and H was approximately 1–2%, with the rest being trace compounds, possibly oxygen. Characteristics of UFPs are summarized in Table 2.

Table 2. *Characteristics of Ultrafine Particles for in vitro experiments.*

	Fuel	Particle size	Composition
Soot-E	ethylene	20-200 nm	graphitic carbon structures
Soot-E/DMF	ethylene/2,5 DMF (80/20 vol.%)	20-200 nm	graphitic carbon structures
NOC-E	ethylene	sub-10 nm	organic carbon
NOC-ED	ethylene/2,5 DMF (80/20 vol.%)	sub-10 nm	organic carbon

We decided to use UFPs with different features compared to that used in the Chapter 1 in order to evaluate the possible impact of different nature and size of noxious particles. All UFPs were dispersed in bidistilled water to obtain a suspension with a concentration of 5 ppm (5 µg/mL). To obtain a stable suspension, 10% DMSO was added to each suspension, and to avoid any deposits we sonicated them.

2.2.4 Cytokine measurements

IL-1α, IL-1β IL-18 and IL-33 release was measured in cell-free supernatants of PBMCs (75 $\times$ 10^4 cells/well) culture after 5 hours of Soot and NOC particles treatment. The assays were performed using commercially available ELISA kits (eBioscience, CA, USA). The measurement of 8-hydroxy-2-deoxyguanosine (8-OH-dG), as critical biomarker of oxidative stress (Valavanidis *et al.*, 2009), was performed following manufacturer's instructions (Elabscience, USA) with in the PBMCs cytosolic extract obtained from UFPs-treated cells for 3 hours.

2.2.5 Flow Cytometry Analysis

In order to assess the expression of NLRP3 inflammasome receptor, we performed flow cytometry analysis (BD FacsCalibur, Milan, Italy) by staining untreated healthy non-smoker-, smoker- and COPD-derived PBMCs (2×10^5 cells/well) with the following antibodies: CD14-PE and NLRP3-PeCy5.5 (eBioscience, San Diego, CA, United States). In order to measure the

levels of mitochondrial-derived ROS (mtROS), cells were stained for MitoSOX Mitochondrial Superoxide Indicator, as indicated in the manufacturer's guide (Life Technologies, USA).

2.2.6 Calcium Measurement

Intracellular calcium (Ca^{2+}) concentrations were measured after 1 hour of treatment (5×10^3 cells/well) as previously reported (Sorrentino *et al*., 2015b). Briefly, intracellular Ca^{2+} concentrations were measured by using the fluorescent dye Fura 2-AM (Sigma Aldrich, Rome, Italy). PBMCs were incubated at 37°C for 1 hour. Thereafter, cells were washed, and Fura 2-AM hydrolysis was allowed in calcium-free medium. Data were expressed as percentage of delta increase of fluorescence ratio (F340/F380 nm) induced by ionomycin (1 μM) or carbonyl cyanide p-trifluoromethoxy-phenylhydrazone (FCCP, 0.05 μM)—basal fluorescence/basal fluorescence ratio (F340/F380 nm).

2.2.7 RT-PCR

To investigate the repair of DNA damage following UFPs-induced mitochondrial dysfunction, 8-oxoguanine DNA glycosylase 1 (OGG1) gene expression, enzyme involved in this process (Tumurkhuum *et al*., 2016), was measured by Real-Time Polymerase Chain Reaction (RT-PCR) in RNA isolated from PBMCs (10^7 cells/well) after 3 hours of treatment with Soot-E, Soot-E/DMF, NOC-E and NOC-ED at the concentration of 100 pg/mL. Total RNA was isolated from treated cells by using the RNA extraction kit according to the manufacturer's instructions (Qiagen, Milan, Italy). Reverse Transcription was performed by using first-strand cDNA synthesis kit (Qiagen, Milan, Italy) followed by PCR. Thermal cycling conditions were as follow:

-5 min at 95°C, followed by 40 cycles of 30 s at 95°C, 60 s at 54°C, 30 s at 60°C for OGG1.

-5 min at 95°C, followed by 40 cycles of 30 s at 95°C, 60 s at 58°C, 30 s at 68°C for β-actin.

Primer pairs were as follow:

OGG1: Forward 5′-GACAAGACCCCATCGAATGC-3′;

Reverse 5′-AGCTTCCTGAGATGAGCCTC-3′.

β-actin: Forward 5′-ACTCTTCCAGCCTTCCTTCC-3′;

Reverse 5′-CGTACAGGTCTTTGCGGATG-3′.

2.2.8 Statistical Analysis

Data are reported as violin plots indicating the median $\pm$ interquartile range or as mean $\pm$ SEM. Statistical differences were assessed with ONE-way analysis of variance (ANOVA) followed by Bonferroni's multiple comparison post-test. *p* values less than 0.05 were considered significant.

2.3 Results

2.3.1 Ultrafine particles led to IL-18 and IL-33 release from PBMCs from unstable/exacerbated COPD patients.

As previously described, the inhalation of noxious particles from air pollution induces chronic inflammation process by affecting lung resident and circulating cells (Perez-Padilla *et al*., 2010). To evaluate the effect of the environmental UFP exposure and the contribution of CS on the pro-inflammatory mechanisms associated with COPD, we investigated the release of IL-1-like cytokines (IL-18, IL-33, IL-1α and IL-1β) in non-smokers-, smokers- and COPD-derived PBMCs. To mimic environmental pollution, PBMCs were treated with four different UFPs, that are Soot-E, Soot-E/DMF, NOC-E and NOC-ED, for 5 hours. We found that PBMCs from non-smokers and smokers (Figure 13, white and dotted violin plots, respectively) were less responsive to Soot and NOC particles treatment in terms of IL-18 release compared to PBMCs obtained from unstable COPD (Figure 13, black violin plots). In particular, the addition of Soot-E (Figure 13A), Soot-E/DMF (Figure 13B), NOC-E (Figure 13C) and NOC-ED (Figure 13D) significantly increased the release of IL-18 from PBMCs obtained from unstable/exacerbated COPD patients compared to untreated cells (CTR) (Figure 13, black violin plots).

Similarly to what observed for IL-18, the administration of Soot-E and Soot E/DMF (Figure 14A and 14B), and NOC-E and NOC-ED (Figure 14C and 14D) significantly increased the release of IL-33 in PBMCs of unstable/exacerbated COPD patients (Figure 14, black violin plots) at the concentration of 50–100 pg/mL. It is to note that no statistical differences in IL-33 release were observed comparing results among non-smoker (Figure 14, while violin plots) and smoker groups (Figure 14, dotted violin plots); however, we observed a statistical difference in IL-33 basal levels (CTR) that were higher in smokers- than unstable COPD-derived PBMCs (Figure 14, dotted vs black violin plots).

These results imply that unstable/exacerbated COPD patients exposed to Soot and NOC particles are more susceptible to UFP-induced inflammation than healthy subjects in terms of IL-18 and IL-33 release. In contrast to these results, we observed that PBMCs of stable COPD patients were not responsive to NOC and Soot particles in terms of IL-1-like cytokines release (data not shown). A possible explanation is that these patients were under corticosteroid treatment, able to down modulate inflammatory/immune responses and inhibit IL-1-like cytokines production (Barnes, 2016).

Figure 13. *PBMCs from unstable/exacerbated COPD patients were more susceptible to combustion-derived UFPs-induced IL-18 release*.

Healthy non-smoker (white violin plots), smoker (dotted violin plots), and exacerbated COPD (black violin plots)-derived PBMCs were treated with combustion-derived UFPs for 5 hours. The administration of Soot-E (**A**), Soot-E/DMF (**B**), NOC-E (**C**), and NOC-ED (**D**) at the concentration of 50–100 pg/mL induced the release of IL-18. Control (CTR) represents untreated cells. Data are presented as violin plot indicating the median ± interquartile range (n = 7). Statistically significant differences were determined by ONE-way ANOVA followed by Bonferroni's multiple comparison post-test.

Figure 14. *PBMCs from unstable/exacerbated COPD patients were more susceptible to combustion-derived UFPs-induced IL-33 release.*

Healthy non-smoker (white violin plots), smoker (dotted violin plots), and exacerbated COPD (black violin plots)-derived PBMCs were treated with combustion-derived UFPs for 5 hours. The administration of Soot-E (**A**), Soot-E/DMF (**B**), NOC-E (**C**), and NOC-ED (**D**) at the concentration of 50–100 pg/mL induced the release of IL-33. Control (CTR) represents untreated cells. Data are presented as violin plot indicating the median ± interquartile range (n = 7). Statistically significant differences were determined by ONE-way ANOVA followed by Bonferroni's multiple comparison post-test.

2.3.2 Combustion-generated UFPs induced oxidative stress in COPD-derived PBMCs during exacerbation.

In our previous study we demonstrated that the release of IL-1-like cytokines after Soot (80-120 nm diameter) exposure was caspase-1- and NLRP3 inflammasome-dependent in PBMCs from healthy smokers (please refer to Chapter 1; De Falco *et al*., 2017b). In order to understand the molecular mechanism underlying the release of IL-18 and IL-33 from unstable COPD patients after organic UFP exposure, we carried on evaluating the role of NLRP3 and mitochondrial-dependent oxidative stress. We observed that the expression of NLRP3 in $CD14^+$ PBMCs in basal conditions was significantly higher in unstable/exacerbated COPD patients (Figure 15A; black violin plots) than non-smokers (Figure 15A; white violin plots) and smokers (Figure 15A; dotted violin plots).

Oxidative stress is considered a characteristic and a key mechanism in many processes associated with COPD (Colarusso *et al*., 2017). In order to evaluate the mitochondrial-dependent oxidative stress in non-COPD and exacerbated COPD patients, we analyzed the levels of mtROS by means of flow cytometry as percentage of $MitoSOX^+$ cells. As reported in Figure 15B, the basal production of mtROS in unstable/exacerbated COPD-derived PBMCs (black violin plots) was more pronounced than in non-smokers- and smoker-derived PBMCs (white and dotted violin plots, respectively).

Starting from these data and based on the concept that NLRP3 activation is strictly dependent on mtROS production (Shimada *et al*., 2012), we measured mitochondria homeostasis under UFPs treatment. We observed that the exposure to UFPs of PBMCs from non-smokers and smokers (Figure 15C, white and dotted violin plots, respectively) increased the release of Ca^{2+} from mitochondria only after an external stimulus (FCCP, 0.05 μM) during the measurement/detection, implying that UFPs treatment did not affect mitochondrial Ca^{2+} stores. In sharp contrast, the levels of Ca^{2+} stores in the mitochondria of unstable COPD-derived PBMCs were lower (Figure 15C, black violin plots) than those observed in non-smokers and

smokers (Figure 15C, white and dotted violin plots, respectively) after Soot-E, Soot-E/DMF, NOC-E, and NOC-ED (100 pg/mL) treatment. These data indicated that the exposure of cells to UFPs had already induced the release of Ca^{2+} from the mitochondria in unstable COPD-derived PBMCs.

Based on the fact that Ca^{2+} from the mitochondria is strictly correlated to the release of mtROS (Sorrentino *et al*., 2015b), and that oxidative stress can generate a wide range of responses, including, damage of protein and DNA, in order to access the effect of UFPs treatment on oxidative stress status, we went on by measuring the levels of 8-OH-dG, a well-known marker of DNA damage derived from oxidative stress (Valavanidis *et al*., 2009). To this purpose and according to previous results (5 hours of treatment) (Figure 13 and 14) we decided to expose all three investigated groups to UFPs at the concentration of 100 pg/mL for 3 hours. We observed that non-smokers- and smokers-derived PBMCs released high levels of 8-OH-dG solely when exposed to NOC particles, missing responsiveness to Soot particles (Figure 15D, white and dotted violin plots, respectively). Nevertheless, 8-OH-dG levels detected were robustly higher from unstable/exacerbated COPD-derived PBMCs after both Soot and NOC particles exposure (Figure 15D, black violin plots). It is important to note that PBMCs from unstable/exacerbated COPD patients were heavily more responsive to NOC-ED treatment (five times higher) compared to non-smokers derived PBMCs in terms of 8-OH-dG (10 ng/mL versus 2 ng/mL, respectively) (Figure 15D; black vs white violin plots). These data demonstrated that all the three different cohorts were subjected to DNA damage, although it was higher in exacerbated COPD patients than healthy non-smoker and smoker subjects.

Therefore, we went on by analyzing the expression of the OGG1, an enzyme involved in the DNA damage repair following oxidative stress (Tumurkhuum *et al*., 2016). We found that the administration of all UFPs at the concentration of 100 pg/mL significantly increased the levels of OGG1 mRNA in PBMCs obtained from non-smokers (Figure 11E, white violin plots). In contrast, we observed a significant decrease of OGG1 levels after UFPs exposure in smokers-

derived PBMCs (Figure 15E, dotted violin plots) compared to the basal levels. Interestingly, OGG1 mRNA levels in unstable/exacerbated COPD-derived PBMCs did not increase after Soot-E, Soot-E/DMF, NOC-E, and NOC-ED exposure (Figure 15E, black violin plots), implying that in these patients UFPs-induced oxidative stress is not countered by repairing enzymes and may be responsible for the activation of a cascade of signaling pathways that mediate the production of pro-inflammatory cytokines.
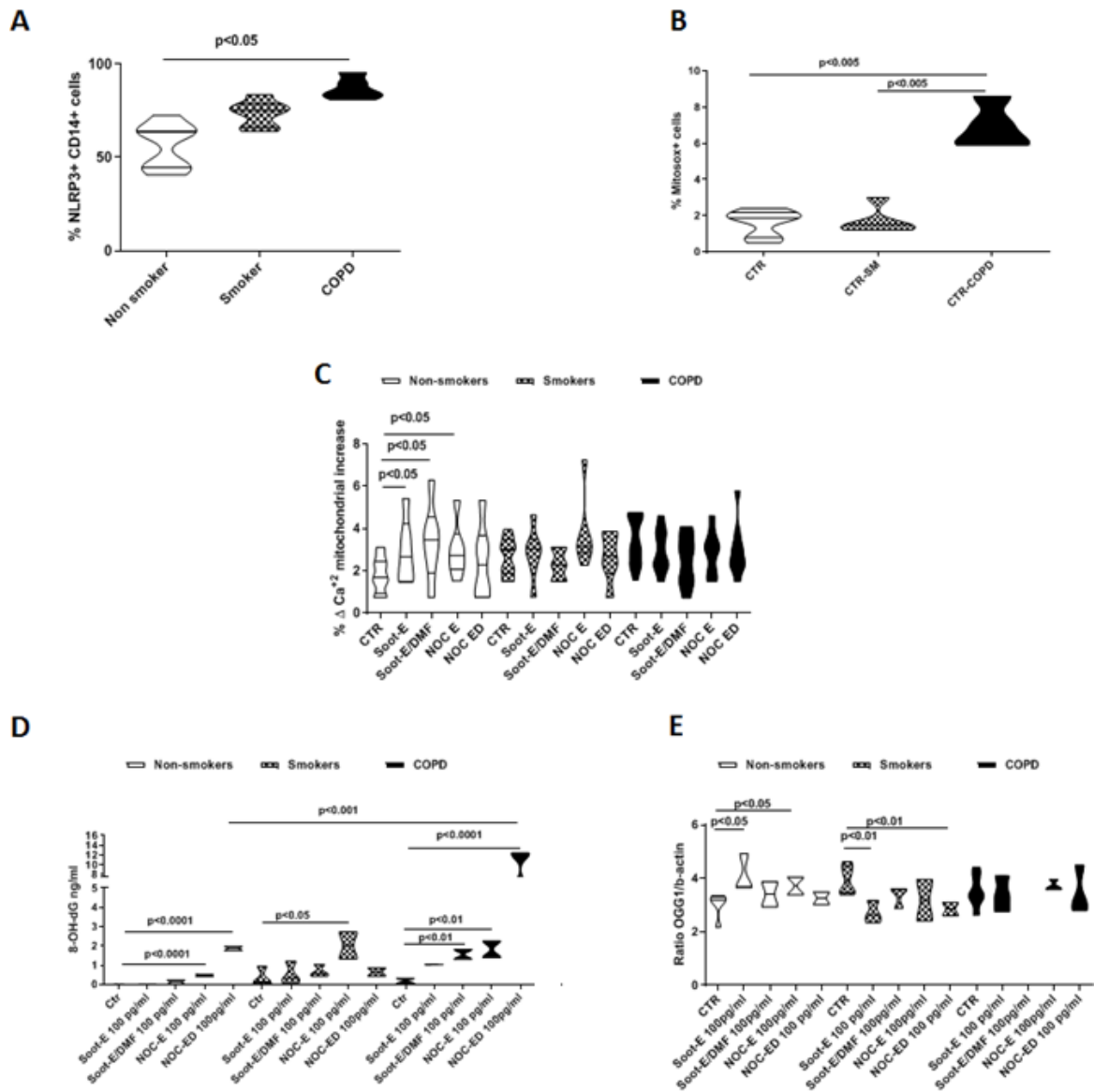
Figure 15. *The exposure to combustion-generated UFPs induced mitochondria-dependent oxidative stress*.

PBMCs isolated from healthy non-smokers and smokers, and exacerbated COPD patients (white, dotted and black violin plots, respectively) were analyzed both in basal condition (CTR) and after UFPs treatment. Flow cytometry analysis showed the expression of NLRP3 inflammasome in untreated CD14$^+$ PBMCs (**A**), and mtROS levels, identified as Mitosox$^+$ cells, (**B**). The levels of Ca^{2+} stores in the mitochondria of PBMCs treated with UFPs were analyzed (**C**). Levels of cytoplasmic 8-OH-dG after 3 hours of treatment were detected by ELISA assay (**D**). RT-PCR analysis showed mRNA levels of OGG1 after 3 hours of treatment (**E**). Data are presented as violin plots indicating the median ± interquartile range (**A**, **B**) and means ± SEM (**C–E**) (n = 7). Statistically significant differences were determined by ONE-way ANOVA followed by Bonferroni's multiple comparison post-test.

2.3.3 The release of IL-18 and IL-33 from unstable COPD-derived PBMCs after UFPs addition was not NLRP3-/caspase-1- and caspase-8-dependent.

Because mtROS release is able to induce the activation of NLRP3 inflammasome (Colarusso *et al*., 2017), and because IL-18 and IL-33 derive from the activation of the inflammasome (Terlizzi *et al*., 2014), we went on by investigating the molecular mechanisms underlying the release of these cytokines from unstable COPD-derived PBMCs after UFPs exposure by using pharmacological inhibitors of inflammasome-related components. We found that the pharmacological inhibition of caspase-1 by means of Ac-YVAD-cmk (YVAD, 1 µg/mL) did not alter the levels of IL-18 from unstable COPD-derived PBMCs after Soot-E (Figure 16A), Soot-E/DMF (Figure 16B), NOC-E (Figure 16C), and NOC-ED (Figure 16D) exposure. Because the inflammasome complex comprises the NLRP3 receptor which can bind ASC leading to the recruitment and activation/autocleavage of caspase-1 (Terlizzi *et al*., 2014), we examined the involvement of NLRP3 inflammasome. We observed that the inhibition of NLRP3 by means of Glybenclamide (Gly, 1 µM) did not alter the levels of IL-18 from unstable/exacerbated COPD-derived PBMCs after treatment with Soot particles (Figure 16A, 16B) and NOC particles (Figure 16C, 16D). In the same way, the pharmacological inhibition of caspase-8, by means of Z-IETD-FMK (IE, 0.5 µg/mL) did not alter IL-18 levels (Figure 16A–D).

Similarly, we observed that the inhibition of caspase-1, NLRP3 and caspase-8 did not alter IL-33 release (Figures 17A–D) from PBMCs obtained from unstable/exacerbated COPD patients exposed to combustion-generated UFPs.

Together these data imply that UFPs induce the release of pro-inflammatory cytokines IL-18 and IL-33, whose release does not involve the canonical, caspase-1-dependent, and non-canonical, caspase-8-dependent, NLRP3 inflammasome pathway.

Figure 16. *The release of IL-18 from unstable/exacerbated COPD-derived PBMCs after UFPs addition was not NLRP3/caspase-1 and caspase-8-dependent.*

The inhibition of caspase-1, NLRP3 and caspase-8, respectively by means of Ac-YVAD-cmk (YVAD,1 µg/mL), Glybenclamide (Gly, 1 µM), and Z-IETD-FMK (IE, 0.5 µg/mL), did not alter IL-18 levels after the administration of Soot-E (**A**), Soot-E/DMF (**B**), NOC-E (**C**) and NOC-ED (**D**) at the concentration of 50-100 pg/mL for 5 hours to PBMCs obtained by unstable/exacerbated COPD patients. Data are presented as violin plots indicating the means ± SEM (n = 7). Statistically significant differences are denoted by *, **; *** and **** indicating $p < 0.05$, $p < 0.01$, $p < 0.0005$ and $p < 0.0001$, respectively, and are determined by ONE-way ANOVA followed by Bonferroni's multiple comparison post-test.
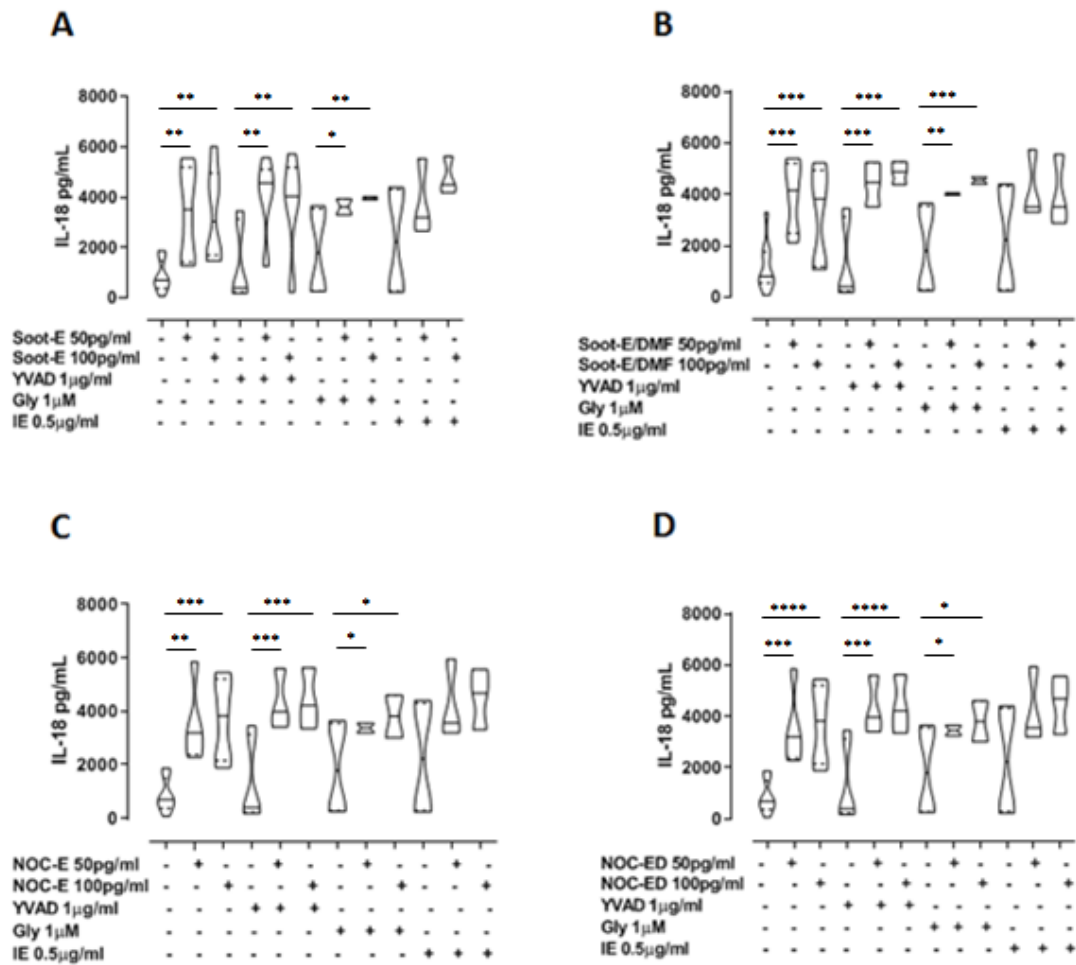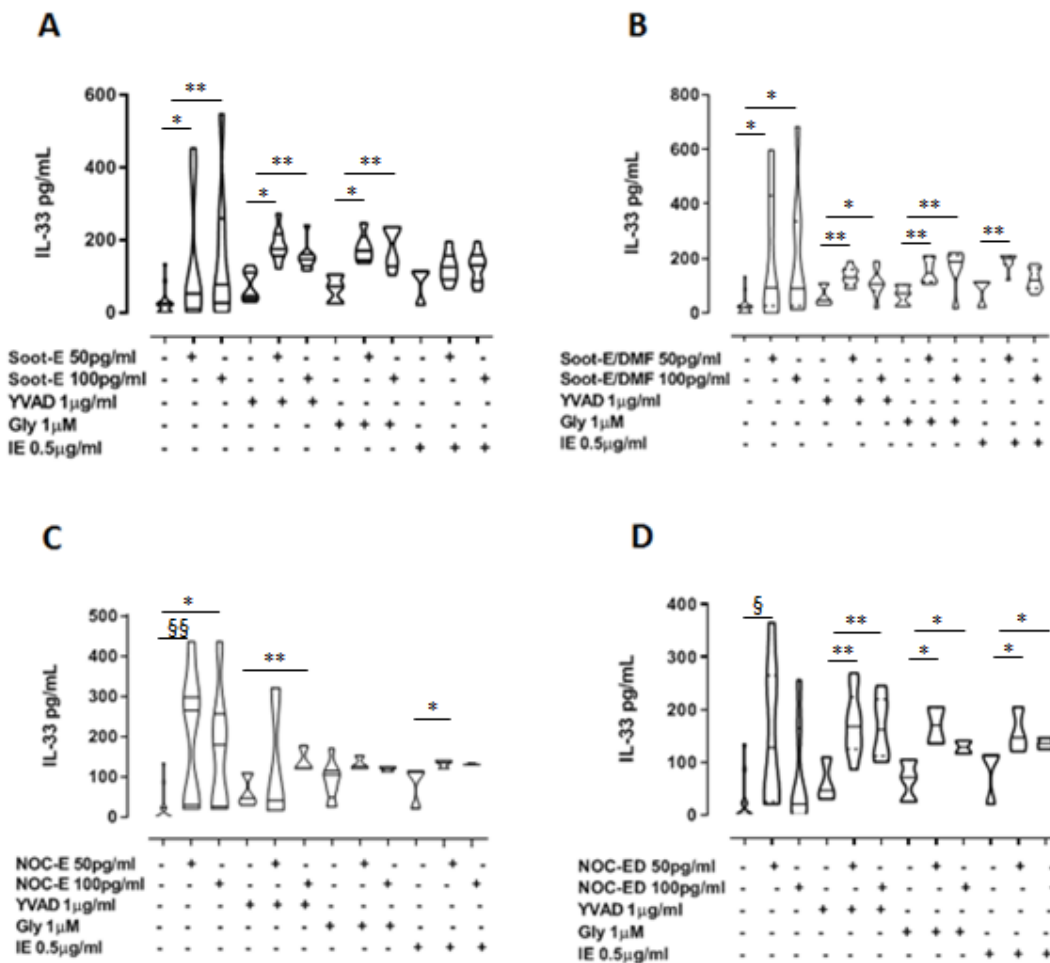
Figure 17. *The release of IL-33 from unstable/exacerbated COPD-derived PBMCs after UFPs addition was not NLRP3/caspase-1 and caspase-8-dependent.*

The inhibition of caspase-1, NLRP3 and caspase-8, respectively by means of Ac-YVAD-cmk (YVAD,1 µg/mL), Glybenclamide (Gly, 1 µM), and Z-IETD-FMK (IE, 0.5 µg/mL), did not alter IL-33 levels after the administration of Soot-E (**A**), Soot-E/DMF (**B**), NOC-E (**C**) and NOC-ED (**D**) at the concentration of 50-100 pg/mL for 5 hours to PBMCs obtained by unstable/exacerbated COPD patients. Data are presented as violin plots indicating the means ± SEM (n = 7). Statistically significant differences are denoted by *, **; § and §§ indicating p<0.05, p<0.01, p<0.005 and p<0.001, respectively, and are determined by ONE-way ANOVA followed by Bonferroni's multiple comparison post-test.

2.4 Conclusions

In this study, we found that human PBMCs derived from unstable/exacerbated COPD patients are more susceptible to combustion-derived particles in terms of IL-1-like cytokines compared to PBMCs isolated from non-smoker and smoker healthy subjects. In particular, we found that combustion-generated UFPs induced mitochondrial-derived oxidative stress, which is not countered by the enzyme OGG1, deputed to repairing oxidative stress damage, leading to the release of IL-18 and IL-33 from PBMCs obtained from unstable/exacerbated COPD patients. Importantly, the release of IL-18 and IL-33 was not dependent on the activation of the canonical, caspase-1-dependent, and non-canonical, caspase-8-dependent, inflammasome pathway. To note, we found that the sole IL-18 and IL-33, but not IL-1α and IL-1β (undetectable), were released after UFPs exposure. This effect was observed when PBMCs were exposed to very low concentrations of UFPs (on the order of pg/mL) compared to what has already been reported in literature (on the order of μg/mL) (Provoost *et al*., 2010; Totlandsdal *et al*., 2010), and in accordance with what we have previously reported in Chapter 1.

Although, the mechanisms involved in the pulmonary effects of air pollution are still not clear, it is possible to speculate that the oxidative stress induced by exposure to noxious particles in the air mediates inflammatory pathways which may trigger activation/alteration of immune cells functions and may lead to the inflammasome activation. Nowadays the precise role of the inflammasome in the establishment and progression of COPD is not fully known and reported data in literature are controversial (Colarusso *et al*., 2017). However, PM is reported as NLRP3 inflammasome activator both in airway epithelia (Hirota *et al*., 2012) and, as reported in the Chapter 1, in immune cells (De Falco *et al*., 2017b). Here we found that the exposure to particles mimicking air pollution induced DNA damage following oxidative stress both in healthy subjects and exacerbated COPD patients. 8-OH-dG levels, a well-known marker of DNA damage (Valavanidis *et al*., 2009), were more pronounced in unstable COPD patients than non-

smoker and smoker subjects, indicating that affected patients are more susceptible to the toxic effect of very small combustion-derived particles and mimicking air pollution. Furthermore, we report that the exposure to UFPs increased the activity of the repairing enzyme OGG1 solely in PBMCs isolated from non-smoker subjects, but not in PBMCs from smoker subjects and from exacerbated COPD patients. Because we found a missing DNA damage response after air pollution exposure both in smokers- and exacerbated COPD-derived PBMCs, we expected a comparable susceptibility to UFPs exposure, due to the fact that smoking habit is a common factor among the two groups. However, smoker subjects were less responsive to UFPs in terms of IL-18 and IL-33 release than exacerbated COPD-derived PBMCs, implying that although tobacco smoke concours to impair DNA repair function, other factors as clinical outcomes/lifestyle of COPD patients are involved in the pro-inflammatory processes associated to air pollutants-induced IL-1-like cytokines production (Eisner *et al*., 2010). Because the production of IL-1-like cytokines is strictly associated to the activation of the multimeric complex inflammasome (Terlizzi *et al*., 2014; Colarusso *et al*., 2017), and because in Chapter 1 (Figure 10, 12) we demonstrated that Soot particles generated in very fuel-rich conditions (80-120 nm diameter) were able to trigger NLRP3/caspase-1-dependent inflammasome pathway in smokers-derived PBMCs, we hypothesized that the NLRP3 inflammasome could be involved in UFPs-induced IL-1-like cytokines release in PBMCs isolated from exacerbated COPD patients. However, we found that neither the canonical, caspase-1-, nor the non-canonical, caspase-8-dependent, NLRP3 inflammasome pathway were involved in the inflammatory response typical of exacerbated COPD patients after exposure to combustion-derived UFPs. The highlighted discrepancy in terms of inflammasome involvement in IL-1-like cytokines release after UFPs exposure between data reported in Chapter 1 and the data showed in this study may reflect the different nature and size of noxious particles in the air. Indeed, in the previous Chapter we used pyrolytic combustion-derived UFPs (80-120 nm diameter), instead here we used non-pyrolytic combustion-derived UFPs (2-40 nm diameter). Moreover,

the main difference between particles consists of the fuel we used to produce them. In this study UFPs were produced burning either a fossil fuel (ethylene) and a mixture with a biofuel (ethylene and 2,5-dimethylfuran), instead Soot particles as in Chapter 1 were obtained by burning acetylene.

It is to point out that this study, for the first time to our knowledge, focus the attention on the effect of particles mimicking air pollution in the exacerbated phase of COPD. Indeed, PBMCs isolated from stable COPD patients, that are patients who received corticosteroid treatment after an exacerbation event, were not responsive to combustion-generated UFPs in terms of IL-1-like cytokines release (De Falco *et al*., 2017). In accordance to our data, Di Stefano *et al*., (2014) reported that the inflammasome may be critical solely in COPD exacerbation in that they found no correlation between NLRP3, caspase-1 and IL-1β responses between smokers and stable COPD patients. An important issue to underlie is the role of oxidative stress as key mechanism in the onset and exacerbation of COPD (Colarusso *et al*., 2017). Although we did not demonstrate that Soot and NOC particles induce mtROS production, we observed that untreated exacerbated COPD-derived PBMCs produced higher mtROS levels compared to healthy subjects in the same conditions, probably due to mitochondrial dysfunction in exacerbated COPD. This data support that COPD patients show evidence of increased oxidative stress, suggesting that endogenous antioxidants may be insufficient to prevent oxidative damage from air pollution exposure. The consequences of augmented oxidative stress in the airway include increased transcription of inflammatory genes, increased protease activity, and increased mucus secretion, and may be of the causes of glucocorticoid resistance, all factors that may worse clinical picture in COPD patients (Bowler *et al*., 2014). Moreover, oxidative stress and following DNA damage are also reported among the causes of the NLRP3 inflammasome activation (Colarusso *et al*., 2017). A plausible explanation for the missing link between oxidative stress in exacerbated COPD patients and the

NLRP3 inflammasome activation after UFPs exposure might be that, as reported by Shimada *et al*., (2012), 8-OH-dG may bind with NLRP3 and may inhibit inflammasome activation.

In conclusion, these data demonstrate that combustion-derived UFPs (2-40 nm diameter) exposure in COPD patients during exacerbation phase of the disease triggers an IL-1-dependent inflammation which is NLRP3-/caspase-1- and caspase-8-independent. In order to better understand the effect of air pollution on the lung, we further investigated the effect of PM exposure by using a mouse model (please refer to Chapter 3).

CHAPTER 3

Air pollution induced caspase-1-independent lung immunesuppression in mice.

3.1 Introduction

Air pollution affects human health (Xia *et al*., 2016). Indeed, WHO recognizes air pollution as a risk factor for many diseases and comorbidities as demonstrated by air pollution-related 4.2 million deaths every year (who.int/health-topics/air-pollution#tab=tab_1); moreover, among human diseases, air pollution is a co-adjuvant for causing 1.8 million deaths for lung diseases. A strict relationship between indoor/outdoor air pollution and the development of respiratory disorders, including COPD and lung cancer, exists, mainly due to the presence of ultrafine particles (UFPs) that can be inhaled and deposit in the lower tract of the respiratory system (Valavanidis *et al*., 2013; Xia *et al*., 2016). Air pollutants consist of particulate matter (PM), ozone (O_3), nitrogen dioxide (NO_2), nitrogen oxides (NOx), sulfur dioxide (SO_2), and Volatile and Semivolatile Organic Carbon (VOC and SOC, respectively) (eea.europa.eu/publications/air-quality-in-europe-2018). Among air pollution components, PM has been shown to play a major role in human morbidity and mortality; PM is a mixture of solid and liquid particles including spores, endotoxin and suspended metals (Sayan & Mossman, 2016). PM can be defined according to different size ranges (PM10 and PM2.5, with smaller size than 10 μm or 2.5 μm, and ultrafine fraction with particles size smaller than 100 nm), to the number concentration or density of particles (which value increases remarkably in the smallest size fractions), and to the chemical composition (e.g., black carbon, organic compounds and heavy metals) (Cassee *et al*., 2013). Inhaled noxious particles from air pollution

are able to penetrate deeply in the lung based on their size, affecting lung resident and circulating cells by inducing chronic inflammation (Xia *et al*., 2016). PM10 and PM2.5 generally deposit in the nasopharyngeal and laryngeal region, and poorly deposit in the alveolar region; instead UFPs can penetrate deeper into the alveolar region due to their smaller size (Oberdoster *et al*., 2005). Based on this, UFPs may represent the component of air pollutants that can cause adverse health effects, especially for the lung where, by depositing into the alveoli, may lead to impairment of its clearance by alveolar macrophages with ensuing pulmonary diseases, such as COPD or lung cancer. In Chapter 2, we demonstrated that UFPs with range size of 2-40 nm triggered an IL-1-dependent inflammation which was NLRP3-/caspase-1- and caspase-8-independent in PBMCs obtained from COPD patients undergoing an exacerbation status. Because the latter *in vitro* data did not give us the opportunity to investigate the effects of environmental pollutants in the respiratory tract, in order to figure out the effect of PM exposure onto the lung immune microenvironment, in this Chapter we describe the effects of environmental pollution by using a mouse model of PM and UFPs exposure.

3.2 Materials and Methods

3.2.1 Mice

Female specific pathogen-free C57Bl/6 mice (6–8 weeks of age) (Charles River Laboratories, Lecco, Italy) were fed with a standard chow diet and maintained in specific pathogen-free conditions at the animal care unit of Department of Pharmacy, University of Salerno. All animal experiments were performed under protocols that followed the Italian (D.L. 26/2014) and European Community Council for Animal Care (2010/63/EU). This study was carried out in strict accordance with the recommendations in the Guide for the Care and Use of Laboratory Animals of the Istituto Nazionale per la Salute. The protocol was approved by the Committee on the Ethics of Animal Experiments Health Ministry with the approval number 985/2017.

3.2.2 PM Exposure Experimental Protocol

In order to understand the molecular and cellular mechanisms underlying the establishment of respiratory disease caused by air pollution exposure, mice were daily intratracheally (i.t.) instilled, under anesthesia (Isoflurane 2%), with 3 different kind of particles mimicking air pollution, that are Soot (90 ng/10 μL/mouse), PM1 (25 ng/10 μL/mouse) or PM10 (30 ng/10 μL/mouse) (Figure 18). Preparation procedure and characteristics of Soot and PM samples are reported in the paragraph 3.2.3. The choose of the working dose for each particle was done according to preliminary data during which mice were treated in a dose-dependent manner and showed lung inflammation after treatments.

To evaluate the possible involvement of the canonical, caspase-1-dependent, inflammasome pathway in the establishment of PM exposure-induced inflammation, Ac-YVAD-cmk (YVAD, 10 μg/mouse), a caspase-1 inhibitor, was intraperitoneally (i.p.) injected every 3 days, as already reported (Zhang *et al*., 2016). Mice were divided in groups as follows:

1. Sham-PBS treated mice, n = 5;

2.Vehicle, mice treated with DMSO 0.1%, which was used as vehicle to dissolve Soot, PM1 and PM10, n = 8;

3. Soot, mice i.t. instilled with Soot, n = 8;

4. Soot+YVAD, mice i.t. instilled with Soot and i.p. injected with YVAD, n = 8;

5. PM1, i.t. instilled with PM1, n = 8;

6. PM1+YVAD, mice i.t. instilled with PM1 and i.p. injected with YVAD, n = 8;

7. PM10, mice i.t. instilled with PM10, n = 8;

8. PM10+YVAD, mice i.t. instilled with PM10 and i.p. injected with YVAD, n = 8.

For time-course experiment, mice were sacrificed at different time points (8, 14, and 28 days, from first instillation of Soot, PM1 or PM10) in order to study the pulmonary susceptibility to particles which mimic air pollution.
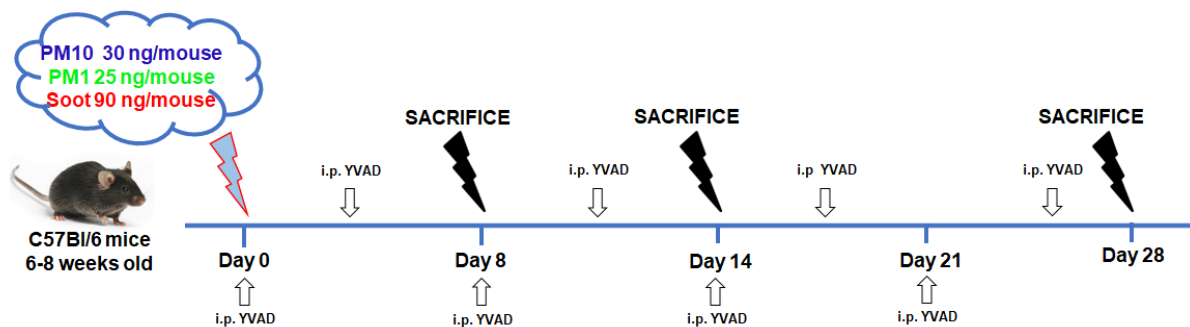
Figure 18. *Experimental plan for PMx-treated mice.*

C57Bl/6 mice (female, 6-8 weeks of age) were intratracheally (i.t.) instilled daily for 28 days with three different air pollutants: PM10 (30 ng/mouse) or PM1 (25 ng/mouse), both collected from atmosphere, or Soot (90 ng/mouse), collected from a laboratory flame. Mice were sacrificed at different time points: 8, 14 and 28 days after the first PMx instillation. In another set of experiment, Ac-YVAD-cmk (YVAD, 10 µg/mouse), a pharmacological caspase-1 inhibitor, was intraperitoneally (i.p.) injected every three days starting from the first day of PMx exposure.

BAL was collected using 0.5 mL of PBS containing 0.5 mM EDTA to measure pro- and anti-inflammatory cytokines levels. Right lung lobes were collected and used after digestion with 1 U/mL of collagenase (Sigma Aldrich, Rome, Italy) for FACS analysis and to perform ELISAs analysis. Left lung lobes were embedded into OCT medium to perform Periodic acid/Alcian blue/Schiff staining (PAS) staining to evaluate lung inflammation.

3.2.3 Preparation and Characteristics of particles for in vivo experiment

Soot samples were collected from a laboratory flame, which was run in fuel-rich conditions feeding an ethylene/air mixture with an equivalence ratio $\Phi = 2.0$ at atmospheric pressure. PM1 and PM10 samples were collected by means of an automatic outdoor station for continuous atmospheric particulate sampling (Tecora Skypost PM HV). The outdoor station was operated in a crowed area characterized by high automotive traffic during 2018 fall season and allowed to collect daily samples of PM on filters. PM was later suspended in DMSO, following a sonication-assisted solvent extraction. Elemental composition and size range of the Soot, PM1 and PM10 is reported in Table 3. Particles morphology and chemical composition were determined by Scanning Electron Microscopy analysis performed by a Hitachi TM3000 SEM, coupled with a built-in energy dispersive Xray detector SwiftED3000.

Table 3. *Characteristics of PM10, PM1 and Soot Particles used for in vivo experiments.*

	PM1	PM10	Soot
Particle size	< 1 mm	< 10 mm	< 200 mm
C %	87,5	77	79,5
H %	n.d.	n.d.	19,5
O %	11,5	19,6	< 1
S %	0,8	0,5	n.d.
K %	0,2	0,25	n.d.
Na %	n.d.	0,3	n.d.
Mg %	n.d.	0,3	n.d.
Al %	n.d.	0,3	n.d.
Ca %	n.d.	0,75	n.d.
Fe %	n.d.	0,25	n.d.
Si %	n.d.	0,75	n.d.

3.2.4 Cytokine measurements

IL-1α, IL-1β, IL-33, IL-13, TNF-α, IFN-γ, and IL-10 were measured in BAL or lung homogenates samples. The assays were performed using commercially available ELISA kits (eBioscience, CA, USA). Cytokines levels in BAL samples were expressed as pg/mL, whereas in lung homogenates as pg/mg protein.

3.2.5 Flow Cytometry Analysis

In order to investigate the immune cells infiltrated into the lung of PMx exposed mice, we performed flow cytometry analysis (BD FacsCalibur Milan, Italy). After lungs digestion, cell suspensions were passed through 70 μm cell strainers, and red blood cells were lysed. Lung cell suspensions were stained with the following antibodies: CD11c, CD11b, Gr-1, F4/80, MHC II, CD80, Arginase I, CD4, CD25, and FoxP3.

3.2.6 PAS Staining

To evaluate lung inflammation degree following PMx exposure of mice, left lung lobes were cut into 7 μm-thick cryosections which were stained by using PAS staining (Sigma Aldrich, Milan Italy) which was performed according to the manufacturer's instructions to detect glycoprotein (Sorrentino *et al*., 2015). The degree of inflammation was scored by blinded observers. PAS+ cryosections were graded with scores 0 to 4 to describe low to severe lung inflammation as follows: 0: <5%; 1: 5 to 25%; 2: 25–50%; 3: 50–75%; 4: <75% positive staining/total lung area.

3.2.7 Airway Responsiveness Measurements

To investigate the possible bronchial dysfunction 28 days post PMx treatment, we performed airway responsiveness measurements in collaboration with Professor Cirino's group (Department of Pharmacy, University of Naples "Federico II", Naples, Italy). Bronchial rings

(1–2 mm length) were cut and placed in organ baths mounted to isometric force transducers (Type 7006, Ugo Basile, Comerio, Italy) and connected to a Powerlab 800 (AD Instruments, Ugo Basile, Comerio, Italy). Rings were initially stretched until a resting tension of 0.5 g was reached and allowed to equilibrate for at least 30 min. To evaluate bronco-contraction, in each experiment bronchial rings were challenged with carbachol in a concentration-dependent manner (1 pM−10 μM); instead, in order to evaluate bronco-dilation, a cumulative concentration-response curve to salbutamol (10 pM−30 μM) on a stable tone, produced by 1 μM of carbachol, was performed.

3.2.8 Statistical Analysis

Data are reported as violin plots indicating median ± interquartile range or as mean ± SEM. Statistical differences were assessed with ONE-way analysis of variance (ANOVA) and TWO-way ANOVA followed by multiple comparison post-tests as appropriate. Mann–Whitney U-test was performed where appropriate. *p* values less than 0.05 were considered significant.

3.3 Results

3.3.1 The exposure to PM led to the development of lung inflammation in mice.

Because toxicological effects of PM are connected both to different size ranges and composition, we exposed mice to 3 different fractions of PM: PM10, which size is around 10 μm; PM1, which size is around 1 μm; Soot, which size is less than 100 nm and represents the organic carbonaceous component of PM1 and PM10. PAS staining performed on left lung lobes of PM-exposed mice showed that the i.t. instillation of PM10 triggered lung inflammation both at 8 and 14 days post-treatment, but not at 28 days after the first i.t. (Figure 19A, 19B blue line) which showed an inflammatory pulmonary milieu comparable to the Vehicle group (DMSO, 0.1%) (Figures 19A, 19B black line). Similarly, PM1 instillation led to a state of pulmonary inflammation at 14 and 28 days post-treatments (Figure 19A, 19C green line), implying a delayed lung inflammation compared to PM10. Mice i.t. instilled with Soot 90 ng/mouse showed a strong hyperplasia around bronchi, which was correlated to higher mucus production at solely 8 and 28 days post-instillation, but not at 14 days where the structural changes were not visible and the state of inflammation seemed to be restored (Figure 19A, 19D red line).
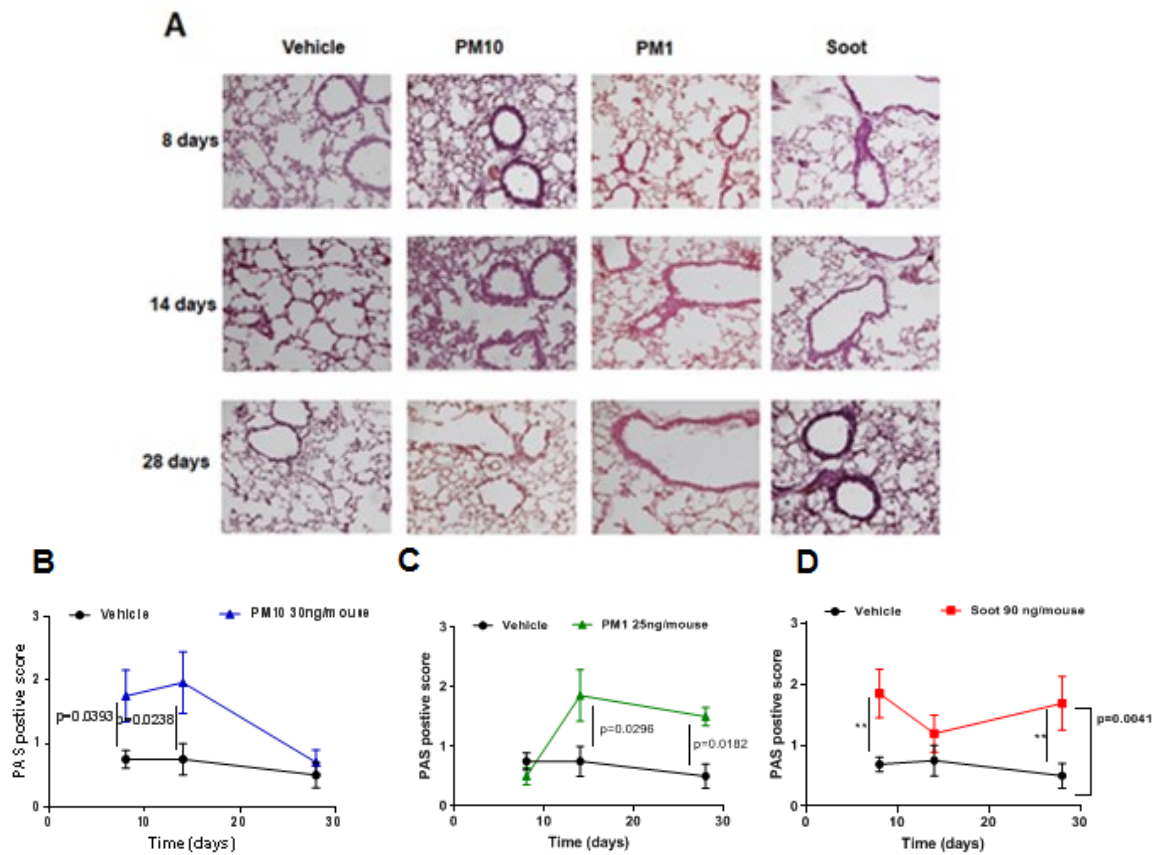
Figure 19. *The exposure to PMx induced lung inflammation in vivo-treated mice.*

Mice were intratracheally (i.t.) daily instilled with PM10 (30 ng/mouse), PM1 (25 ng/mouse), or Soot (90 ng/mouse) and sacrificed at 8, 14 and 28 days after the first exposure. Representative images of PAS staining performed on lung cryosection (**A**). Quantitative analysis of PAS staining showed increased lung inflammation after PM10 (**B**), PM1 (**C**), and Soot (**D**) treatment. Data are represented as mean ± SEM (n = 8). Statistically significant differences were determined according to TWO-way ANOVA followed by Tukey's post-hoc test.

To prove any bronchial dysfunction after PMx exposure, we assessed bronchial reactivity to carbachol and salbutamol *in vitro*, in bronchi collected after 28 days of treatment. We found that bronchi of PM10- and PM1-treated mice showed a hyper-reactivity to carbachol, a clear evidence of altered airway responsiveness (Figure 20A and 20B, respectively) compared to the Vehicle group. Instead, we did not find any alteration in airway responsiveness in Soot-treated mice compared to the Vehicle group (Figure 20C). In contrast to latter data on the reactivity to carbachol, the data from bronchial dilation by salbutamol, showed that bronchi of both mice i.t. instilled with PM10 (Figure 20D) and PM1 (Figure 20E) did not have any statistical alteration in bronco-dilation; in contrast, bronchi from mice i.t. instilled with Soot showed a strong reduction of bronco-dilation under salbutamol challenge compared to the Vehicle group (Figure 20F, red vs black line).
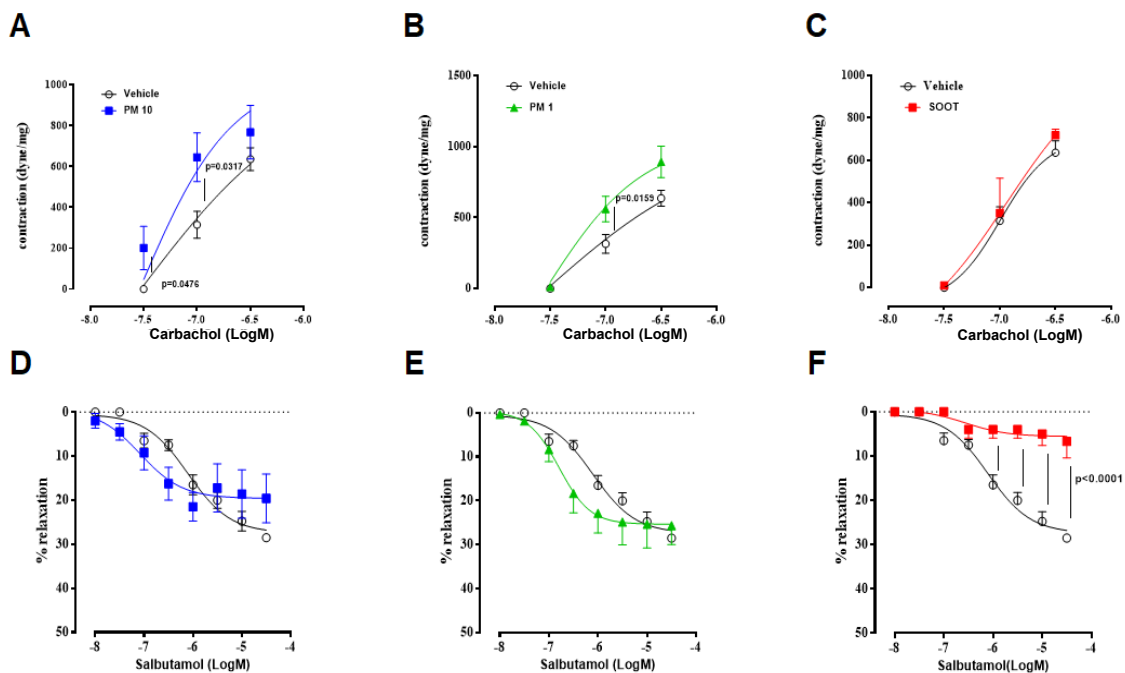

Figure 20. *The exposure to PMx altered bronchial responsiveness*.
Bronchi from mice exposed to PM10 (30 ng/mouse, blue line), PM1 (25 ng/mouse, green line), and Soot (90 ng/mouse, red line) were tested to carbachol or salbutamol. PM10 (**A**) and PM1 (**B**) treatment increased carbachol responsiveness, contrarily Soot treatment did not modify carbachol responsiveness (**C**). On the other hand, bronchial dilation by salbutamol was not altered in PM10- (**D**) and PM1- (**E**) treated mice, instead Soot-treated mice showed significantly reduced bronchial dilation (**F**). Data are represented as mean ± SEM (n = 8). Statistically significant differences were determined according to TWO-way ANOVA followed by Tukey's post-hoc test.

These data suggest that the exposure to PMx induce lung inflammation in mice, although in a different way in that all tested particles induced mucus hypersecretion (PAS$^+$ staining) but solely the smallest component, Soot (size ranging from 20–40 nm, typical of the primary Soot particles, to 100–200 nm typical of the chain-like aggregates) alter the physiological bronchial dilation, likely by damaging the lung epithelium.

3.3.2 PM exposure induced lung immunesuppression in mice.

Because the exposure to inhaled irritants can trigger inflammatory cells by changing their phenotype (Colarusso *et al.*, 2017), we went on by analyzing lung immune microenvironment in mice exposed to PM10, PM1 and Soot by means of flow cytometry. We evaluated the recruitment of the following cell populations into lung: dendritic cells (DCs), identified as CD11c^{high} CD11b^{int}; macrophages, identified as CD11c^{int} CD11b^{high} F4/80$^+$; myeloid-derived suppressor cells (MDSCs), identified as CD11b^{high} Gr-1$^+$; T regulatory cells (Treg,), identified as CD4$^+$ CD25$^+$ FoxP3$^+$.

The instillation of PM10 significantly increased the recruitment of DCs at 8 days (Figure 21A, blue line), of macrophages at 14 days (Figure 21D, blue line), of MDSCs, at 14 and 28 days (Figure 21G, blue line) and of Treg at 14 and 28 days (Figure 21J, blue line) compared to the Vehicle and Sham group (Figure 21, black and gray line, respectively). Similarly, in PM1 treated mice we found no differences in the number of DCs (Figure 21B, green line) compared to the Vehicle and Sham group (Figure 21B, black and gray line, respectively), a significant increase in the percentage of recruited macrophages at 14 days (Figure 21E, green line), of MDSCs at 14 days (Figure 21H, green line) and of Treg at 14 and 28 days post-instillation (Figure 21K, green line) compared to the Vehicle group (Figure 21, black line).

Surprisingly, we found similarities between Soot particles and PM10/PM1, in that Soot instillation significantly increased the recruitment of DCs (Figure 21C, red line) at 8 days, of macrophages at 14 days (Figure 21F, red line), of MDSCs at 14 days (Figure 21I, red line) and of Treg at 28 days (Figure 21L, red line) compared to the Vehicle and Sham group (Figure 21, black and gray line, respectively).
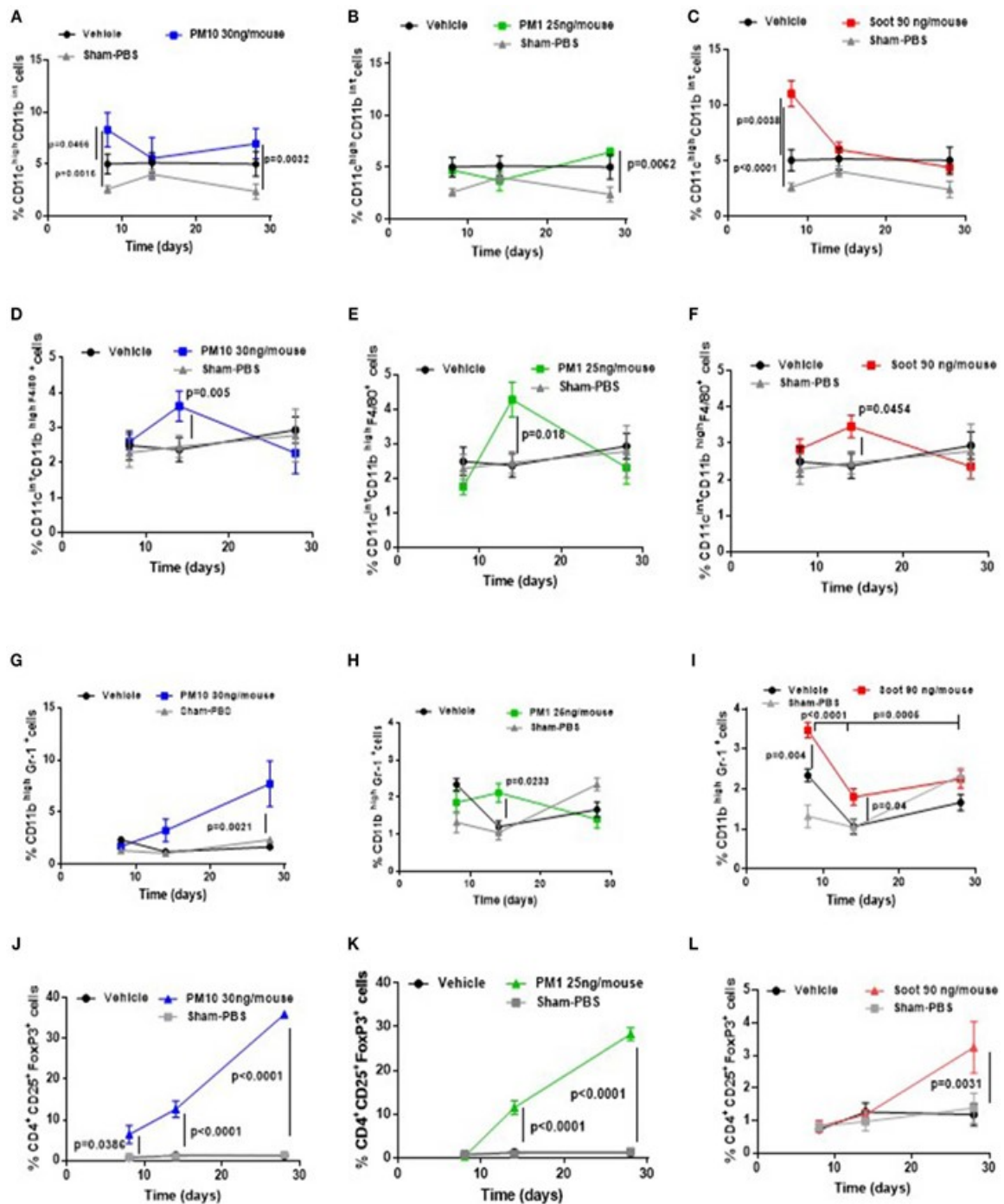
Figure 21. *Exposure to PMx altered lung immune microenvironment in a time-dependent manner*.

Lungs from mice intratracheally (i.t) exposed to PM10 (30 ng/mouse, blue line), PM1 (25 ng/mouse, green line), and Soot (90 ng/mouse, red line) were digested with collagenase and flow cytometry analysis was performed. PM10 (**A**) and Soot (**C**), but not PM1 (**B**) induced higher recruitment of DCs at early time point. Similarly, PM10 (**D**), PM1 (**E**), and Soot (**F**) induced higher recruitment of macrophages at 14 days. Higher recruitment of MDSCs was observed after PM10 (**G**), PM1 (**H**), and Soot (**I**) treatment. This effect was associated to higher presence of Treg after PM10 (**J**), PM1 (**K**), and Soot (**L**) exposure. Data are represented as mean ± SEM (n = 8). Statistically significant differences were determined according to TWO-way ANOVA followed by Tukey's post-hoc test.

In order to better understand the role of recruited cells in lung microenvironment after PMx exposure, we moved on by analyzing the phenotype of innate immune cells by evaluating the expression of the costimulatory molecule CD80 and cell surface MHC II on both DCs and macrophages. Based on previous data, we focused our attention on Soot, in that it seemed to play the most relevant effect (pulmonary inflammation and reduced airway responsiveness to salbutamol, as shown in Figure19D and 20F, respectively).

The percentage of CD80$^+$ DCs (Figure 22A), but not of MHC II$^+$ DCs (Figure 22B) was high in Soot-treated mice. To note, Sham mice had very low expression of CD80 on DCs than the Vehicle group (Figure 22A). Similarly, we found that macrophages showed higher expression of CD80 (Figure 22C) but lower levels of MHC II (Figure 22D) in Soot-treated mice compared to the Vehicle and Sham group.

Because of lung macrophages assume a different phenotype according to the environment they encounter, to better define macrophages phenotype and the role of MDSCs in this context, we evaluated the expression of Arginase I (Arg I), enzyme involved in inflammation-induced lung immunesuppression (Steggerda *et al*., 2017). We observed, in Soot instilled mice, a significant increase in immunesuppressive Arg I$^+$ macrophages and MDSCs compared to Vehicle group (Figure 22E, 22F, respectively). Similarly, PM10- and PM1-treated mice showed an higher expression of the immunesuppressive Arg I on both macrophages (Vehicle: 27.1 ± 2.60 vs. PM10: 48.5 ± 3.60 or PM1: 42.0 ± 3.04) and MDSCs (Vehicle: 32.1 ± 1.16 vs. PM10: 59.3 ± 1.43 or PM1: 55.2 ± 1.06) respect to the Vehicle group.
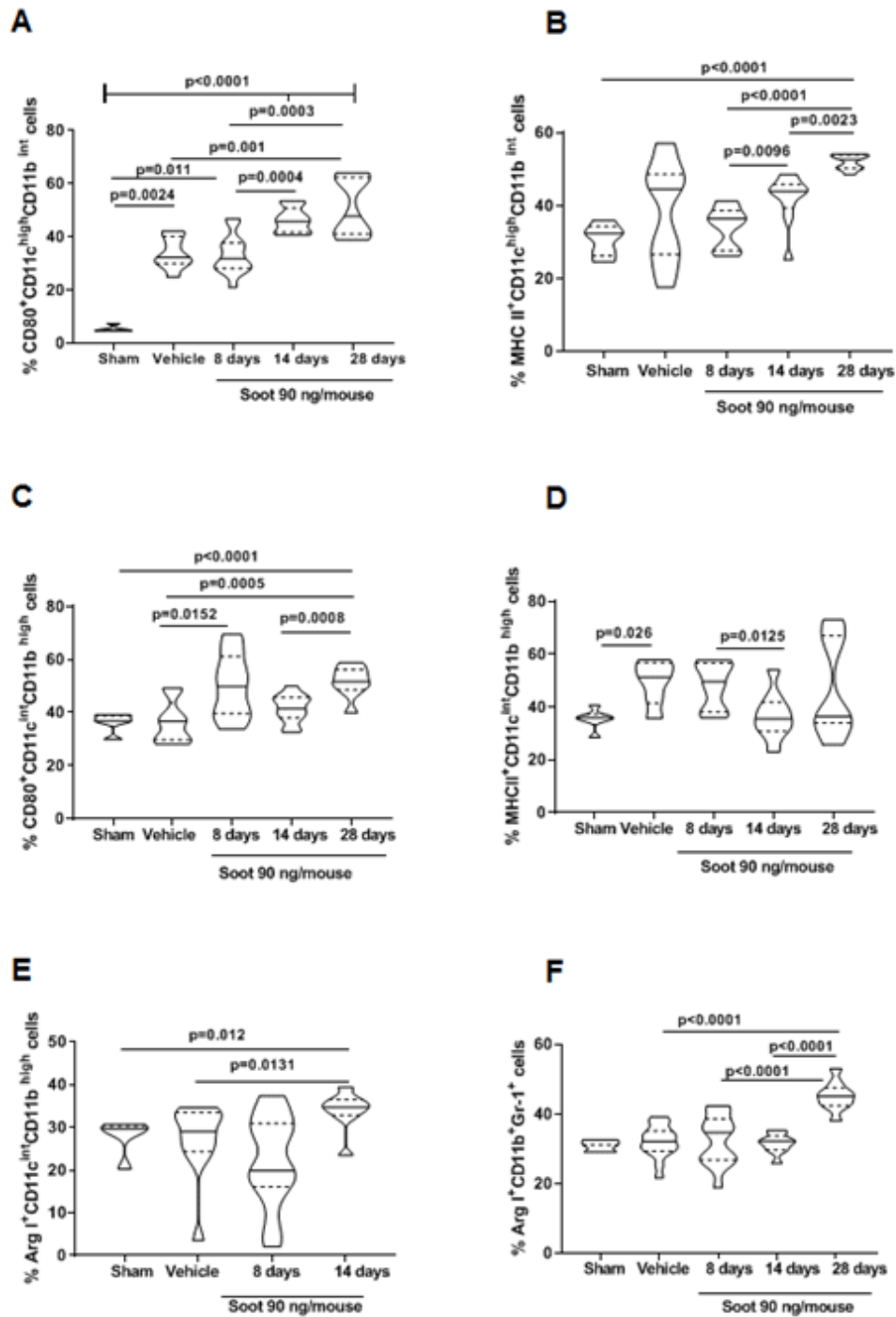
Figure 22. *Exposure to Soot altered the innate phenotype of immune cells recruited into lung*.

Soot-treated mice showed higher levels of CD80 (**A**), but not MHC II (**B**) on DCs. Similar effect was observed for macrophages regarding CD80 (**C**) but not MHC II (**D**) expression. Macrophages (**E**) and MDSCs (**F**) recruited to the lung of Soot-treated mice showed significantly higher levels of Arginase I. Data are presented as violin plots showing median $\pm$ interquartile range (n = 8). Statistically significant differences were determined according to ONE-way ANOVA followed by Dunn's post-hoc test.

To improve the meaning of the previous data and to better understand the immune microenvironment induced by PMx exposure, we performed pro- and anti-inflammatory cytokines measurements in lung homogenates or in BAL samples. IL-1α and IL-33 levels were evaluated in lung tissue homogenates in that they were undetectable in BAL samples, most probably due to a limit of the ELISA kits sensitivity; whereas IL-1β, IL-13, IL-10, TNF-α and INF-γ levels were tested in BAL.

We found a not significant upward trend of IL-1α levels at 14 days in lung homogenates from Soot-treated mice (Figure 23A, red line), whereas PM10- (Figure 23B, blue line) and PM1- (Figure 23C, green line) treated mice showed a significant increase in this cytokine at later time points. These differences could be explained by the different composition of particles used, as the presence of metals and oxides in addition to carbonaceous components. The levels of IL-1β in BAL samples were higher at earlier time points (8 and 14 days) both in Soot- (Figure 23D, red line), PM10- (Figure 23E, blue line) and PM1- (Figure 23F, green line) treated mice respect to Vehicle group (Figure 23, black line). In the same way, the levels of IL-33 were higher at earlier time points in Soot-treated mice compared to the Vehicle group (Figure 23G, red vs black line); as far as PM10- (Figure 23H, blue line) and PM1- (Figure 23I, green line) treated mice we observed that IL-33 levels highly augmented starting from 8 days up to 28 days of treatment, probably due to the presence of non-carbonaceous components.

Figure 23. *IL-1α, IL-1β and IL-33 release in PMx-treated mice*.

Mice were intratracheally (i.t) instilled with Soot (90 ng/mouse, red line), PM10 (30 ng/mouse, blue line), and PM1 (25 ng/mouse, green line). IL-1α (**A-C**) and IL-33 (**G-I**) were analyzed in lung homogenates obtained from PMx-treated mice, wheares IL-1β (**D-F**) were tested in the BAL of PMx-treated mice. Data are represented as mean ± SEM (n = 8). Statistically significant differences were determined according to TWO-way ANOVA followed by Tukey's post-hoc test.

Moreover, we found that solely Soot treatment was able to induce the secretion of IL-13 in lung homogenates compared to the Vehicle group (Figure 24A, red vs black line), in that we did not observe the same effect in PM10 (Figure 24B, blue line) and PM1 group (Figure 24C, green line). Based on these data we could speculate that the different levels of IL-13 in the three groups reflect both the reduced bronchial dilation observed in Soot group (Figure 20F), and the increased bronchial reactivity to carbachol observed in PM10 and PM1 groups (Figure 20A and 20B). We observed any difference in terms of TNF-α levels detected in the BAL collected from of Soot-, PM10- and PM1-treated (Figures 24D, 24E and 24F, respectively) mice. Similarly, no differences were found in terms of and IFN-γ levels in Soot and PM10-treated mice (Figure 24G and 24H, respectively); instead IFN-γ levels significantly reduced in PM1-treated mice compared to Vehicle group (Figure 24I, green vs black line).
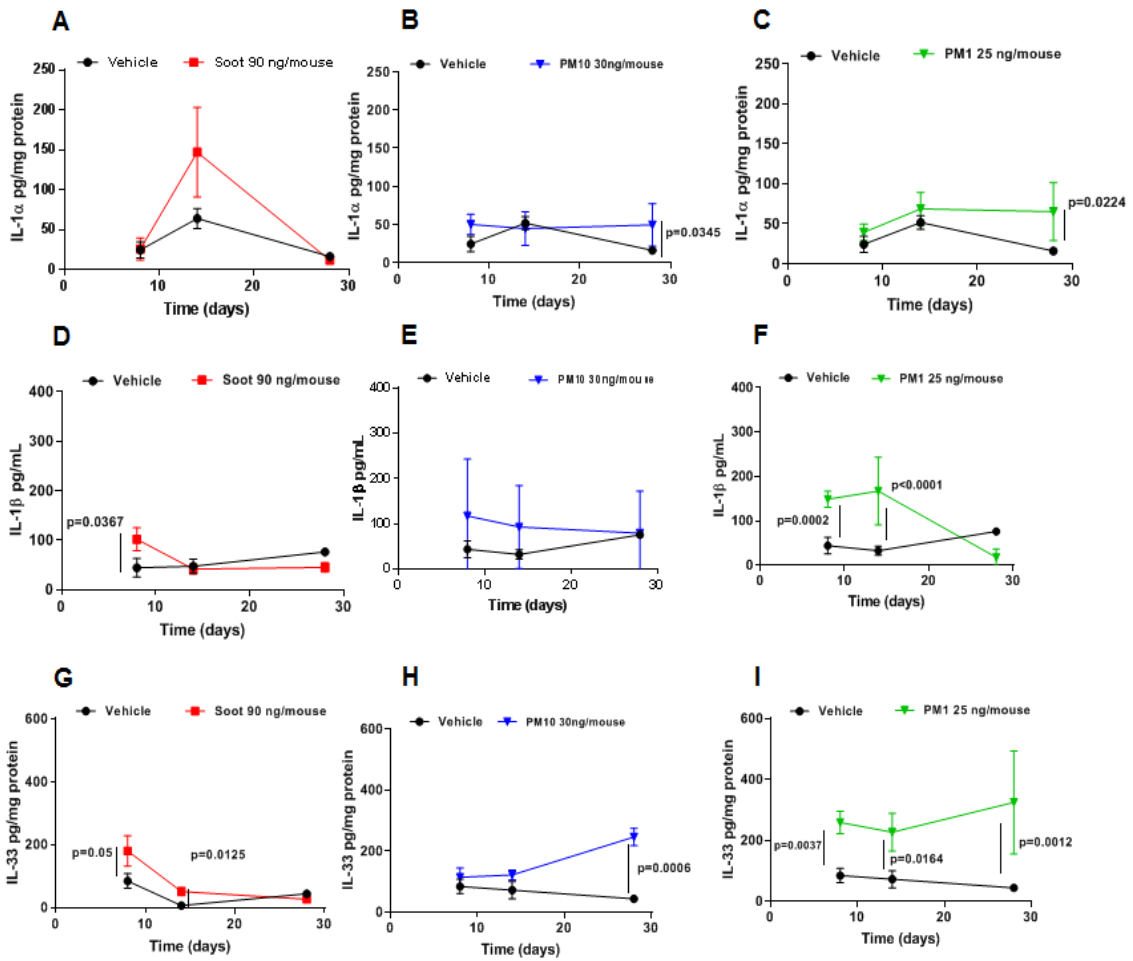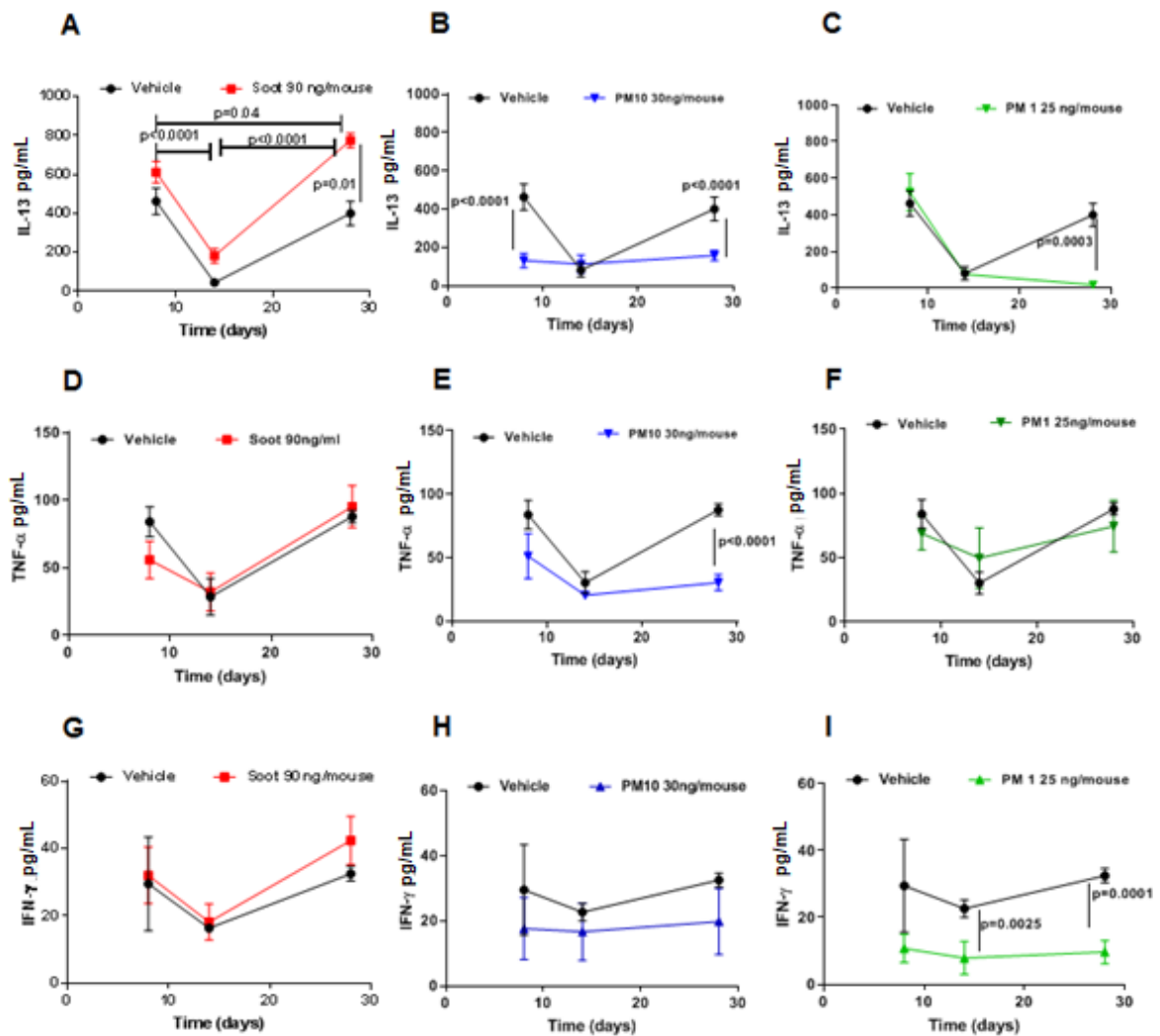
Figure 24. *IL-13, TNF-α and IFN-γ release in PMx-treated mice*.

Mice were intratracheally (i.t) instilled with Soot (90 ng/mouse, red line), PM10 (30 ng/mouse, blue line), and PM1 (25 ng/mouse, green line). IL-13 (**A-C**), TNF-α (**D-F**) and IFN-γ (**G-I**) were analyzed in the BAL of PMx-treated mice by means of ELISAs. Data are represented as mean ± SEM (n = 8). Statistically significant differences were determined according to TWO-way ANOVA followed by Tukey's post-hoc test.

More importantly, we observed that the levels of IL-10, an immunesuppressive cytokine (Mittal *et al.*, 2015), in the BAL of mice treated with Soot (Figure 25A, red line), PM10 (Figure 25B, blue line) and PM1 (Figure 25C, green line), were significantly higher compared to Vehicle group (Figure 25, black lines), further confirming the immunesuppressive lung microenvironment due to PMx exposure.
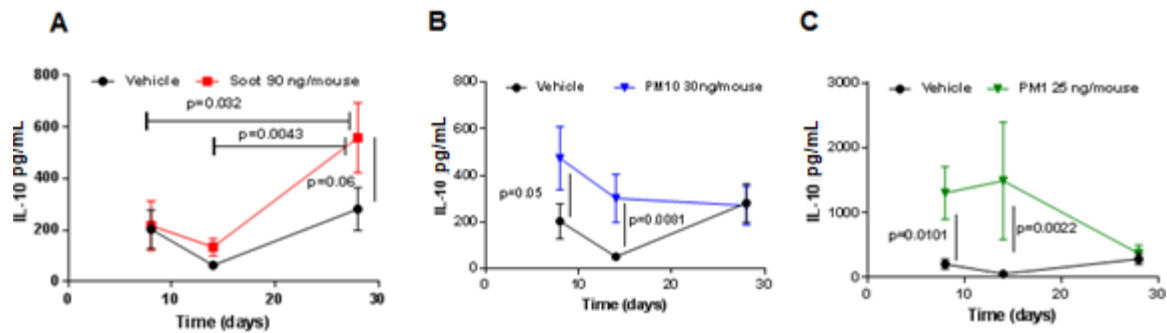
Figure 25. *PMx exposure in vivo led to high release of IL-10 into lung*.

Mice were intratracheally (i.t) instilled with Soot (90 ng/mouse) (**A**, red line), PM10 (30 ng/mouse) (**B**, blue line), and PM1 (25 ng/mouse) (**C**, green line). IL-10 levels were analyzed in the BAL of PMx-treated mice by means of ELISA. Data are represented as mean ± SEM (n = 8). Statistically significant differences were determined according to TWO-way ANOVA followed by Tukey's post-hoc test.

3.3.3 Caspase-1 was not involved in Soot-induced lung immunesuppression in mice.

In order to clarify the mechanisms underlying the establishment of the lung immunesuppressive microenvironment in mice exposed to PMx, we focused our attention on caspase-1, key enzyme in the activation cascade of the inflammasome (Terlizzi *et al.*, 2014). Therefore, we moved on by using a specific pharmacological inhibitor, Ac-YVAD-cmk (YVAD, 10 µg/mouse) in our *in vivo* model of PMx exposure, as reported in Materials and Methods (paragraph 3.2.2). PAS staining performed on left lung lobes of Soot-exposed mice i.p. injected with YVAD showed that the inhibition of caspase-1 led to a reduction of bronchial hyperplasia and mucus production at 8 days, but not at 14 days, after Soot instillation (Figure 26A, 26B).

To better define the possible role of caspase-1 in our mouse model of PMx exposure, we went on by analyzing the immune lung microenvironment when caspase-1 was inhibited during Soot instillation. We found that the percentage of DCs into the lung of Soot-treated mice significantly decreased after caspase-1 inhibition at solely 8 days (Figure 26C); moreover we found that caspase-1 inhibition did not alter macrophages (Figure 26D) and MDSCs (Figure 26E) recruitment neither at 8 and 14 days after Soot instillation.
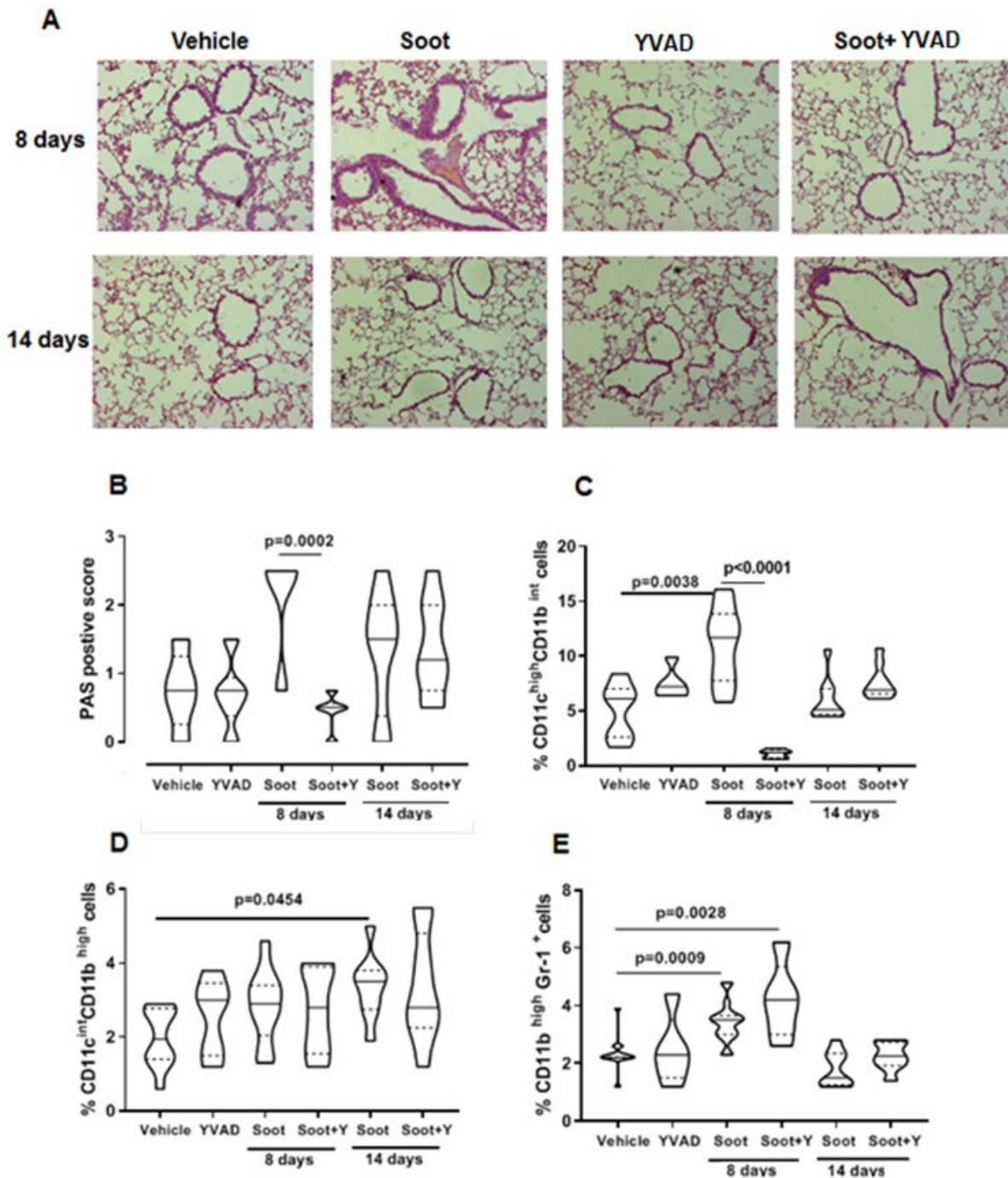
Figure 26. *Effect of Ac-YVAD-cmk (YVAD), an inhibitor of caspase-1, on Soot-induced lung inflammation in mice.*

The inhibition of caspase-1 by means of Ac-YVAD-cmk (YVAD, i.p. 10 μg/mouse/twice/week) reduced lung inflammation, evaluated by PAS staining, in mice exposed to Soot at the sole early time point (8 days) (**A**, **B**). In support, DCs (**C**), macrophages (**D**), and MDSCs (**E**) were still recruited to the lung in Soot+YVAD-treated mice after 14 days. Data are presented as violin plots showing median ± interquartile range (n = 8). Statistically significant differences were determined according to TWO-way ANOVA followed by Tukey's post-hoc test.

It is to underlie that, similarly to what we observed in Soot-treated mice (Figure 26A, 26B), we found a significant decrease of PAS positive staining in PM1+YVAD-treated mice compared to PM1 and Vehicle treated mice (Figure 27A, dark green vs green and black line) at 14 days, and a downward trend of PAS positive staining in PM10+YVAD-treated mice compared to PM10 and Vehicle treated mice (Figure 27B) at 8 and 14 days.
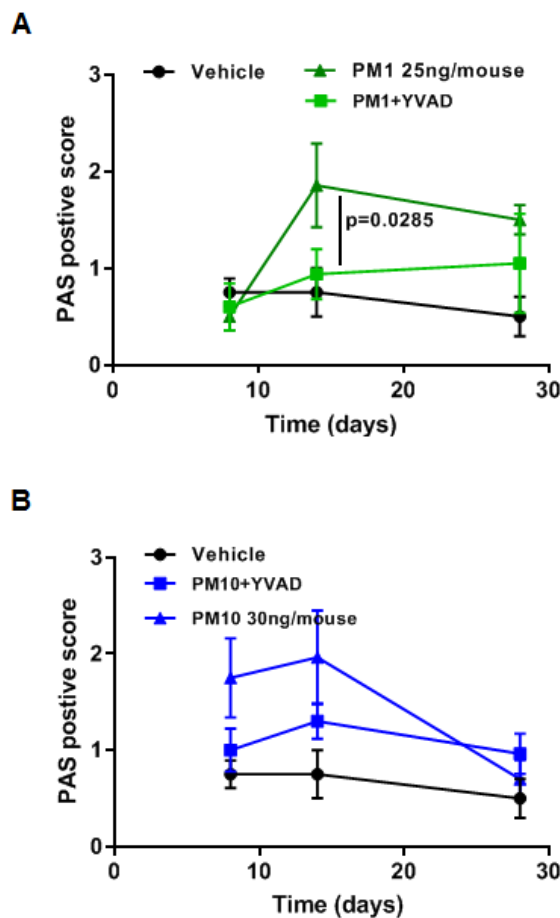
Figure 27. *Effect of Ac-YVAD-cmk (YVAD), an inhibitor of caspase-1, on PM1- and PM10-induced lung inflammation in mice.*
PAS positive staining analyzed in a time dependent manner in PM1- (**A**) and PM10- (**B**) treated mice in the presence or not of the caspase-1 inhibitor, Ac-YVAD-cmk (YVAD, i.p. 10 μg/mouse/twice/week). Data are represented as mean ± SEM (n = 8). Statistically significant differences were determined according to TWO-way ANOVA followed by Tukey's post-hoc test.

These data were consistent with results obtained by means of ELISAs, which highlighted that YVAD treatment did not alter the release of IL-1α, IL-33 and IFN-γ (Figures 28A, 28C, 28D, respectively) induced by Soot treatment. However, we detected that Soot-induced IL-1β release (Figure 28B) was lower at the sole 8 days when caspase-1 was inhibited (Soot+YVAD group).
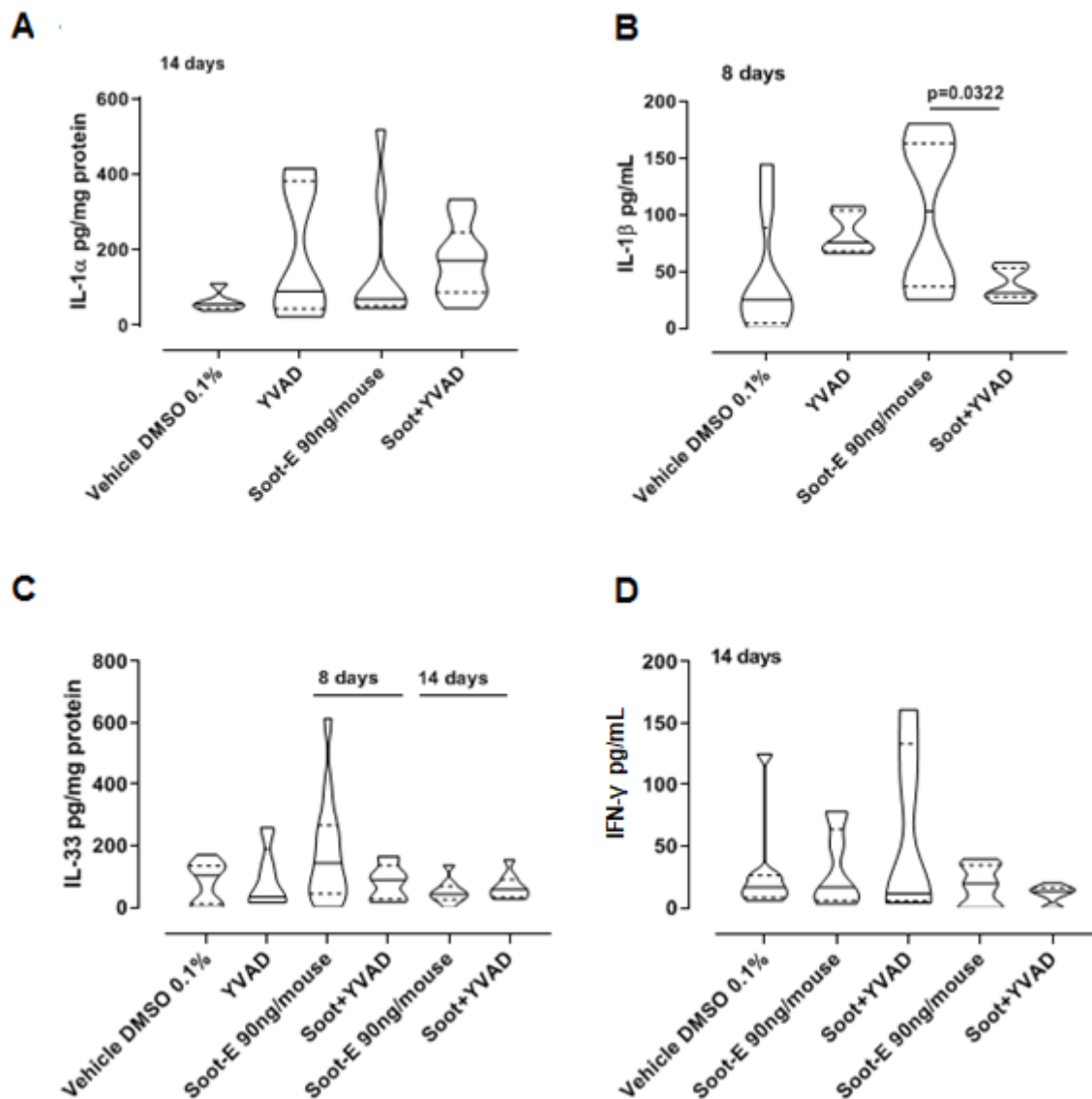
Figure 28. *Effect of caspase-1 inhibition on Soot-induced cytokines production in mice.* IL-1α (**A**) and IL-33 (**C**) were analyzed in lung homogenates obtained from Soot±YVAD-treated mice. IL-1β (**B**) and IFN-γ (**D**) were tested in the BAL of Soot-treated mice in the presence of Ac-YVAD-cmk (YVAD, i.p. 10 μg/mouse/twice/week). Data are represented as mean ± SEM (n = 8). Statistically significant differences were determined according to Mann Whitney U-test.

3.4 Conclusions

In this Chapter we show data that demonstrate that the exposure to particles that mimic air pollution leads to a state of latent lung inflammation in mice, associated to the establishment of lung immunesuppressive microenvironment, populated by MDSCs and characterized by IL-10, and by the alteration of the bronchial tone. This scenario is not altered by the pharmacological inhibition of caspase-1.

In recent reports air pollution was associated to COPD establishment and comorbidities (Song *et al*., 2014; Xia *et al*., 2016). In addition, it should be considered that cigarette smoking is the main cause of COPD onset (who.int/gard/publications/Risk%20factors.pdf). However, if we consider that only 15-20% of smokers develop COPD (Eisner *et al*., 2010), air pollution may represent another key environmental risk factor for the pathogenesis of this pulmonary disease. Here we show that PM10, PM1 and Soot particles led to an increased lung recruitment of innate immune cells in their immunesuppressive phenotype in mice. Indeed, DCs and macrophages showed higher CD80 but lower MHC II levels. Concomitantly, macrophages and MDSCs counted higher levels of Arginase I. Arginase I catalyzes the hydrolysis of the amino acid L-Arginine to produce L-ornithine and urea and its expression defines an immunesuppressive signature in myeloid cells (Steggerda *et al*., 2017) in that Arginase I positive innate immune cells educate Th2- or Treg to exert their anti-inflammatory and tolerogenic activity. Therefore, exposure to air pollution increased the tolerogenic DCs which were not able to present antigens, and together with Arginase I positive macrophages, favored the establishment of an immunesuppressive microenvironment. In this context, immunesuppression overtakes immunostimulatory activity of innate immune cells which, in their tolerogenic phenotype, can facilitate the immunesuppressive arm of the adaptive immune system (Sorrentino *et al*., 2015), making the lung more susceptible to the harmful stimuli and, potentially, to the establishment of respiratory disorders, such as COPD, fibrosis and, even worse, cancer. Therefore, this *in vivo* study, for the first time, to our knowledge, highlights that

the exposure to particles mimicking air pollution can favor the establishment of an immunesuppressive environment in the airways of mice which may promote to the onset of lung disorders.

Moreover, in tune with the data showed in Chapter 1 and 2, we find that the nature of different PM instilled into mice plays a critical role for lung function. As reported in Table 3, the main difference between PM10, PM1 and Soot is the presence of inorganic components (metals, sulfur and nitric oxide). We believe that the most relevant pulmonary effect is revealed by Soot which is critical in the induction of lung inflammation and alter lung physiology, especially the airway responsiveness. Indeed, the sole Soot, which represents the carbonaceous component of PM10 and PM1 and has the smallest range size, led to a reduction of bronchodilation following the challenge with Salbutamol, a β2 agonists used for the pharmacological therapy in COPD patients (goldcopd.org/wp-content/uploads/2018/11/GOLD-2019-POCKET-GUIDE-FINAL_WMS.pdf). Although our study does not prove that small noxious particles in the air induce damage to lung epithelium, we found that the exposure to PM and Soot triggers the production of IL-1-like cytokines, which could be downstream the inflammasome pathway in mice never exposed to pollutants. Therefore, in order to evaluate the possible involvement of the canonical inflammasome pathway, we performed PMx exposure experiments during which caspase-1 was pharmacologically inhibited by a specific inhibitor, Ac-YVAD-cmk (YVAD). However, we found that neither the recruitment of DCs, macrophages and MDSCs, neither the immunesuppression were altered in PMx-exposed mice when caspase-1 was inhibited. It is to point out that, although caspase-1 inhibition in Soot-instilled mice did not affect IL-1α, IL-33 and IFN-γ levels, we found that the levels of IL-1β were lower at the sole 8 days in Soot+YVAD group of mice compared to Soot-treated mice. These data may suggest that caspase-1 is involved in lung inflammation at early time points, however, it does not play a critical role for the establishment of late lung inflammation after PM and Soot exposure. The evidence showed

in this study, which are strictly correlated to our previous data about the effect of UFPs on smokers- (Chapter 1) and exacerbated COPD-derived PBMCs (Chapter 2), demonstrate that the canonical, caspase-1-dependent, inflammasome pathway does not play a role in the inflammatory and immunesuppressive processes induced by particles mimicking air pollution.

In conclusion, these data demonstrate that air pollution exposure creates an immunesuppressive environment in the lung, which is not associated to the canonical, caspase-1-dependent, inflammasome pathway. Our data provide new prospective to improve the knowledge about the pulmonary effect of air pollution, which, together with other dangerous insults can pave the way for the onset of chronic lung disorders, as COPD, fibrosis and lung cancer.

CHAPTER 4

The axis IL-1α/AIM2 led to the release of the pro-fibrotic TGF-β in exacerbated COPD-derived PBMCs.

4.1 Introduction

Chronic lung inflammation is a key process in the pathogenesis of COPD and is responsible for progressive and irreversible decline of lung function (Sugimoto *et al*., 2016). Recent evidence demonstrated that IL-1-like cytokines characterize lung microenvironment of COPD patients (Colarusso *et al*., 2017). Indeed, some clinical trials against IL-1R and IL-1β were promoted, although with disappointing results (clinicaltrials.gov/ct2/show/NCT00581945; clinicaltrials.gov/ct2/show/NCT01448850). Nevertheless, IL-1-like cytokines are strictly correlated to the activation of the inflammasome (Terlizzi *et al*., 2014).

A central mechanism driving inflammation in immune cells is orchestrated by the inflammasome (Lasithiotaki *et al*., 2018), a multimeric complex that mediates the activation of caspase-1 and is responsible for the secretion of the pro-inflammatory cytokines IL-1β and IL-18, which exert pleiotropic effects in inflammation and tumorigenesis (Terlizzi *et al*., 2014). The most characterized inflammasome is NLRP3 which is activated, exogenously and/or endogenously, by various PAMPs and DAMPs; ROS, potassium efflux, changes in cell volume, calcium signaling, and lysosomal disruption have been proposed as critical upstream signals for NLRP3 activation. Emerging scientific evidence suggest that a number of inhaled triggers, i.e. cigarette smoking, one of the main risk factor for COPD, can cause NLRP3 inflammasome activation (De Nardo *et al*., 2014) which leads ASC specks to circulate in the bloodstream with the ensuing cell-to cell communication, ending up to the propagation of inflammatory patterns,

even in distant areas (Franklin *et al*., 2014). In the latter study, the authors demonstrated that following cigarette smoking, ASC specks were detectable in the broncho-alveolar lavage fluid (BAL) in mice, implying that ASC specks may be part of a chronic inflammatory response to smoke-induced damage to cells and tissues. Thus, it was obvious to think that the inflammasome is active in COPD patients. But, data in literature regarding NLRP3 are very discordant, most probably due to experimental limitation in that in most studies human samples were obtained from patients at different status, exacerbated or stable disease. Moreover, in our previous study (De Falco *et al*., 2017b), we found that PBMCs from smokers were more susceptible to the release of IL-1 like cytokines after the stimulation with air pollutants (Chapter 1), but that the stimulation of NLRP3 by means of LPS±ATP was not able to induce a statistical increase of the levels of these cytokines (Chapter 1, Figure 8).

Therefore, the aim of this study was to understand the role of the inflammasome in COPD by using human blood samples.

4.2 Materials and Methods

4.2.1 Human Samples

Peripheral blood samples were collected from hospitalized patients affected or not by COPD at the "Monaldi-Azienda Ospedaliera (AORN)-Ospedale dei Colli" Hospital in Naples, Italy, after their approval according to the Review Board of the hospital. All participants involved in this study signed the informed consent. The experimental protocol was performed according to the guidelines and regulations provided by the Ethical Committee of the "Monaldi-Azienda Ospedaliera (AORN)-Ospedale dei Colli" (protocol n. 604/2017). COPD patients, all former or current smokers, were divided into two groups as previously reported in the Materials and Methods section of the Chapter 2 (paragraph 2.2.1): unstable/exacerbated and stable. Instead, healthy subjects were identified as non-smokers and smokers. All subjects recruited in this study were 50 ± 10 years of age. Blood samples were collected and used within 24 hours in order to isolate mononuclear cells.

4.2.2 Isolation of Human PBMCs

As already reported in Materials and Methods section of Chapter 1 (paragraph 1.2.2) and Chapter 2 (paragraph 2.2.2), PBMCs were isolated according to Ficoll's protocol. Collected PBMCs were plated and treated at different time points (1, 5 or 24 hours). PBMCs were treated with NLRP3 inflammasome activators, as LPS (0.1 μg/mL) and ATP (0.5 mM) (Terlizzi *et al.*, 2014) or with AIM2 inflammasome ligand Poly (dA:dT) (dA:dT, 1 μg/mL) (Sorrentino *et al.*, 2015b). The activation of the inflammasomes was performed in the presence or absence of Ac-YVAD-cmk (YVAD, 1 μg/mL), a caspase-1 inhibitor; Z-LEVD-FMK (z-LEVD, 10 μM), a caspase-4 inhibitor (Eric, 2011); Pirfenidone (PIRF, 0.1 μg/mL), an inhibitor of fibroblasts, actually used in therapy for pulmonary fibrosis; Nintedanib (10 nM), a tyrosine-kinase inhibitor used in clinic for pulmonary fibrosis and NSCLC, and monoclonal antibody anti-IL-1α (aIL-1α, 1 ng/mL) or isotype control IgG. Concentrations of the above treatments were chosen

according to published data (Sorrentino *et al*., 2015b; Terlizzi *et al*., 2015; Terlizzi *et al*., 2016; Terlizzi *et al*., 2018).

4.2.3 Cytokine Measurements

IL-1α and TGF-β were measured in cell-free supernatants (75×10^4 cells/well) after 5 and 24 hours of treatment, using commercially available ELISA kits (eBioscience, CA, United States; R&D Systems, United States). The levels of 8-hydroxy-2-deoxyguanosine (8-OH-dG) were measured following manufacturer's instructions (Elabscience, Houston, TX United States) after 1 hour of treatment in PBMC-derived cytosolic extract.

4.2.4 Flow Cytometry Analysis

In order to assess the expression of AIM2 inflammasome receptor, we performed flow cytometry analysis (BD FacsCalibur, Milan, Italy) by staining cells with the following antibodies: AIM2-FITC and CD14-PE (eBioscience, San Diego, CA, United States). PBMCs were stained for the extracellular CD14 and then fixed and permeabilized by means of BD Cytofix/Cytoperm solutions before adding anti-AIM2.

4.2.5 Statistical Analysis

Data are reported as violin plots indicating median ± interquartile range. Each experiment was performed in duplicate. Statistical differences were assessed with ONE-way ANOVA followed by multiple comparisons Bonferroni's or Dunn's post-test, or Mann-Whitney U test or Student's t test as appropriate. *p* values less than 0.05 were considered as significant.

4.3 Results

4.3.1 Activation of AIM2 inflammasome led to the release of IL-1α from unstable/exacerbated COPD-derived PBMCs in a caspase-1- and caspase-4-dependent manner.

In Chapter 2 we previously reported that NLRP3 expression was significantly increased in exacerbated COPD-derived circulating cells (Figure 15A).

Similarly, we found that the percentage of CD14^{+} cells that expressed AIM2 was significantly higher in exacerbated COPD patients compared to healthy non-smoker and smoker subjects (Figure 29A, 29B).
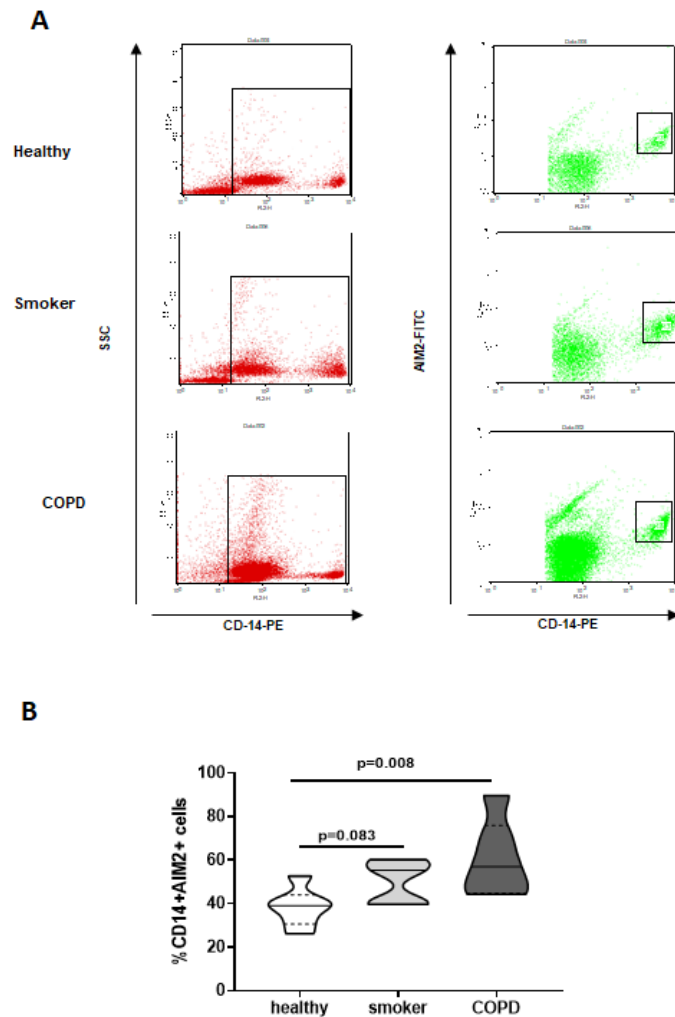
Figure 29. *Exacerbated COPD-derived CD14$^+$ PBMCs expressed higher levels of AIM2.*

Isolated PBMCs from healthy non-smoker and smoker subjects, and exacerbated COPD patients were analyzed by flow cytometry for CD14$^+$ and AIM2 expression, based on SSC-CD14$^+$ gate (**A**). PBMCs isolated from exacerbated COPD patients showed increased expression of AIM2 (**B**). Data are represented as violin plots showing median ± interquartile range (n = 7). Statistically significant differences were determined by ONE-way ANOVA followed by Bonferroni's multiple comparison post-test.

In order to understand the involvement of both inflammasomes in COPD condition, we moved on by stimulating isolated PBMCs from unstable COPD patients and healthy subjects with NLRP3 and AIM2 inflammasome ligands. Particularly, we triggered NLRP3 inflammasome by means of LPS (0.1 μg/mL) ± ATP (0.5 mM), according to the two-signal model (Terlizzi *et al.*, 2014; Colarusso *et al.*, 2017), whereas AIM2 activation was induced by Poly (dA:dT) (dA:dT, 1 μg/mL) treatment (Sorrentino *et al.*, 2015b). Both PBMCs isolated from healthy non-smokers (Figure 30A) and smokers (Figure 30B) were not able to release IL-1α after NLRP3 and AIM2 stimulation. To note, we were not able to detect IL-1β in these samples. In sharp contrast, exacerbated COPD-derived PBMCs were responsive to the sole AIM2 triggering compared to NLRP3 stimulation (Figure 30C), indeed the levels of IL-1α after dA:dT addition significantly increased compared to untreated cells (CTR).
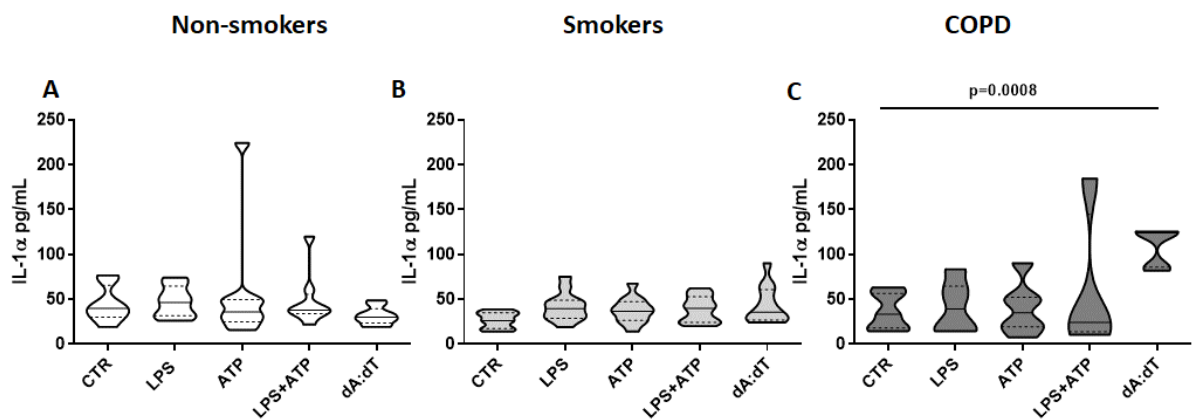
Figure 30. *Activation of AIM2 inflammasome led to IL-1α release from PBMCs obtained from exacerbated COPD patients.*

Non-smoker- (**A**), smoker- (**B**) and exacerbated COPD-derived PBMCs (**C**) were treated with LPS (0.1 μg/mL) ± ATP (0.5 mM) or Poly (dA:dT) (dA:dT, 1 μg/mL) for 5 hours. AIM2 triggering significantly increased IL-1α release only from COPD-derived PBMCs isolated. CTR represents untreated cells. Data are represented as violin plots showing median ± interquartile range (n = 10). Statistically significant differences were determined by ONE-way ANOVA followed by Bonferroni's multiple comparison post-test.

Because of oxidative stress plays a key role in COPD onset and progression (Colarusso *et al.*, 2017), we took into consideration the measurement of a marker of oxidized DNA, 8-hydroxy-2-deoxyguanosine (8-OH-dG) (Valavanidis *et al.*, 2009; Shimada *et al.*, 2012). We found that the release of 8-OH-dG during basal conditions (CTR) was significantly higher in PBMCs from exacerbated COPD patients than non-smokers and smokers (Figure 31A). Moreover, AIM2 inflammasome stimulation by means of dA:dT treatment further increased 8-OH-dG levels from COPD patients (Figure 31B).
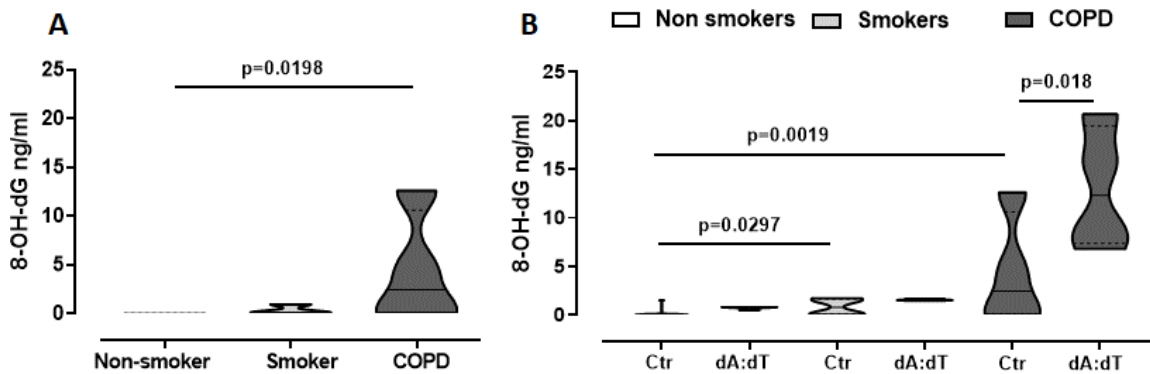
Figure 31. *AIM2 stimulation in exacerbated COPD-derived PBMCs led to higher levels of 8-OH-dG.*

Levels of 8-OH-dG were measured in untreated PBMCs from healthy non-smoker and smoker subjects, and COPD patients (**A**). AIM2 stimulation statistically increased the levels of 8-OH-dG in exacerbated COPD patients treated with Poly (dA:dT) (dA:dT, 1 µg/mL) (**B**, dark grey). Data are represented as violin plots showing median ± interquartile range (n = 5). Statistically significant differences were determined by ONE-way ANOVA followed by Bonferroni's multiple comparison post-test.

In order to understand and define the molecular mechanism associated with AIM2-dependent IL-1α release from COPD-derived PBMCs, we treated the cells with a caspase-1 inhibitor, Ac-YVAD-cmk (YVAD, 1 μg/mL) (Sorrentino *et al*., 2015b), or caspase-4 inhibitor, Z-LEVD-FMK (z-LEVD, 10 μM) (Eric, 2011; Terlizzi *et al*., 2018), in the presence or not of dA:dT. The pharmacological inhibition of caspase-1 (Figure 32A) or caspase-4 (Figure 32B) significantly reduced IL-1α levels.

Because COPD is characterized by airway remodeling correlated to fibrosis of airway wall (Barnes, 2008) and because we recently demonstrated that AIM2 inflammasome activation is involved in pro-fibrotic processes (Terlizzi *et al*., 2018), we went on to evaluate whether AIM2-dependent IL-1α release was affected by two antifibrotic drugs. Therefore, we exposed PBMCs from unstable COPD patients to Pirfenidone (PIRF, 0.1 μg/mL) (Figure 32C), an inhibitor of TGF-β release (Terlizzi *et al*., 2018), and Nintedanib (10 nM) (Figure 32D), a tyrosine kinase inhibitor (Terlizzi *et al*., 2018). Our results showed that the treatment with antifibrotic drugs significantly reduced IL-1α release from exacerbated COPD-derived PBMCs in the presence of dA:dT (Figure 32C, 32D).
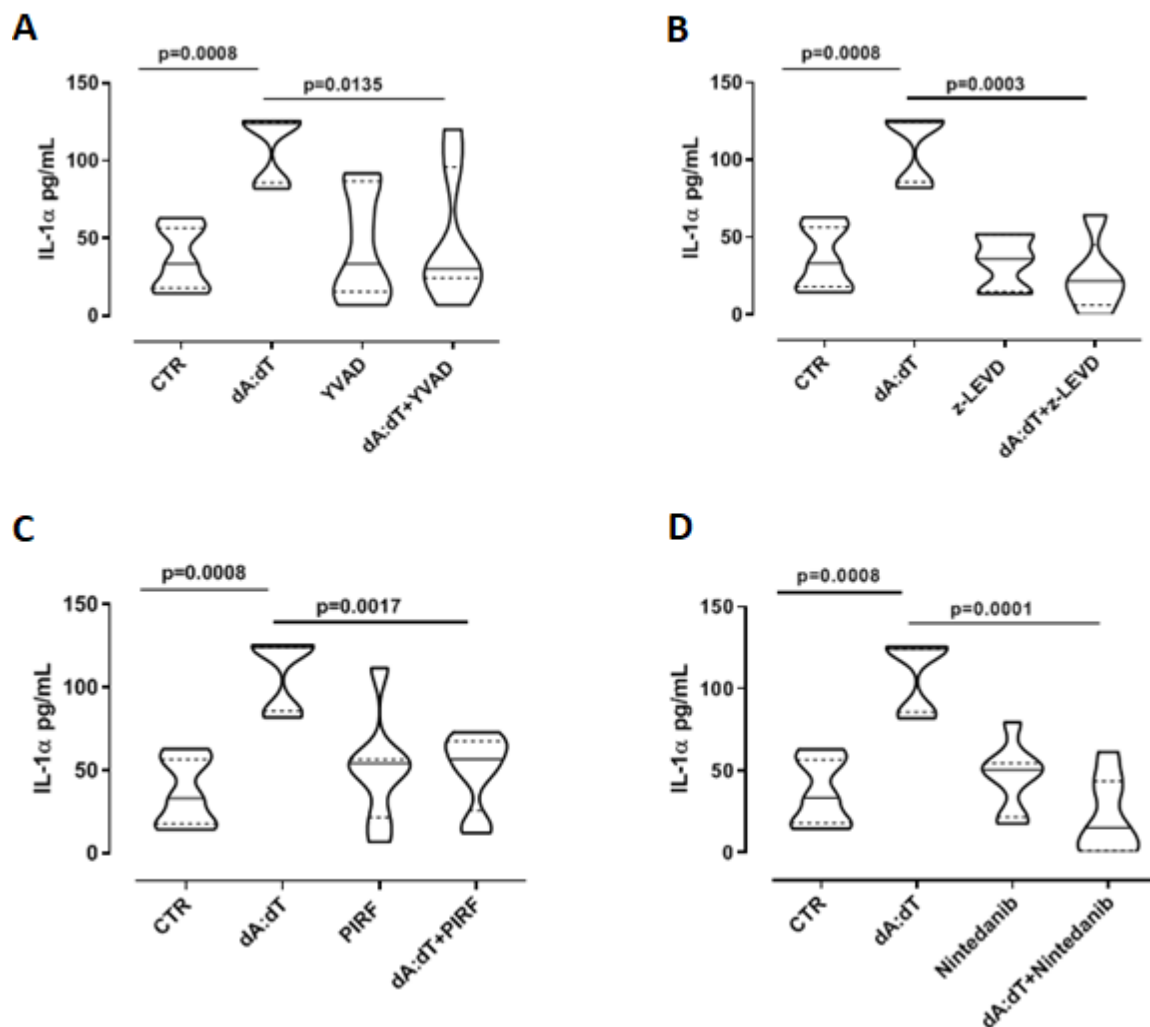
Figure 32. *The release of IL-1α from exacerbated COPD-derived PBMCs after AIM2 stimulation was caspase-1 and caspase-4-dependent.*

The addition of Ac-YVAD-cmk (YVAD, 1µg/mL), caspase-1 inhibitor (**A**), Z-LEVD-FMK (z-LEVD (10 µM), caspase-4 inhibitor (**B**), Pirfenidone (PIRF, 0.1 µg/mL) (**C**) and Nintedanib (10 nM) (**D**) significantly reduced IL-1α release after AIM2 activation by means of Poly (dA:dT) (dA:dT, 1 µg/mL). Data are represented as violin plots showing median ± interquartile range (n = 10). Statistically significant differences were determined by ONE-way ANOVA followed by Bonferroni's multiple comparison post-test.

4.3.2 AIM2/IL-1α axis led to TGF-β release from exacerbated COPD-derived PBMCs in a caspase-1- and caspase-4-dependent manner.

Small airway fibrosis is key point for progression and exacerbation of COPD and is well-known to be the resultant of chronic inflammation (Barnes, 2008). Therefore, we analyzed the release of TGF-β as both an immunesuppressive and pro-fibrotic cytokine (Barnes, 2013). We found that the stimulation of AIM2 significantly increased the release of TGF-β from exacerbated COPD-derived PBMCs after 24 hours of treatment (Figure 33). To investigate the molecular mechanisms associated to AIM2-dependent TGF-β release, we treated exacerbated COPD-derived PBMCs with AIM2 ligand in the presence or not of caspase-1 and caspase-4 inhibitors, YVAD and z-LEVD respectively. Both the pharmacological inhibition of caspase-1 (Figure 33A) and caspase-4 (Figure 33B) significantly reduced TGF-β levels after dA:dT addition, implying that there was a direct effect of the inflammasome on the release of this cytokine.

Based on the fact that caspase-1 and caspase-4 are likely to be upstream IL-1α (Gross *et al*., 2012; Casson *et al*., 2013; Terlizzi *et al*., 2014), to understand whether IL-1α was upstream AIM2-dependent TGF-β release, we neutralized IL-1α by using a monoclonal antibody (aIL-1α, 1 ng/mL) after AIM2 stimulation. We found that IL-1α neutralization significantly reduced the release of TGF-β from exacerbated COPD-derived PBMCs (Figure 33C). The isotype control IgG did not alter the basal levels of TGF-β (data not shown). In support, the addition of Pirfenidone, which mechanism of action is not related to AIM2 inflammasome, but rather to the inhibition of TGF-β by down-regulation of its transcription (Knüppel *et al*., 2017), did not abrogate AIM2-dependent TGF-β secretion (Figure 33D). Moreover, the treatment of COPD-derived PBMCs with Nintedanib, a tyrosine kinase inhibitor, significantly decreased TGF-β release after dA:dT treatment (Figure 33E), implying that tyrosine kinases may be involved in AIM2/IL-1α-dependent pro-fibrotic processes in exacerbated COPD patients.
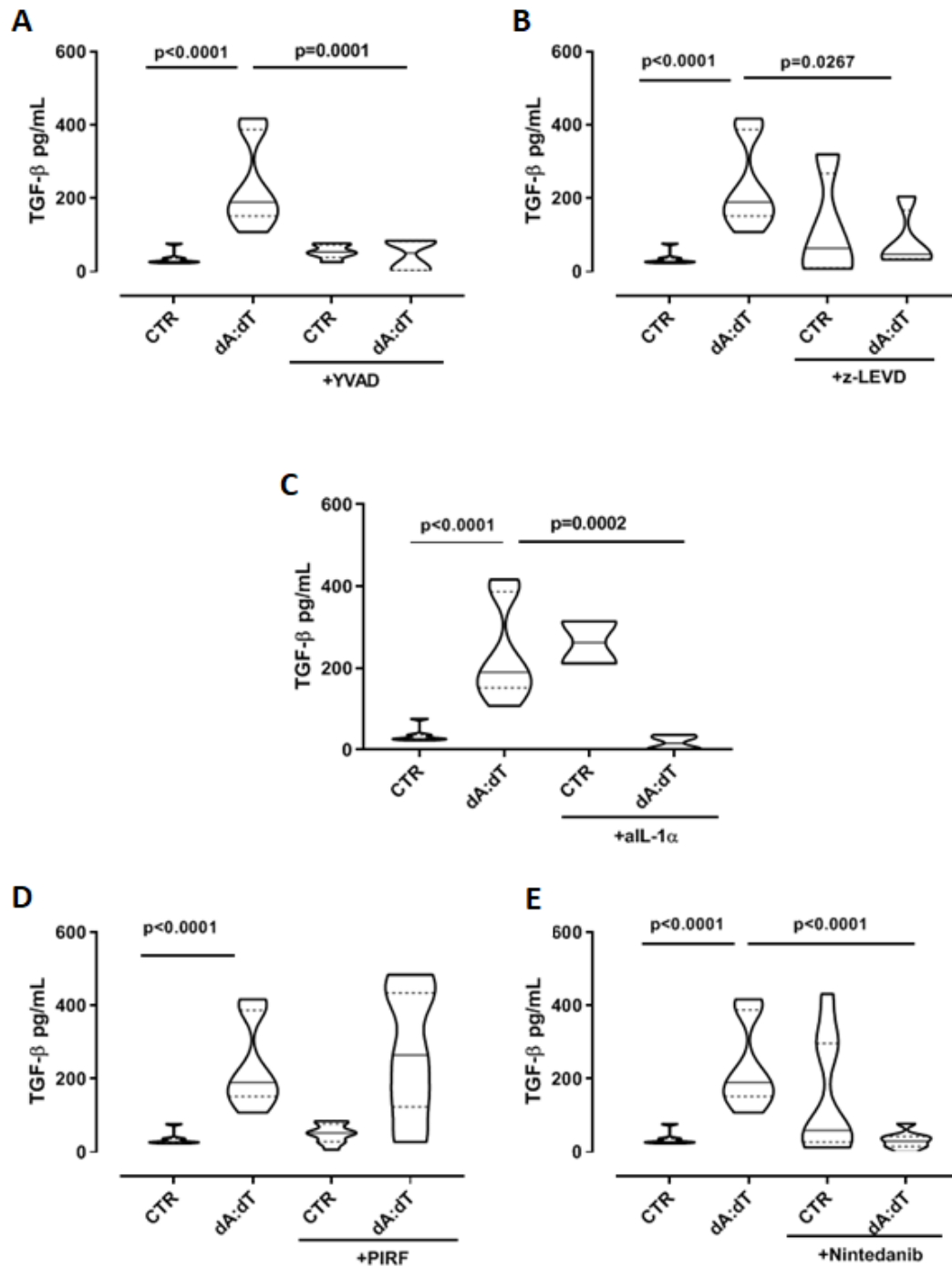
Figure 33. *Activation of AIM2 was responsible for caspase-1/caspase-4/IL-1α-dependent TGF-β release from exacerbated COPD-derived PBMCs.*

The addition of Ac-YVAD-cmk (YVAD, 1 µg/mL), caspase-1 inhibitor (**A**), Z-LEVD-FMK (z-LEVD, 10 µM), caspase-4 inhibitor (**B**), monoclonal antibody against IL-1α (aIL-1α, 1 ng/mL) (**C**), Nintedanib (10 nM) (**E**), but not Pirfenidone (PIRF, 0.1 µg/mL) (**D**), significantly reduced TGF-β release at 24 hours post treatment with AIM2 activator, Poly (dA:dT) (dA:dT, 1 µg/mL). Data are represented as violin plots showing median ± interquartile range (n = 10). Statistically significant differences were determined by ONE-way ANOVA followed by Bonferroni's multiple comparison post-test.

Together these data suggest that PBMCs from exacerbated COPD patients are responsive to AIM2 inflammasome stimulation. The activation of AIM2 triggers IL-1α release, which in turn is responsible for TGF-β secretion through both canonical, caspase-1-dependent, and non-canonical, caspase-4-dependent, inflammasome pathways.

4.4 Conclusions

The role of the inflammasome in COPD development and progression has been suggested, although it is still elusive and controversial. The literature focused especially on NLRP3 inflammasome. In particular, it was demonstrated that various molecules can trigger NLRP3. Extracellular ATP, which acts as an endogenous danger signal for the activation of NLRP3 inflammasome, is elevated in BAL fluid of patients with COPD compared to healthy subjects (Colarusso *et al*., 2017), and its concentration is associated to a decline of lung function (Lommatzsch *et al*., 2010). Moreover, NLRP3 is overexpressed in lung of stable COPD patients rather than non-smoker and smoker subjects, implying the correlation between NLRP3 mRNA and the severity of airflow obstruction (Faner *et al*., 2016). In contrast, the same authors found that NLRP3 is not responsible for caspase-1-dependent increase of IL-1β and IL-18 levels (Faner *et al*., 2016). Similarly, we found (Figure 30) that the stimulation of NLRP3 by means of LPS±ATP did not induce neither non-smoker-, nor smoker-, nor-COPD-derived PBMCs to release IL-1-like cytokines. Instead, we found that, rather, AIM2 stimulation leads to the release of IL-1α in a canonical, caspase-1-dependent, and non-canonical, caspase-4-dependent manner. It has to point out that the basal levels of NLRP3 (Chapter 2, Figure 15A) compared to AIM2 (Figure 29B) were still higher, but NLRP3 receptor was not functional, as instead in the case of AIM2. Indeed, the stimulation of AIM2 via Poly dA:dT significantly increased IL-1α, but not IL-1β levels, which, in turn, is responsible for the induction of TGF-β. In contrast, Eltom *et al*., (2014) reported that AIM2 inflammasome is not involved in IL-1α/caspase-1/11 axis in a CS-induced neutrophil inflammation in mice. This discrepancy probably stands on the difference between studies performed on humans and mice.

IL-1α is a dual-function cytokine that can act directly via cell surface receptor ligation or, as an un-cleaved full-length alarmin binding to IL1R1 and instructing the adaptive immune system to trigger 'sterile inflammation' (Terlizzi *et al*., 2014; Borthwick, 2016). The mechanism/s governing IL-1α release are less clear, but recently, it was described that IL-1α can be processed

by caspase-11 in mice (homolog of caspase-4 in humans) via a non-canonical inflammasome (Gross *et al*., 2012), besides by caspase-1 (Casson *et al*., 2013; Terlizzi *et al*., 2014). Although the role of caspase-1 in COPD, has been already reported (Faner *et al*., 2016; Müller *et al*., 2011), the involvement of caspase-4 has been poorly studied.

To note, our study demonstrates that caspase-1 and caspase-4 inhibition abrogates the secretion of AIM2-induced IL-1α in COPD, however we are not able to predict whether caspase-1 or caspase-4 plays the main role in AIM2 inflammasome activation, or rather, whether they act synergistically. The limitations to reach this goal are that primary cells are difficult to genetically manipulate. However, because caspase-4 has been described to be upstream caspase-1 activation (Sollberger *et al*., 2012), we speculate that AIM2 activation leads first to caspase-4 and then to caspase-1 activation, responsible for IL-1α release.

Moreover, we found that caspase-4 inhibition by means of Z-LEVD-FMK (z-LEVD) (Figure 32B) completely reduced the levels of IL-1α compared to caspase-1 inhibition by means of Ac-YVAD-cmk (YVAD) (Figure 32A), suggesting that caspase-4 could be upstream caspase-1 for IL-1α induction when AIM2 is stimulated. The results here reported are in line with others about the involvement of IL-1α in chronic lung diseases (Sorrentino *et al*., 2015b; Borthwick, 2016; Terlizzi *et al*., 2018).

Another issue of these data is that IL-1α led to the induction and release of TGF-β, an immunesuppressive and pro-fibrotic cytokine (Barnes, 2013; Terlizzi *et al*., 2018). IL-1α together with TGF-β can play a crucial role for lung inflammation and fibrosis. Fibrotic processes play a pivotal role in COPD causing significant lung dysfunction by remodelling small airways and contributing to airflow limitation (Barnes, 2013). Indeed, oxidative lung damage processes stimulate airway epithelial cells to release pro-fibrotic mediators, such TGF-β, which stimulates small airway fibroblasts to produce collagens resulting in peribronchiolar fibrosis.

In conclusion this study highlights a novel molecular mechanism by which AIM2 inflammasome drives, via the canonical and non-canonical pathway, the release of pro-inflammatory and pro-fibrotic factors involved in the exacerbation stage of COPD.

Based on the results reached in this study, in the next Chapter we focus our attention on the effect of smoke as COPD-driven factor and we try to define the relationship between COPD and lung cancer evaluating the inflammasome involvement in lung carcinogenesis by using animal models of cigarette smoke (CS) and carcinogen exposure.

CHAPTER 5

Crosstalk between COPD and lung cancer: AIM2 inflammasome and IL-1α were highly expressed in a mouse model of smoke-induced COPD and carcinogen-induced lung cancer.

5.1 Introduction

The main goal of this research project is to highlight potential molecular mechanisms that at the crossroad between COPD and lung cancer. Since 1980s up to nowadays, epidemiological studies have been demonstrating that COPD is a high-risk pathology in that COPD patients are 6.35 times more likely to develop lung cancer compared to the normal population (Butler *et al*., 2019). It is well-known that both COPD and lung cancer are separately of high prevalence and that coexistence of both conditions can occur; however, the molecular mechanism/s that underlie the relationship between COPD and lung cancer still remain an object of open discussion and scientific investigation.

Based on the literature (Duhram & Adcock, 2015), we can summarize several cross-talks between COPD and lung cancer as follows:

    1. cigarette smoke exposure;

    2. environmental pollution;

    3. genetic and epigenetic changes.

Lung exposure to cigarette smoking as well as to environmental pollution can trigger oxidative stress with an ensuing inflammatory process that translate into an evolving long-term chronic inflammation (Talikka *et al*., 2012; Li *et al*., 2017), which is at the basis of lung dysfunction. Chronic release of pro-inflammatory cytokines could exploit into airway

destruction, air trapping and lung hyperinflation (Duhram & Adcock, 2015) resulting in lung structural damage and functional impairment (Colarusso *et al.*, 2017), all events that link COPD to lung carcinogenesis.

In our previous data we demonstrated that the deregulation of the oxidative stress pattern (Chapter 2 and 4) is associated to the release of IL-1-like cytokines, in particular IL-1α which can lead to a fibrotic TGF-β-dependent process (Chapter 4). To note, the release of TGF-β was strictly correlated to IL-1α which release was triggered by an inflammasome receptor, AIM2 (Colarusso *et al.*, 2019b). Because these data were performed by using blood samples of COPD patients, in the attempt to understand the impact of COPD on lung carcinogenesis, in this Chapter we took advantage of a cigarette smoking mouse model compared to carcinogen-induced mouse model to highlight any potential crosstalk between COPD and lung cancer.

5.2 Materials and Methods

5.2.1 Mice

Female specific pathogen-free C57Bl/6N mice (6-8 weeks of age) (Charles River Laboratories, Lecco, Italy) were fed with a standard chow diet and maintained in specific pathogen-free conditions at the animal care facility of Department of Pharmacy, University of Salerno. This study was carried out in strict accordance with the recommendations in the Guide for Care and Use of Laboratory Animals of the Istituto Nazionale per la Salute. The experimental protocol was approved by the Committee on Ethics for Animal Studies of the University of Salerno and Health Ministry with the approval number 985/2017.

In another set of experiments, female C57Bl/6j mice (6-8 weeks of age) (The Jackson Laboratory) were housed at the Center for Animal Models of Disease at the University of Patras, Department of Physiology, Faculty of Medicine, Greece. This study was approved by the Veterinary Administration of the Prefecture of Western Greece (approval protocol 67696/192/05.03.2019).

All animal experiments were performed under protocols that followed the Italian (D.L. 26/2014) and European Community Council for Animal Care (2010/63/EU). Experiments were performed with n = 9 mice per group and were repeated twice.

5.2.2 Cigarette Smoke Exposure Protocol.

In order to create a mouse model of cigarette smoke (CS)-induced COPD, mice were exposed to second- and first-hand smoking (Figure 34).
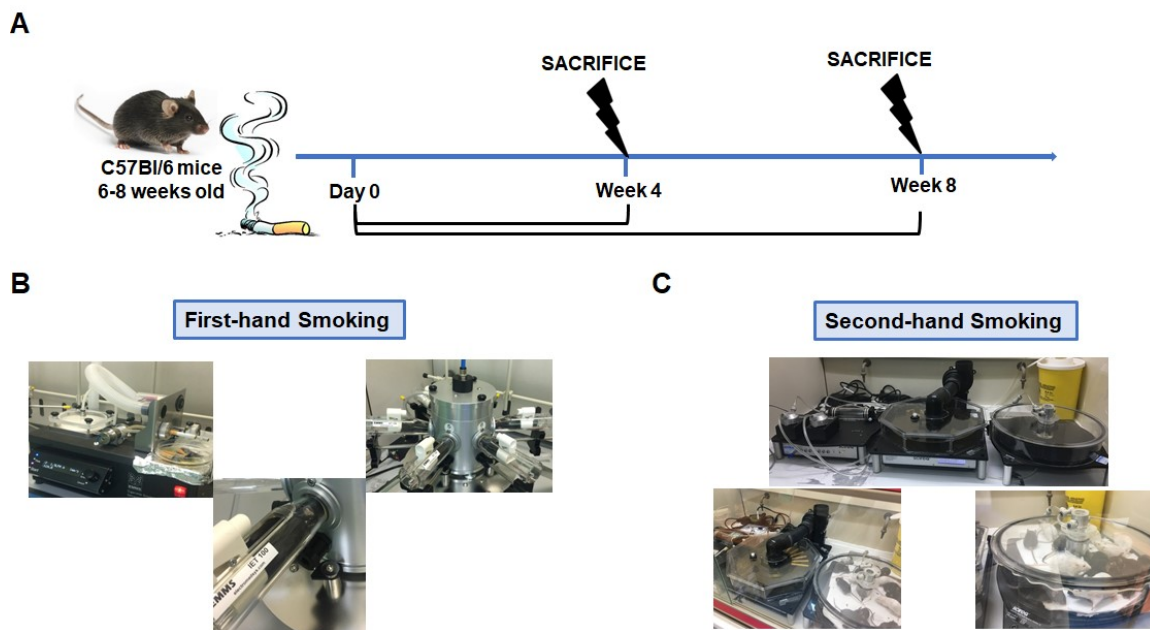
Figure 34. *Smoke Exposure Protocol.*
C57Bl/6N and C57Bl/6j mice (female, 6-8 weeks of age) were exposed for (**A**) 4-8 weeks to first- and second-hand smoking by using a (**B**) nose-only and (**C**) whole-body exposure apparatus, respectively. Control mice, Room Air group, breathed filtered air for the same time.

In CS exposure experiment, the concentration of total particulate matter (TPM) inhaled by mice was determined according to the following equation:

$$TPM = \frac{TAR * p}{n * V\ bias}$$

(Equation 1)

where *TAR* content for each cigarette is expressed as mg per cigarette (mg/cig); *p* is the puff rate expressed as puffs per minute (puffs/min); *n* is the number of puffs to completely smoke the cigarette, expressed as puffs per cigarette (puffs/cig); *V bias* is the bias flow set to achieve a certain number of complete air exchanges within the exposure apparatus over a fixed period of time for the exposure, expressed as liters per minute (L/min).

To mimic smoke inhalation as in smokers, mice were exposed to first-hand smoking once a day at the concentration of 1 μg/cm^3 of TPM, generated from Red Marlboro cigarettes (TAR =

12 mg/cig), 5 days/week for 4 and 8 weeks by using a nose-only exposure apparatus (EMMS, UK). Each cigarette was smoked through 6 puffs (1 puff/min) and the generated smoke was delivered in 5-second puffs with 55 seconds of normal air between each puff. Control mice, here defined as Room Air group, breathed filtered air for the same time. No mortality was registered following this experimental plan. Therefore, according to set parameters, and to the selected value of bias flow (2 L/min), inserting these parameters into Equation 1, the TPM concentration which was inhaled by mice in first-hand smoking experiment was:

$$TPM = \frac{12 \frac{mg}{cig} * 1 \; puff/min}{6 \; puffs \; * 2 \; L/min} = 1 \frac{mg}{L} = 1 \; \mu g/cm3$$

(Equation *1.1*)

Instead, to mimic the inhalation profile associated to second-hand smoking, mice were allocated in a total body exposure smoking apparatus (Scireq, Canada) for 50 minutes twice/day (with a recovery period of 30 minutes between two sessions), 5 days/week for 4 and 8 weeks. Mice received a concentration of 0.715 µg/cm^3 of TPM generated by 1R6F research cigarettes (Tobacco Research Institute, University of Kentucky; TAR = 10 mg/cig). During each session, smoke was generated from 7 cigarettes, each of them was smoked through 7 puffs (1 puff/min; each puff was of 2 seconds followed by 58 seconds of air); a bias flow of 2 L/min was set. Therefore, as previously, inserting set parameters into the Equation 1, the TPM concentration which was inhaled by mice in second-hand smoking experiment was:

$$TPM = \frac{10 \frac{mg}{cig} * 1 \; puff/min}{7 \; puffs \; * 2 \; L/min} = 0.715 \; mg/L = 0.715 \; \mu g/cm3$$

(Equation *1.2*)

The working dose of TPM was chosen based on published data (Beckett *et al.*, 2013; John-Schuster *et al.*, 2014) and on preliminary data performed by exposing mice in a dose-dependent manner.

In another set of experiments, nose-only CS-exposed mice were intraperitoneally (i.p.) injected every 3 days with Ac-YVAD-cmk (YVAD, 10 μg/mouse), a caspase-1 inhibitor, as already reported (Zhang *et al.*, 2016), starting from the first exposure to CS (Figure 35). Mice were sacrificed 24 hours after the last CS exposure.
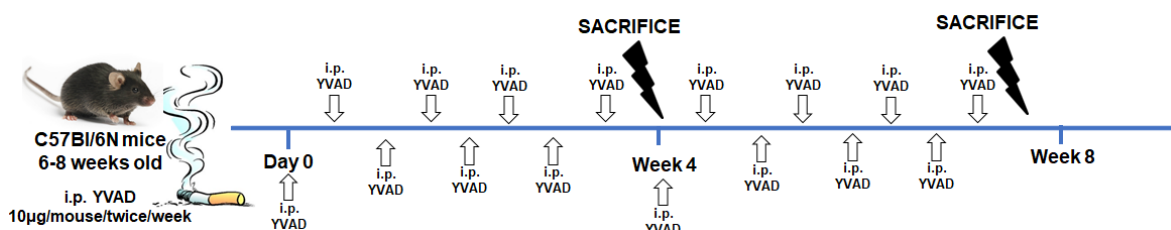
Figure 35. *Pharmacological inhibition of caspase-1 in nose-only CS-exposed mice.* Starting from the first day of CS exposure, C57Bl/6N mice (female, 6-8 weeks of age) were intraperitoneally (i.p.) treated with Ac-YVAD-cmk (YVAD, 10 μg/mouse) twice/week. Mice were sacrificed at different time points: 4 and 8 weeks after the first smoke exposure.

Isolated lungs were embedded in paraffin or OCT, cut (5 μm-thick sections or 7 μm-thick cryosections) and stained with Hematoxylin & Eosin (H&E) to calculate mean linear intercept (MLI) by means of ImageJ software (NIH, USA). Please refer to the paragraph 5.2.4 for the calculation/analysis of MLI.

Moreover, broncho-alveolar lavage fluid (BAL) was collected using 0.5 mL of PBS containing 0.5 mM EDTA to measure pro- and anti-inflammatory cytokines levels. Right lung lobes were collected and used after enzymatic digestion with 1 U/mL of collagenase (Sigma Aldrich, Rome, Italy). Flow cytometry (BD FacsCalibur Milan, Italy), ELISA, RT-PCR and western blotting analysis were performed.

5.2.3 Carcinogen-induced mouse model of lung cancer

To mimic lung cancer, a carcinogen-induced mouse model was used. Mice (C57Bl/6N, 6-8 week of age) were intratracheally (i.t.) exposed to N-methyl-N-nitrosourea (NMU), a well-known carcinogen and mutagen agent due to its alkylating activity (Freire *et al.*, 2013; Terlizzi *et al.*, 2015) under anesthesia (Isoflurane 2%). Briefly, mice were treated with NMU at the dose of 50 µg/mouse (10 µL of saline) at day 0, week 5, week 8 and week 12, followed by another two low doses of 10 µg/mouse at weeks 1, 2, 6, 9, 10, 13 and 14.

Mice were sacrificed at different time points: 4, 8 and 16 weeks after the first instillation of NMU, as reported in the Figure 36. The following groups were considered:

1. Naïve, non-treated, mice;

2. 4 weeks NMU-treated mice;

3. 8 weeks NMU-treated mice;

4. 16 weeks NMU-treated mice.

BAL fluid and lungs were collected to perform the above described biochemical analyses.
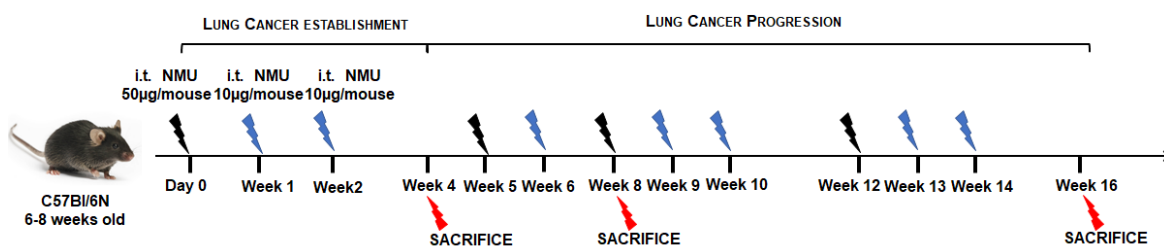
Figure 36. *Experimental protocol for carcinogen-induced lung cancer mouse model*. C57Bl/6N mice (female, 6-8 weeks of age) were intratracheally (i.t.) exposed to N-methyl-N-nitrosourea (NMU) for 16 weeks. Black arrows represent the administration of the high dose of NMU, 50 µg/10 µL/mouse; whereas blue arrows represent the instillation of the low dose of NMU, 10 µg/10 µL/mouse. Mice were sacrificed at different time points: 4, 8 and 16 weeks after the first NMU exposure.

5.2.4 Quantitative lung morphometry

Air space enlargement was assessed by using the mean linear intercept (MLI) technique, which is a standard parameter to assess alveolar diameter in mice (Horvat *et al.*, 2010). MLI was obtained by using three pictures of H&E stained right lung lobe (magnification 10X, Zeiss microscope, Germany). Briefly, a fixed grid of 7 horizontal lines was overlapped on the lung section image by means of ImageJ software. Intercepts of lines with alveolar septa (I septa) were counted, and the distance (in μm, L_m) of each alveolar space was measured (Figure 37).

Figure 37. *Example of representative H&E pictures used for MLI calculation.*
A fixed grid of 7 horizontal (black) lines was overlapped on the lung section stained for H&E. Intercepts of lines with alveolar septa (I septa) were counted, and the distance (in μm) of each alveolar space (light blue arrows), indicated as Lm, was measured.
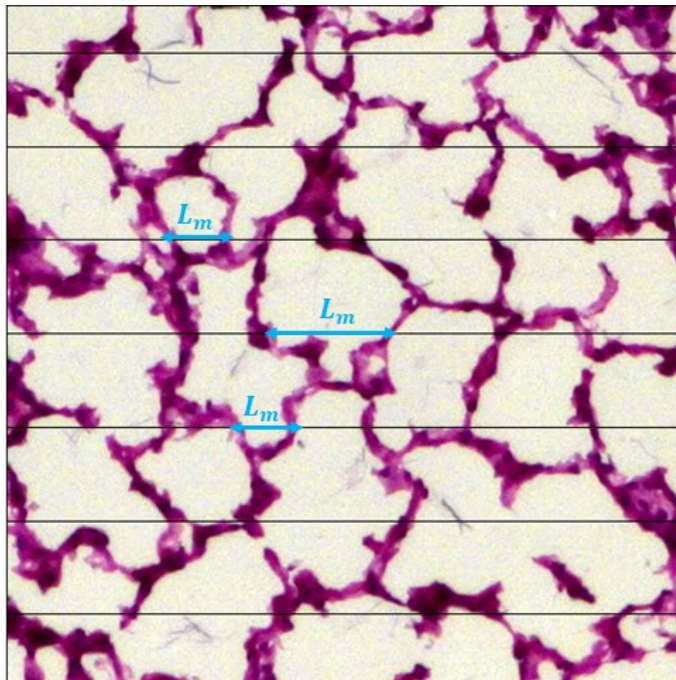
MLI was calculated according to the following equation:

$$MLI = \frac{\sum_{i=1}^{n} Lm_i}{I\ septa}$$

(Equation 2)

5.2.5 Airway Responsiveness Measurements

To evaluate the bronchial tone, we performed airway responsiveness. Briefly, bronchial rings (1–2 mm length) were cut and placed in organ baths mounted to isometric force transducers (Type 7006, Ugo Basile, Comerio, Italy) and connected to a Powerlab 800 (AD Instruments, Ugo Basile, Comerio, Italy). Rings were initially stretched until a resting tension of 0.5 g was reached and allowed to equilibrate for at least 30 min. To evaluate bronco-contraction, in each experiment bronchial rings were challenged with carbachol in a concentration-dependent manner (1 pM−10 μM).

5.2.6 Cytokine measurements

IL-1α, IL-1β and TGF-β were measured in BAL or lung homogenates samples. The assays were performed using commercially available ELISA kits (eBioscience, CA, USA). Cytokines levels in BAL samples were expressed as pg/mL, whereas in lung homogenates as pg/mg protein.

5.2.7 Western blot analysis

Lung homogenates were used to examine the expression of caspase-1 (active form 20 kDa) (Santa Cruz Biotechnology, CA, United States) and AIM2 (45 kDa) (Proteintech Group, USA).

5.2.8 Flow Cytometry Analysis

In order to investigate the immune cells infiltrated into the lung of nose-only CS-exposed mice, we performed flow cytometry analysis (BD FacsCalibur Milan, Italy). After lung digestion, cell suspensions were passed through 70 μm cell strainers, and red blood cells were lysed. Lung cell suspensions were stained with the following antibodies: CD11c, CD11b, F4/80, MHC II and IDO (Indoleamine 2, 3-dioxygenase).

5.2.9 RT-PCR

AIM2 gene expression was measured by RT-PCR. Total RNA was isolated from frozen tissues isolated from naïve and NMU-treated mice by using an RNA extraction kit according to the manufacturer's instructions (Qiagen, Milan, Italy). Reverse Transcription was performed by using first-strand cDNA synthesis kit (Qiagen, Milan, Italy) followed by PCR. Thermal cycling conditions were as follows:

-45 cycles of 20s at 95°C, 20s at 60°C, 20 s at 72°C

Primer pairs were as follows:

AIM2: Forward 5′-TCCTGATGCTGCTCCTTGAA-3′;

Reverse 5′-GTGTCTGGGTTTGGTGGTTG-3′

GAPDH: Forward 5′-CCCACTCTTCCACCTTCGAT-3′;

Reverse 5′-CTTGCTCAGTGTCCTTGCTG-3′.

5.2.10 Immunoprecipitation and western blot analysis

Protein G Magnetic Agarose Beads (25%) (ABT) were coated and incubated with 100 μL (250 μg/mL) of proteins obtained by lung homogenates of NMU-treated mice. Anti-AIM2 antibody (Proteintech Group, USA) (2 μg/mL) was added to the above solution, containing binding Buffer and beads, gently mixing gently for 1 hour. AIM2-immunoprecipitated samples were subjected to electrophoresis and analyzed by western blotting. IgG was used as negative control (NC).

5.2.11 Statistical Analysis

Data are reported as violin plots indicating the median ± interquartile range or as mean ± SEM. Statistical differences were assessed with Mann Whitney t test and TWO-way analysis of variance (ANOVA) followed by Sidak's post-test, where appropriate. p values less than 0.05 were considered significant.

5.3 Results

5.3.1 First-hand smoking induced alveolar enlargement in mice.

To mimic COPD, mice were exposed to cigarette smoking, and MLI was evaluated. MLI represents a parameter to highlight any alteration of the alveolar structure as alveolar enlargement (Horvat *et al*., 2010). The exposure of mice to first-hand smoking for 4 weeks did not induce alveolar enlargement (Figure 38A and 38B, green violin plots). In sharp contrast, a longer exposure for 8 weeks significantly increased MLI, implying an enlargement of alveoli at 8 weeks compared to 4 weeks (Figure 38A and 38B, purple vs green violin plots). However, it has to be point out that the Room Air group at 8 weeks still had, although not significant, higher MLI than the Room Air group at 4 weeks (Figure 38B, purple vs green violin plots), suggesting a potential role of the age of animals.

On the other hand, mice exposed to second-hand smoking did not show any difference in terms of alveolar enlargements (Figure 38C) and MLI values among Room Air and Smoke groups, both at 4 and 8 weeks after smoke exposure (Figure 38D, green vs purple violin plots). These data support the difference between first- and second-hand smoking exposure model, and they underlie that the nose-only CS-exposure could be able to induce an emphysematous pattern typical of COPD in a mouse model at early time points, as already reported in literature (Beckett *et al*., 2013). Nevertheless, more experiments at longer time points are needed to evaluate an emphysema-like pathology induced by smoke exposure.

Because significant changes in lung architecture were observed, the bronchial responsiveness to carbachol was measured. CS-exposed mice had a significant reduction of the bronchial tone following a cumulative administration of carbachol (Figure 38E, green and purple line). This effect was more pronounced at 4 weeks (Figure 38E, green line), time point when we did not observe any alteration of the alveolar structure compared to the Room Air group of mice (Figure 38B, green violin plots). In particular, 4 weeks CS-exposed mice showed a statistically significant decrease of bronchial responsiveness to carbachol starting from 0.1

µM compared to Room Air group (Figure 38E, green vs black line). Instead, the bronchial tone of mice exposed for 8 weeks had higher bronchial responsiveness than mice exposed for 4 weeks (Figure 38E, purple vs green line), but still a lower tone than Room Air group (Figure 38E, purple vs black line).

These data may suggest that the exposure to smoke for 4 weeks was able to damage first the bronchial smooth muscle cells and then induce an alveolar enlargement, most likely to compensate airflow alteration. On the other hand, at 8 weeks alveolar spaces were increased while the bronchial tone tended to be rescued, speculating on potential morphological feedback to rescue lung function.
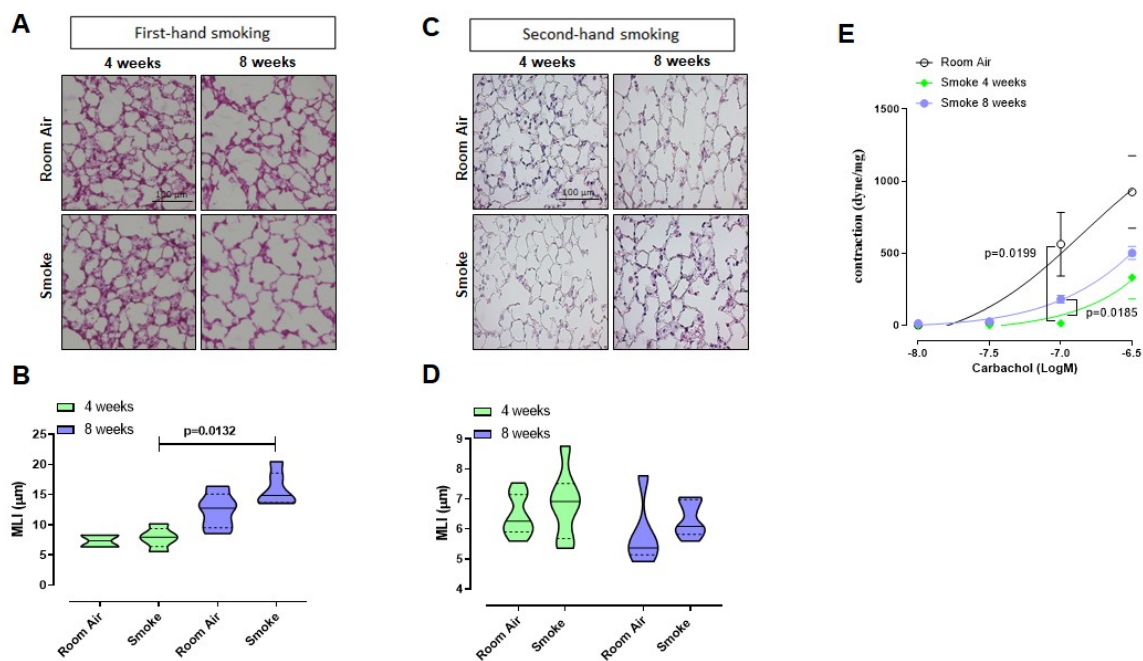
Figure 38. *First-hand smoking induced alveolar enlargement and altered bronchial responsiveness.*

Representative pictures of first-hand (**A**) and second-hand smoking exposure (**C**) at 4 and 8 weeks compared to Room Air group. Analysis of MLI, expressed as µm, at 4 and 8 weeks post first- (**B**) and second-hand (**D**) exposure (green vs purple violin plots). Bronchial tone after Carbachol (10^{-8} -$10^{-6.5}$ M) stimulation of bronchial rings obtained from mice exposed to first-hand smoking or Room air group at 4 and 8 weeks (**E**). Data are presented as violin plots showing median $\pm$ interquartile range and mean $\pm$ SEM (n = 9). Statistically significant differences were determined by TWO-way ANOVA followed by Sidak's post-test.

5.3.2 IL-1-like cytokines in the lung of first-hand smoking exposed mice.

Based on data previously reported in Chapter 4, PBMCs isolated from unstable-exacerbated COPD patients released IL-1α after AIM2 inflammasome activation (Colarusso *et al*., 2019b). Therefore, in order to investigate the role of the inflammasome in this mouse model of CS-exposure, we first evaluated the levels of IL-1-like cytokines, which are strictly associated to the multimeric complex activation (Terlizzi *et al*., 2014). The exposure of mice to first-hand smoking for 4 weeks showed higher presence of IL-1α in lung homogenates than mice exposed for 8 weeks (Figure 39A, green vs purple violin plots). It is to point out that, although we did not find any significant difference when we compared Room Air and Smoke groups at both time points, an upward trend of IL-1α levels was observed in CS-exposed mice than Room Air group at 4 weeks (Figure 39A, green violin plots). Instead, no differences were found in the levels of IL-1β in the BAL fluid obtained from CS-exposed mice at both 4 and 8 weeks (Figure 39B).

These latter data together with the data about the bronchial tone could suggest that an earlier inflammatory pattern could lead to bronchial dysfunction as observed by higher levels of IL-1α at 4 weeks, implying smooth muscle cell damage, with an ensuing feedback on the alveolar space at later time point (8 weeks).
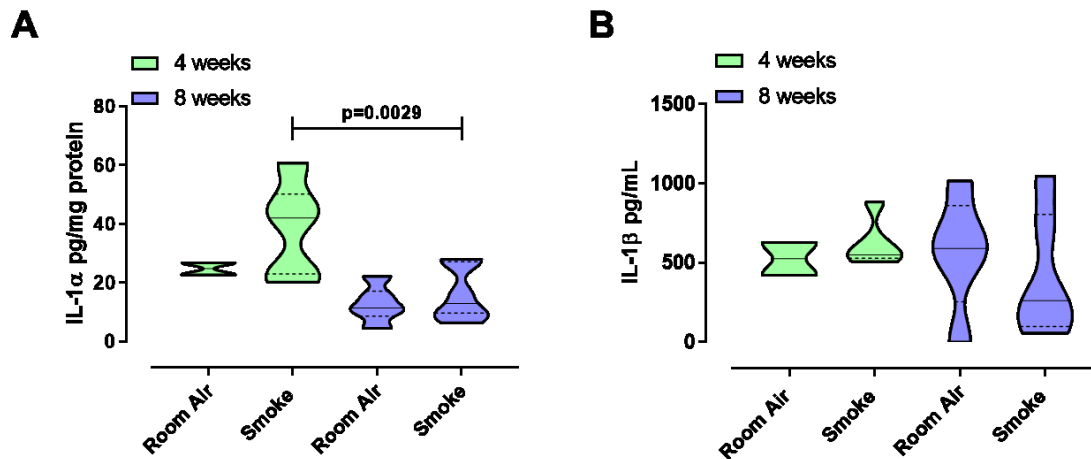
Figure 39. *IL-1α, but not IL-1β, was released at 4 weeks post smoke exposure.*

Lung homogenates and BAL obtained from first-hand smoking mice were analyzed by means of ELISAs, to evaluate IL-1α and IL-1β levels, respectively. Smoke exposure led to higher levels of IL-1α (**A**) in lung homogenates, but not of IL-1β (**B**) in the BAL fluid. Data are presented as violin plots showing median ± interquartile range (n = 9). Statistically significant differences were determined according to Mann Whitney t test.

5.3.3 Smoke-induced alveolar enlargement was not caspase-1-dependent.

In our previous data, as reported in Chapter 4, we demonstrated that AIM2 stimulation induced the release of IL-1α from COPD-derived PBMCs in a caspase-1- and caspase-4-dependent manner. Therefore, we went on by evaluating the possible involvement of caspase-1, enzyme involved in the canonical inflammasome pathway (Terlizzi *et al.*, 2014), in our experimental conditions.

Western blotting analyses performed on lung homogenates obtained from first-hand smoking-exposed mice sacrificed at 4 and 8 weeks, showed that caspase-1 was present and cleaved solely at 8 weeks after CS exposure compared to 4 weeks (Figure 40A and 40B, purple vs green violin plots). To note, we did not find significant differences in terms of caspase-1 protein expression between Room Air and Smoke groups at both time points. These data were to what observed for IL-1β (Figure 39B).

Nevertheless, we treated mice with a well-known pharmacological inhibitor of caspase-1, Ac-YVAD-cmk (YVAD; i.p.: 10 µg/mouse/twice/week), following the experimental protocol reported in Figure 35. The pharmacological inhibition of caspase-1 did not alter the alveolar structure (Figure 40C) and MLI values (Figure 40D) in smoking mice at both 4 and 8 weeks. These data suggest that caspase-1 was not involved in lung structural changes (alveolar enlargement) induced by first-hand smoking exposure.
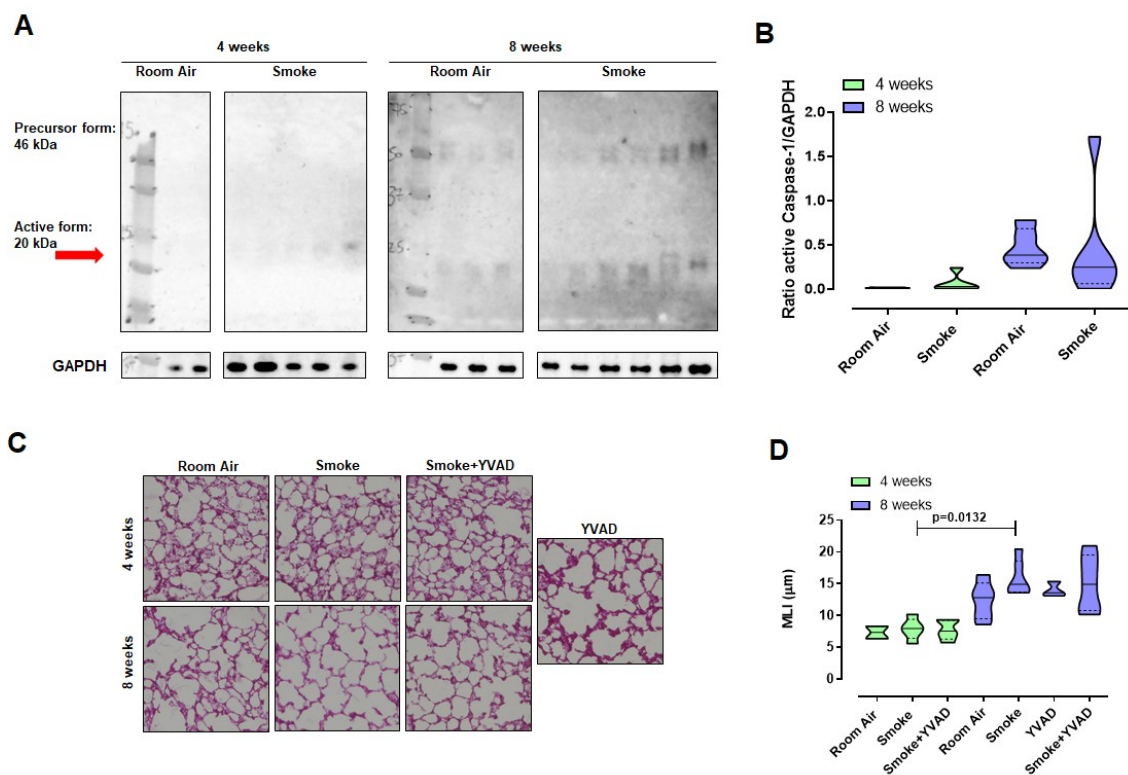
Figure 40. *Caspase-1 was not involved in the mouse model of smoke-induced COPD.*

Representative western blots (**A**) and western blotting analyses (**B**) performed on lung homogenates obtained from first-hand smoking mice showed the presence of active caspase-1 at 8, but not at 4, weeks post CS exposure. Representative histology of mouse lung after CS-exposure in presence or not of the pharmacological inhibitor of caspase-1, Ac-YVAD-cmk (YVAD, i.p.: 10 µg/mouse/twice/week) showed no differences in terms of alveolar enlargement (**C**) and MLI values (**D**) at both 4 and 8 weeks. Data are presented as violin plots showing median ± interquartile range (n = 9). Statistically significant differences were determined according to Mann Whitney t test and TWO-way ANOVA followed by Sidak's post-test, where appropriate.

5.3.4 The exposure of mice to first-hand smoking led to pulmonary recruitment of immunesuppressive cells.

It was recently emphasized that smoking has an impact on the immune system function, implying an involvement in the pathogenesis and progression of COPD (Zuo *et al.*, 2013). Therefore, we evaluated immune cell infiltration in the lung of Room Air and Smoke groups after smoke exposure and caspase-1 inhibition by means of flow cytometry analysis performed on lung homogenates. We did not observe any differences in the percentage of lung dendritic cells (DCs, identified as $CD11c^{high}$ $CD11b^{int}$ $F4/80^{neg}$) (Figure 41A) in both Room Air and smoking groups at the two experimental time points. Similarly, the inhibition of caspase-1 did not alter the scenario. Nevertheless, the phenotype of DCs was altered at the earlier time point in terms of MHC II expression, in that smoking mice at 4 weeks had higher levels of MHC II than smoking mice at 8 weeks (Figure 41B, green vs purple violin plots). In addition, although the levels of MHC II at 8 weeks post smoking were lower than those at 4 weeks, they were still higher than those for Room Air mice (Figure 41B, purple vs green violin plots). In contrast, lung DCs showed higher levels of the immunesuppressive indoleamine-2,3-dioxygenase (IDO) at 8 weeks compared to Room Air and mice exposed to CS for 4 weeks (Figure 41C, purple vs green violin plots). Interestingly, the inhibition of caspase-1 did not alter the expression MHC II (Figure 41B) and IDO (Figure 41C).

Similarly, the recruitment of macrophages (identified as $CD11c^{int}$ $CD11b^{high}$ $F4/80^{pos}$) was not altered in CS-exposed mice at both time points (Figure 41D). Interestingly, macrophages, similarly to DCs, expressed higher levels of IDO after 8 weeks than 4 weeks post smoking exposure (Figure 41E, purple vs green violin plots). To note, there were no statistical differences between Room Air and Smoke group at 8 weeks, although the median in smoking mice was higher than the other group (19 ± 4.8 vs 21.95 ± 10.6). In addition, the pharmacological inhibition of caspase-1 did not reduce lung percentage of IDO^+ macrophages, rather it significantly increased IDO^+ macrophages (Figure 41E).

Taken together these data indicate that first-hand smoking leads to an immunesuppressive lung microenvironment in mice in a caspase-1-independent manner.
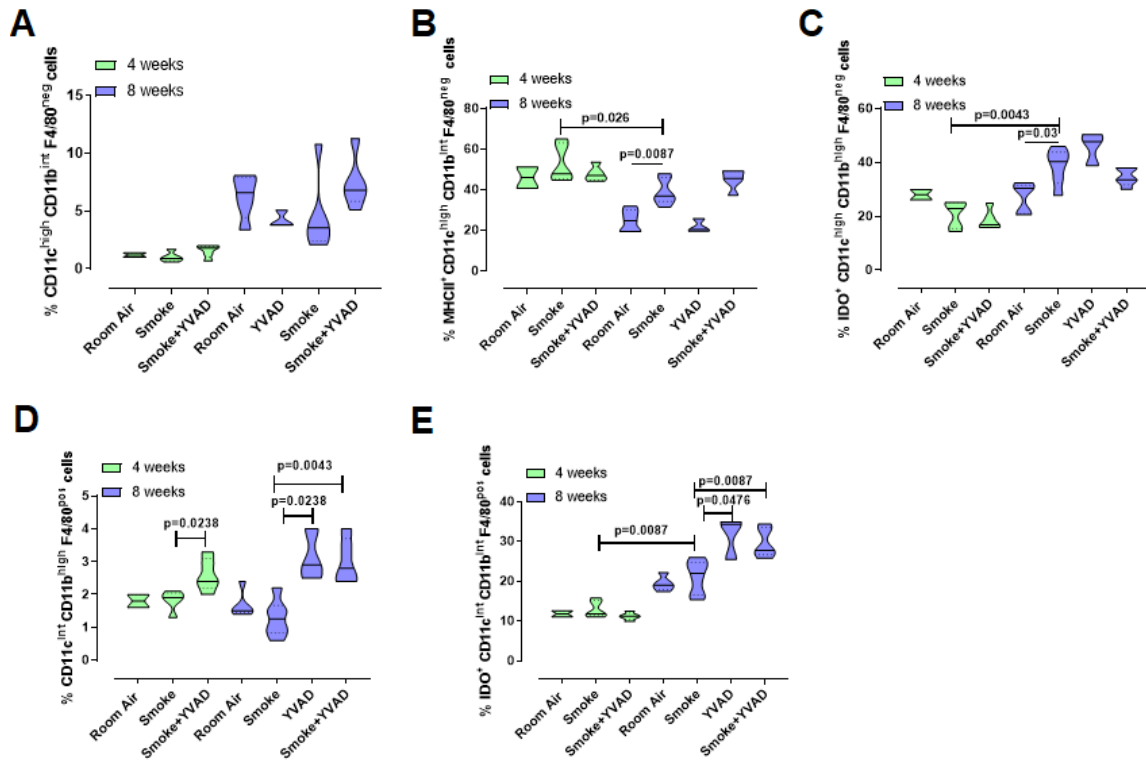
Figure 41. *First-hand smoking induced an immunesuppressive environment in the lung.*

Lungs from CS-exposed mice were digested and flow cytometry analysis was performed to identify DCs (**A**) and the expression of MHC II (**B**) and intracellular IDO (**C**). Similarly, the recruitment of macrophages (**D**) and their IDO expression (**E**) was analyzed. Data are presented as violin plots showing median ± interquartile range (n = 9). Statistically significant differences were determined according to Mann Whitney t test and TWO-way ANOVA followed by Sidak's post-test, where appropriate.

5.3.5 AIM2 inflammasome was highly expressed into lung of smoke-exposed mice.

According to our previous data (Chapter 4) AIM2 inflammasome was highly expressed in basal condition in CD14^{+} COPD-derived PBMCs and its activation was responsible for IL-1α-induced TGF-β release in a caspase-1- and caspase-4-dependent manner (Colarusso *et al.*, 2019b). Therefore, in order to understand the possible involvement of the AIM2 inflammasome in our mouse model of smoking exposure, western blotting analyses were performed on lung homogenates. The expression of AIM2 was significantly higher in smoking mice at 8 weeks than Room Air (Figure 42A, 42B, red vs black line) and Smoke group at 4 weeks (Figure 42A, 42B).
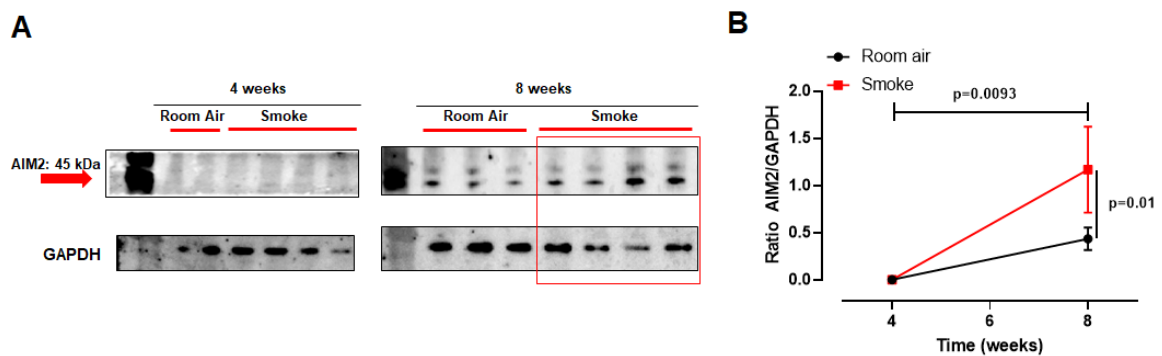

Figure 42. *AIM2 protein expression in CS-exposed mice.*

Representative (**A**) and quantitative analysis (**B**) of western blots indicated that AIM2 protein levels were higher after 8 weeks of smoke exposure. Data are represented as mean ± SEM (n = 9). Statistical analysis was performed according to TWO-way ANOVA followed by Sidak's post-test.

5.3.6 AIM2 inflammasome, IL-1α and TGF-β were highly expressed in the lung of a mouse model of carcinogen-induced lung cancer.

To pursue the main goal of this project to evaluate any potential crosstalk between COPD and lung cancer, we compared the experimental data from smoking mice to mice who were treated with a well-known carcinogen, mimicking lung adenocarcinoma (Terlizzi *et al*., 2015).

The expression of AIM2 in the lung of mice exposed to NMU was detected either by means of western blotting (Figure 43A) and confirmed by RT-PCR (Figure 43B), which showed a time-dependent increase of the receptor. The higher levels of AIM2 inflammasome in the lung of carcinogen-treated mice were associated to higher levels of IL-1α (Figure 43C) and TGF-β (Figure 43D).
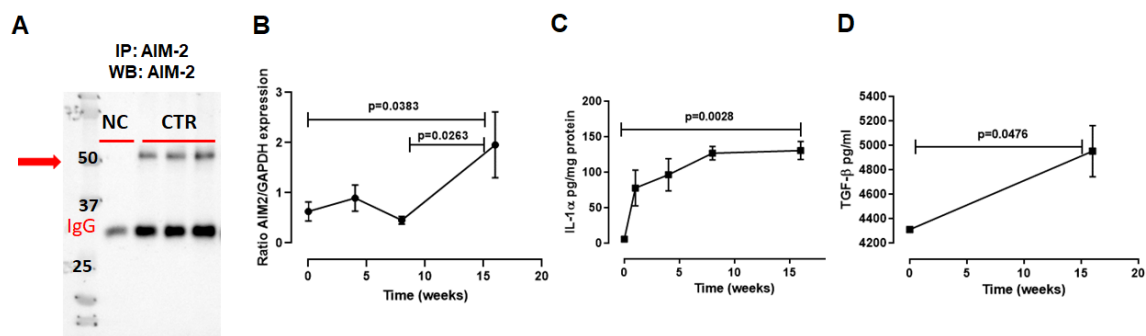
Figure 43. *Expression of AIM2, IL-1α and TGF-β in NMU-treated mice.*
Representative western blots performed on lung homogenates after immunoprecipitation in NMU-treated mice, reported as CTR (**A**) (NC stands for negative control of the antibody used for the immunoprecipitation). RT-PCR for mRNA AIM2 levels at different time points after NMU exposure, 4-8-16 weeks. The value 0 on the x axis represents naïve/non-treated mice (**B**). Levels of IL-1α in lung homogenates (**C**) and TGF-β in BAL (**D**) fluid in NMU-treated mice compared to naïve group (represented by 0 at the x axis). Data are represented as mean ± SEM (n = 15). Statistical analysis was performed according to TWO-way ANOVA followed by Sidak's post-test.

Taken together these results highlight that AIM2, IL-1α and TGF-β expression was increased in NMU-induced lung cancer. Similarly, we found that smoking increased the levels of AIM2 and IL-1α in mice. Therefore, based on these preclinical data and under patent data obtained from human samples (ImmunePharma srl intellectual property) we can suggest that AIM2 inflammasome, IL-1α and TGF-β maybe at the crossroad between COPD and lung cancer.

5.4 Conclusions

Inhalation of cigarette smoke (CS), including exposure to second-hand smoke, is the leading cause and the most common risk factor for COPD establishment, accounting for at least 80% of cases (Fricker *et al.*, 2014). During the last decades, many studies were performed in order to understand the molecular basis of COPD to find new pharmacological targets to improve the therapeutic approaches. However, both the lack of animal models that recapitulate the hallmarks of COPD in humans and the ethical limitations for using human lung COPD samples have hampered the dichotomy between COPD and lung cancer (Colarusso *et al.*, 2017). In this Chapter, to circumvent the limitations on human COPD-derived lung tissues, we used a preclinical approach. Mice were exposed both to first- and second-hand smoking. In the first case we used a nose-only exposure system which is able to mimic the inhalation profile of human smokers; in the second case, mice passively inhaled smoke produced by cigarettes burning through a whole-body exposure apparatus. We found that solely the exposure to first-hand smoking led to alveolar enlargement, a typical feature of COPD (Horvat *et al.*, 2010). In line with what reported by Beckett *et al.*, (2013), we found that CS-exposed mice presented alteration of the alveolar structure at 8 weeks post CS exposure, associated to bronchial tone impairment and IL-1α, the latter especially at earlier time point.

The overexpression of IL-1α in lung epithelium of mice exposed to smoke is involved in the development of COPD-like phenotype consisting of emphysema, lung inflammation and fibrosis (Rovina *et al.*, 2013). Moreover, the role of IL-1α, in this mouse model of smoke-induced COPD, is strongly associated to our data (Chapter 4) obtained in COPD-derived PBMCs and demonstrating that the AIM2/IL-1α axis drives the release of pro-fibrotic mediators. However, differently from COPD-derived PBMCs, the pharmacological inhibition of caspase-1 was not involved in the alteration of lung structure after smoking. In contrast, the inhibition of caspase-1 statistically reduced the levels of IL-1α and TGF-β (Chapter 4). The discrepancy between the human data on PBMCs and preclinical data in mice could stand first

on the nature of the biological samples, but more importantly on the type of cell we are looking at. In the first case, PBMCs could represent what happens in immune cells, instead in the second case, the evaluation of the inflammasome was performed in the whole murine lung, which did not have a human counterpart to be compared to. Nevertheless, it is worthy to point out that we found that in both cases, AIM2 inflammasome was involved.

To pursue the main goal of this research project we used a mouse model of lung cancer. We found that both protein and mRNA levels of AIM2 were significantly increased in mice treated with NMU compared to non-treated mice. Interestingly we found that the expression of AIM2 was time-dependent in NMU-exposed mice in the same manner as in smoking mice, indicating that AIM2 expression could augment with tumor progression. Nowadays, the precise role of AIM2 inflammasome in cancer is still elusive (Terlizzi *et al*., 2014). However, our group demonstrated that AIM2 inflammasome could play a pro-carcinogenic role in lung cancer, in that its activation in tumor-associated pDCs leads to high IL-1α levels which favor lung tumor cell proliferation (Sorrentino *et al*., 2015b). Surprisingly, we found that the levels of IL-1α and TGF-β were highly expressed in lung homogenates and BAL fluid obtained from NMU-treated mice, similar to what observed for COPD-derived PBMCs (Chapter 4) and CS-exposed mice. In support to these data, we found that human samples of lung cancer had higher levels of AIM2 protein expression than healthy paired samples (data not shown; under patent-ImmunePharma srl intellectual property).

Another important issue is the immunesuppressive environment in the lung of smoking mice. We found that smoke exposure increased the tolerogenic phenotype of DCs and macrophages, events that are usually observed in both COPD (Tsoumakidou *et al*., 2014; Kaku *et al*., 2014) and lung cancer (Lu *et al*., 2019). In sharp contrast to what reported by others (Churg *et al*., 2009), we found that the inhibition of caspase-1 did not abrogate the alveolar enlargement induced by CS exposure, although this enzyme was present in its active form in lung homogenates. To note, we found that COPD-derived PBMCs exposed to Poly dA:dT (Chapter

4) increased the levels of IL-1α and thus of TGF-β in a caspase-1-dependent manner. As reported above, this discrepancy could stand both on the nature of the samples and on the role of the structural vs hematopoietic cell in the pathogenesis of COPD.

In conclusion, in this study we demonstrated that the exposure to first-hand smoking leads to an alteration of the alveolar structure induced by CS exposure typical of human COPD and an immunesuppressive lung microenvironment which is not associated to the canonical, caspase-1-dependent, inflammasome pathway. Most importantly, we found that AIM2 inflammasome and IL-1α are at the crossroad between COPD and lung cancer in that their expression are increased in our experimental models of COPD and lung cancer, data supported by human lung cancer samples.

Although some questions are still open on the role of AIM2 and IL-1α, the data obtained so far pave the way for a novel scientific approach for COPD patients that develop lung cancer, focusing on the biology of AIM2 inflammasome.

DISCUSSION

The main goal of this PhD project was to understand the crosstalk between COPD and lung cancer, focusing on the role of the inflammasome.

Epidemiological evidence indicate that patients with COPD have a 6.35-fold higher risk to develop lung cancer compared to the normal population (Butler *et al*., 2019) and that 40% to 70% of patients diagnosed with lung cancer have evidence of COPD (Young *et al*., 2009). Chronic airway inflammation seems to play a critical role in lung carcinogenesis among COPD patients and it may represent a link between these pathologies in that lung inflammation is one of the main feature of COPD (Colarusso *et al*., 2017), and it represents the seventh hallmark of cancer (Colotta *et al*., 2009). Chronic inflammation typical of COPD and lung cancer patients could reflect the site of deposition of inhaled irritants, especially cigarette smoke and environmental pollution, shared risk factors by the two diseases (Valavanidis *et al*., 2013).

The inflammasome, an intracellular multimeric complex associated to IL-1-like pro-inflammatory cytokines release, was suggested to be involved in COPD pathogenesis (Colarusso *et al*., 2017). Besides, Prof. Sorrentino's group already demonstrated that it may play a pro-carcinogenic role in lung cancer establishment (Terlizzi *et al*., 2015; Sorrentino *et al*., 2015b; Terlizzi *et al*., 2016). While inflammasomes play crucial roles in the clearance of pathogens, the precise role of inflammasome/s in COPD and lung cancer establishment and progression is still unclear.

Therefore, the rationale of this project was that, defined that the inflammasome plays a role in both diseases, then it could be at the crossroad for both the establishment of COPD and lung cancer. Another issue that prompted us to focus on the inflammasome in both pathologies was that it was demonstrated that oxidative stress, double strand-DNA (dsDNA) and other DAMPs

can activate the inflammasome. In particular, because it is well known that both air pollution and cigarette smoke are high-risk factors for both COPD and lung cancer, and that they are, either directly or indirectly, able to induce the release/generation of oxidative stress-related DAMPs (Valavanidis *et al.*, 2013), they could trigger the inflammasome with an ensuing chronic inflammation, pivotal driver of both diseases (Colotta *et al.*, 2009; Colarusso *et al.*, 2017).

In Chapter 1 we found that both smoking and air pollution can prompt toward pulmonary inflammation in an IL-1-like manner. The exposure of PBMCs isolated from smokers to Soot (pyrolytic combustion-derived UFPs, 80-120 nm diameter), led to an inflammatory process that was responsible for IL-1α, IL-18 and IL-33 release and was associated to the activation of the canonical, caspase-1-dependent, NLRP3 inflammasome (De Falco *et al*, 2017b). This effect was not assessed in healthy non-smoker subjects. Because inflammation plays a key role in cancer establishment, and air pollution was defined by IARC as cancer-causing agent (Loomis *et al.*, 2013), these results indicate that smokers, a high-risk population, once exposed to air pollution may be more susceptible to the inflammatory processes involved into lung cancer development, than non-smokers. Based on the strict relationship between air pollution and the pathogenesis of COPD, we went on by investigating the possible role of the inflammasome in COPD after the exposure to ultrafine particles (non-pyrolytic combustion-derived UFPs, 2-40 nm diameter). We found that UFPs mimicking small-size pollutants induced the release of IL-18 and IL-33, but not of IL-1α and IL-1β, from PBMCs obtained from COPD patients undergoing an exacerbation status (Chapter 2). Instead, healthy non-smoker and smoker subjects were not susceptible to the smaller UFPs, defined as Soot and NOC particles. Most importantly, the release of IL-18 and IL-33 from unstable/exacerbated COPD patients induced by UFPs was not abrogated by the pharmacological inhibition of caspase-1, NLRP3 and caspase-8. These effects were associated to mitochondria-derived oxidative stress, which was not countered by 8-oxoguanine DNA glycosylase 1 (OGG1), enzyme involved in repairing

mitochondria-derived oxidative stress. OGG1 was induced in both non-smokers and smokers than COPD, implying that the repairing engine for DNA damage was dysfunctional in COPD-derived circulating cells than healthy non-smokers and smokers (De Falco *et al*., 2017). Taken together these data imply that smoking and air pollution in COPD alters the genomic/epigenomic signature, that however needs to be further investigated in our experimental conditions. Nevertheless, the presence of IL-18 and IL-33 in immune cells is increased in inflammation, a condition which is strictly correlated to smoke- and air pollution-induced oxidative stress (Valavanidis *et al*., 2013). IL-18 and IL-33, as immunostimulatory cytokines, can promote and regulate lung and systemic immunity by stimulating the production of Th1-like and Th2-like mediators (Nakanishi *et al*., 2001; Chan *et al*., 2019). It is to point out that, besides their immunological activity, these cytokines play a critical role in lung structural cells (lung alveolar type II pneumocytes and bronchial epithelial cells) where could influence the development of chronic airway inflammation and tissue remodelling (Yasuda *et al*., 2012; Kearley *et al*., 2015).

These data were, though, conducted on circulating cells. Therefore, to circumvent ethical and *in vitro* limitations, we decided to investigate the effects of environmental pollutants and smoking in the respiratory tract by using mouse model (Chapter 3). The exposure to pollutants led a state of latent lung inflammation and bronchial dysfunction in mice, associated to lung recruitment of innate immune cells in their immunesuppressive phenotype. PM10, PM1 and Soot particles exposure *in vivo* led to a lung microenvironment highly populated by tolerogenic DCs which were not able to present antigens, and together with Arginase I positive macrophages and MDSCs, favored the establishment of an immunesuppressive microenvironment, as further confirmed by higher levels of IL-10. Combining together the data on this mouse model (Colarusso *et al*., 2019) and circulating cells obtained from non-smokers, which differently from the murine data were not responsive to NLRP3 and AIM2 inflammasome activation (Chapter 4, Figure 30A; Colarusso *et al*., 2019b), we could speculate

that the release of IL-1-like cytokines after air pollution starts from structural cells which then instruct the recruited innate cells to prompt toward a tolerogenic environment, which on one side could fire off an acute inflammation but on the other could lead to latent patterns which could behave as adjuvant for both COPD and lung cancer establishment. In support to this hypothesis, that still needs to be proved, healthy non-smoker-derived PBMCs released IL-10 after the exposure to air pollutants (Chapter 1, Figure 9; De Falco et al., 2017b).

To carry on the investigation regarding the role of the inflammasome in COPD, we stimulated PBMCs with both LPS±ATP to trigger NLRP3, or Poly dA:dT to trigger AIM2 inflammasome. We found that, although both NLRP3 and AIM2 receptors were expressed in CD14^{+} exacerbated COPD-derived PBMCs compared to healthy non- and smoker subjects (Chapter 2 and 4; De Falco et al., 2017; Colarusso et al., 2019b), the sole AIM2 inflammasome was functional in than its stimulation led to the release of IL-1α, but not of IL-18, IL-1β and IL-33. Interestingly IL-1α release was caspase-1- and caspase-4-dependent, and strictly correlated to the basal levels of 8-hydroxy-2-deoxyguanosine (8-OH-dG), well-known marker for DNA damage derived from oxidative stress (Valavanidis et al., 2009), which levels were further increased after AIM2 activation (Chapter 4; Colarusso et al., 2019b). This latter result was pivotal to understand why, although the strong link between NLRP3 activation and oxidative stress, NLRP3 receptor was not responsive in COPD-derived PBMCs. Indeed, as reported by Shimada et al., (2012) 8-OH-dG can sequester NLRP3 avoiding its activation. Moreover, we found that AIM2-dependent IL-1α release was responsible for TGF-β release, an immunesuppressive cytokine that can drive pro-fibrotic processes during COPD exacerbation (Barnes, 2013). It is to point out that these effects were not observed in PBMCs isolated from stable COPD patients.

These data were of great relevance because, for the first time to our knowledge, they highlighted that AIM2 inflammasome, via the canonical and non-canonical pathway, plays a critical role in the exacerbation stage of COPD. To circumvent the limitation of exacerbated

COPD-derived circulating cells and the difficulty to obtain lung samples from COPD patients, we moved on by evaluating the role of the inflammasome in an *in vivo* complex by taking advantage of a mouse model of cigarette smoke-induced COPD (Chapter 5). Solely the exposure to first-hand smoking, which mimics the inhalation profile of smokers, induced bronchial dysfunction at shorter time point (4 weeks of exposure) and alveolar enlargement after 8 weeks. Moreover, lungs of first-hand smoking mice were populated by immunesuppressive DCs and macrophages, expressing higher levels of indoleamine-2,3, dioxygenase (IDO), an enzyme that makes innate immune cells unable to induce cytotoxic and effective adaptive immunity (Hwu *et al*., 2000). To date, the inhibition of caspase-1 did not reduce the alveolar enlargement and did not alter lung immune microenvironment induced by smoke exposure, although this enzyme was present in its active form in lung homogenates. This could further support our previous hypothesis that structural cells play a significant role at instructing innate immune cells and thus the ensuing microenvironment. This effect is likely to be caspase-1-independent.

It is noteworthy that the inhalation of smoke led to a state of inflammation characterized by high levels of IL-1α in lung homogenates at 4 weeks, as observed in human COPD circulating cells after AIM2 activation (Chapter 4; Colarusso *et al*., 2019b). Moreover, the expression of AIM2 was time-dependently increased in the airways of smoking mice. The presented data were of crucial importance to point at IL-1α and AIM2 inflammasome as critical players in both COPD-derived PBMCs during the exacerbation stage of the disease and in our mouse model of COPD induced by smoke inhalation.

In order to pursue the main goal of this project and understand whether the inflammasome is at the crosstalk between COPD and lung cancer, we considered crucial to compare the above results to a mouse model of carcinogen-induced lung cancer. We found that IL-1α and TGF-β were highly expressed in lung homogenates and BAL fluid obtained from NMU-treated mice. These data highlight a first crosstalk between COPD and lung cancer, in that we found that

these two cytokines are highly expressed both in COPD (blood-derived cells and mouse model) and in our experimental model of lung cancer. Therefore, driven by these results, we asked about the role of AIM2 inflammasome in lung cancer. We proved that both protein and mRNA levels of AIM2 were significantly increased in mice treated with NMU compared to naïve (non-treated mice) in a time-dependent manner. In support to these data, AIM2 expression was evaluated in human lung cancerous tissues, and was higher than non-tumor tissues (data under patent-ImmunePharma srl intellectual property).

Altogether these data could suggest that air pollution and cigarette smoke, two common risk factors for COPD and lung cancer (who.int/gard/publications/Risk%20factors.pdf), can lead the activation of the inflammasome complex in that they induced the release of IL-1-like cytokines. This effect was observed both in circulating cells and in lung structural cells (Figure 44). However, it is to underlie that whether on one side IL-1-like cytokines were released in a caspase-1-dependent manner by circulating cells derived from healthy subjects after treatment with air pollutants (Chapter 1; De Falco *et al*., 2017b), and after AIM2 stimulation from COPD-derived PBMCs (Chapter 4; Colarusso *et al*., 2019b), on the other, smoke- and PMx-induced inflammation and immunesuppression in lung structural cells (*in vivo* exposure) seemed to be caspase-1-independent (Chapter 5 and 3; Colarusso *et al*., 2019). Based on these data, we could speculate that air pollution and smoke stimulate the canonical, caspase-1-dependent, inflammasome pathway in circulating cells, but induce the activation of the non-canonical, caspase-1-independent, inflammasome pathway in structural cells (Figure 44).
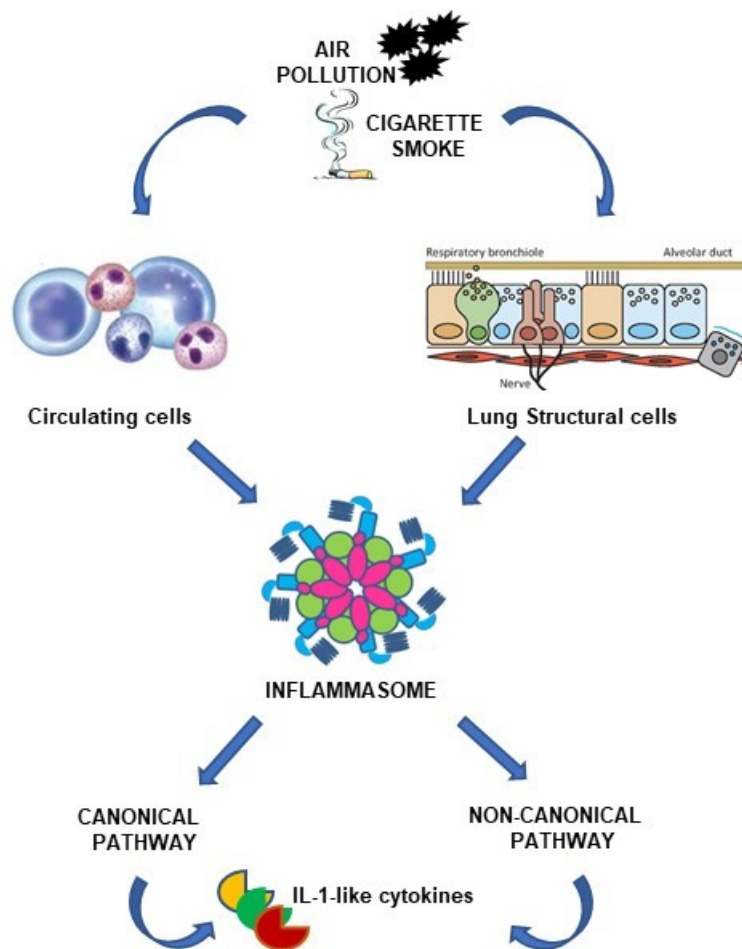
Figure 44. *Air pollution and cigarette smoke lead to inflammasome activation*.

Data presented in this PhD research suggested that air pollution and cigarette smoke, risk factors for COPD and lung cancer, induce the release of IL-1-like cytokines in a canonical, caspase-1-dependent, inflammasome pathway in circulating cells. In sharp contrast, caspase-1 is not involved in air pollution- and smoke-induced inflammasome activation in lung structural cells, suggestion that the ensuing IL-1-like cytokines release could be dependent on a non-canonical pathway.

In conclusion, data presented in this PhD research demonstrate that AIM2 and IL-1α could be at the crossroad between COPD and lung cancer in that their expression are increased both in COPD-derived circulating cells and our preclinical model of COPD, and in our mouse model of carcinogen-induced lung cancer, supported by human lung cancer samples (Figure 45).
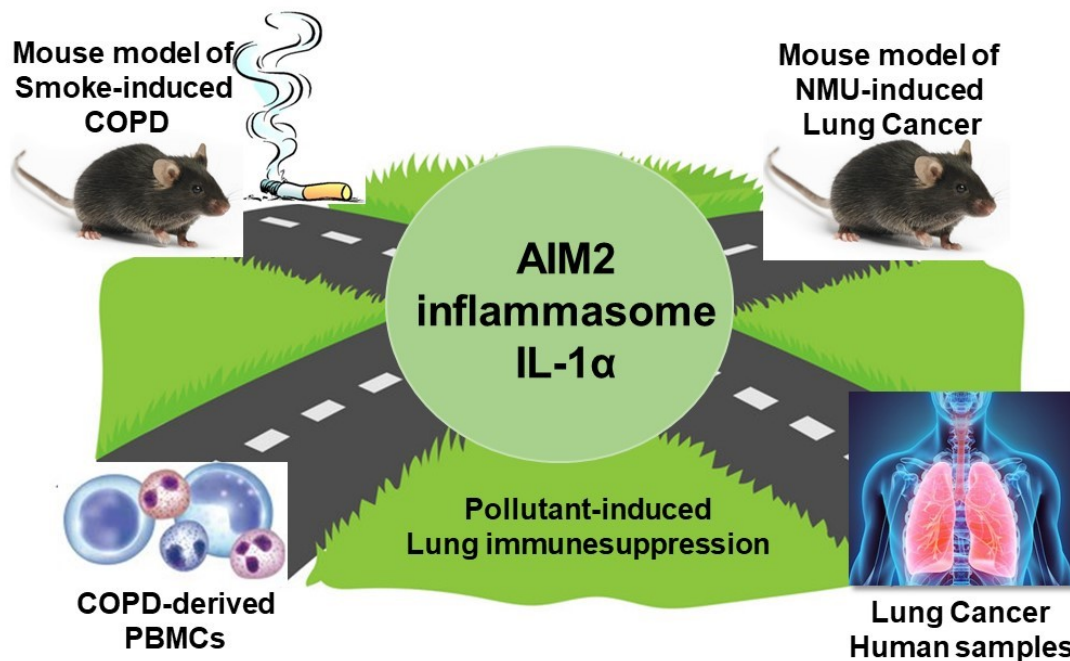
Figure 45. *AIM2 and IL-1α: suggested crossroad between COPD and lung cancer*.

These results improve the knowledge on the inflammasome biology in COPD and lung cancer and pave the way for new therapeutic options for the management of exacerbated COPD patients focusing on AIM2 inflammasome. It is to point out that, whether for lung cancer previous studies have already suggested the possible pro-carcinogenic role of IL-1α and AIM2, both in humans (Sorrentino *et al*., 2015b) and mice (Terlizzi *et al*., 2015, Terlizzi *et al*., 2016), their role in COPD establishment and progression is far from clear.

Nevertheless, many questions still remain unanswered and further studies are needed in order to figure out the molecular mechanism/s to better define AIM2 and IL-1α as oncogenic in COPD patients. Understanding the pro-tumorigenic activity of AIM2 inflammasome and IL-1α in COPD and lung cancer may contribute to the identification of specific biological targets, that on one side could help early identify patients with COPD who are more likely to develop lung cancer and improve the screening strategy, and on the other open new therapeutic perspectives.

BIBLIOGRAPHY

Barnes, P. J., (2008), Immunology of asthma and chronic obstructive pulmonary disease. *Nature Reviews Immunology*, **8**, 183-192. DOI: 10.1038/nri2254.

Barnes, P. J., (2016), Inflammatory mechanisms in patients with chronic obstructive pulmonary disease, *J Allergy Clin Immunol*, **138** (1), 16-27. doi: 10.1016/j.jaci.2016.05.011.

Barnes, P.J., (2013), Corticosteroid resistance in patients with asthma and chronic obstructive pulmonary disease, *J Allergy Clin Immunol*, **131** (3), 636-45. doi: 10.1016/j.jaci.2012.12.1564.

Barton, D. B., Betteridge, B. C., Earley, T. D., Curtis, C. S., Robinson, A. B., and Reynolds, P. R., (2014), Primary alveolar macrophages exposed to diesel particulate matter increase RAGE expression and activate RAGE signaling, *Cell Tissue Res*, **358** (1), 229–238. doi: 10.1007/s00441-014-1905-x.

Beckett, E. L., Stevens, R. L., Jarnicki, A. G., Kim, R. Y., Hanish, I., Hansbro, N. G., Deane, A., Keely, S., Horvat, J. C., Yang, M., Oliver, B. G., van Rooijen, N., Inman, M. D., Adachi, R., Soberman, R. J., Hamadi, S., Wark, P. A., Foster, P. S., and Hansbro, P. M., (2013), A new short-term mouse model of chronic obstructive pulmonary disease identifies a role for mast cell tryptase in pathogenesis, *J Allergy Clin Immunol*, **131** (3), 752-62. doi: 10.1016/j.jaci.2012.11.053.

Bengalli, R., Molteni, E., Longhin, E., Refsnes, M., Camatini, M., and Gualtieri, M., (2013), Release of IL-1 β triggered by Milan summer PM10: molecular pathways involved in the cytokine release, *Biomed Res Int*, **2013**, 158093, doi: 10.1155/2013/158093.

Borthwick, L. A., (2016), The IL-1 cytokine family and its role in inflammation and fibrosis in the lung, *Semin Immunopathol*, **38**, 517–534. DOI 10.1007/s00281-016-0559-z.

Bowler, R. P., Barnes, P. J., and Crapo, J. D., (2004), The role of oxidative stress in chronic obstructive pulmonary disease, *COPD*, **1** (2), 255-77. DOI: 10.1081/copd-200027031.

Butler, S. J., Ellerton, L., Goldstein, R.S., and Brooks, D., (2019), Prevalence of lung cancer in chronic obstructive pulmonary disease: A systematic review, *Respiratory Medicine*: *X*, **1**, 100003. https://doi.org/10.1016/j.yrmex.2019.100003

Calabrò, E., Randi, G., La Vecchia, C., Sverzellati, N., Marchianò, A., Villani, M., Zompatori, M., Cassandro, R., Harari, S., and Pastorino, U., (2010), Lung function predicts lung cancer risk in smokers: a tool for targeting screening programmes, *Eur Respir J*, **35** (1), 146-51. doi: 10.1183/09031936.00049909.

Calverley, P. M. A., Sethi, S., Dawson, M., Ward, C. K., Finch, D. K., Penney, M., Newbold, P., ans van der Merwe, R., (2017), A randomised, placebo-controlled trial of anti-interleukin-1 receptor 1 monoclonal antibody MEDI8968 in chronic obstructive pulmonary disease, *Respir Res*, **18** (1),153. doi: 10.1186/s12931-017-0633-7.

Carr, L. L., Jacobson, S., Lynch, D. A., Foreman, M. G., Flenaugh, E. L., Hersh, C. P., Sciurba, F. C., Wilson, D. O., Sieren, J. C., Mulhall, P., Kim, V., Kinsey, C. M., and Bowler, R. P., (2018), Features of COPD as Predictors of Lung Cancer, *Chest*, **153** (6), 1326-1335. doi: 10.1016/j.chest.2018.01.049.

Cassee, F. R., Héroux, M. E., Gerlofs-Nijland, M. E., and Kelly, F. J., (2013), Particulate matter beyond mass: recent health evidence on the role of fractions, chemical constituents and sources of emission, *Inhal Toxicol*, **25**, 802–12. doi: 10.3109/08958378.2013.850127.

Casson, C. N., Copenhaver, A. M., Zwack, E. E., Nguyen, H. T., Strowig, T., Javdan, B., Bradley, W. P., Fung, T. C., Flavell, R. A., Brodsky, I. E., and Shin, S., (2013), Caspase-11 activation in response to bacterial secretion systems that access the host cytosol, *PLoS Pathog*, **9** (6), e1003400. doi: 10.1371/journal.ppat.1003400.

Celli, B. R., and Wedzicha, J. A., (2019), Update on Clinical Aspects of Chronic Obstructive Pulmonary Disease, *N Engl J Med*, **381**(13), 1257-1266. doi: 10.1056/NEJMra1900500.

Chan, B. C. L., Lam, C. W. K., Tam, L. S., and Wong, C. K., (2019), IL33: Roles in Allergic Inflammation and Therapeutic Perspectives, *Front Immunol*, **10**, 364. doi: 10.3389/fimmu.2019.00364.

Churg, A., Zhou, S., Wang, X., Wang, R., and Wright, J., (2009), The role of interleukin-1beta in murine cigarette smoke-induced emphysema and small airway remodeling, *Am J Respir Cell Mol Biol*, **40**, 482–490. doi: 10.1165/rcmb.2008-0038OC.

Colarusso, C., De Falco, G., Terlizzi, M., Roviezzo, F., Cerqua, I., Sirignano, M., Cirino, G., Aquino, R. P., Pinto, A., D'Anna, A., and Sorrentino R., (2019), The Inhibition of Caspase-1- Does Not Revert Particulate Matter (PM)-Induced Lung Immunesuppression in Mice, *Front Immunol*, **10**, 1329. doi: 10.3389/fimmu.2019.01329.

Colarusso, C., Terlizzi, M., Molino, A., Imitazione, P., Somma, P., Rega, R., Saccomanno, A., Aquino, R. P., Pinto, A., and Sorrentino, R., (2019b), AIM2 Inflammasome Activation Leads to IL-1α and TGF-β Release From Exacerbated Chronic Obstructive Pulmonary Disease-Derived Peripheral Blood Mononuclear Cells, *Front Pharmacol*, **10**, 257. doi: 10.3389/fphar.2019.00257.

Colarusso, C., Terlizzi, M., Molino, A., Pinto, A., and Sorrentino, R., (2017), Role of the inflammasome in chronic obstructive pulmonary disease (COPD), *Oncotarget*, **8** (47), 81813-81824. doi: 10.18632/oncotarget.17850.

Colotta, F., Allavena, P., Sica, A., Garlanda, C., and Mantovani, A., (2009), Cancer-related inflammation, the seventh hallmark of cancer: links to genetic instability, *Carcinogenesis*, **30** (7), 1073–1081. DOI: 10.1093/carcin/bgp127

D'Anna, A., (2009), Combustion-formed nanoparticles, *Proc Combust Inst*, **32**, 593–613. doi:10.1016/j.proci.2008.09.005.

De Falco, G., Colarusso, C., Terlizzi, M., Popolo, A., Pecoraro, M., Commodo, M., Minutolo, P., Sirignano, M., D'Anna, A., Aquino, R. P., Pinto, A., Molino, A., and Sorrentino R., (2017) Chronic Obstructive Pulmonary Disease-Derived Circulating Cells Release IL-18 and IL-33 under Ultrafine Particulate Matter Exposure in a Caspase-1/8-Independent Manner, *Front Immunol*, **26**, 8:1415. doi: 10.3389/fimmu.2017.01415.

De Falco, G., Terlizzi, M., Sirignano, M., Commodo, M., D'Anna, A., Aquino, R. P., Pinto, A., and Sorrentino, R., (2017b), Human peripheral blood mononuclear cells (PBMCs) from smokers release higher levels of IL-1-like cytokines after exposure to combustion-generated ultrafine particles, *Sci Rep*, **7**, 43016. doi: 10.1038/srep43016.

De Nardo, D., De Nardo, C. M., and Latz, E., (2014), New Insights into Mechanisms Controlling the NLRP3 Inflammasome and Its Role in Lung Disease, *The Americal Journal of Pathology*, **184** (1), 42–54. doi: 10.1016/j.ajpath.2013.09.007.

de Torres, J. P., Marín, J. M., Casanova, C., Cote, C., Carrizo, S., Cordoba-Lanus, E., Baz-Dávila, R., Zulueta, J. J., Aguirre-Jaime, A., Saetta, M., Cosio, M. G., and Celli, B. R., (2011), Lung cancer in patients with chronic obstructive pulmonary disease-- incidence and predicting factors, *Am J Respir Crit Care Med*, **184** (8), 913-9. doi: 10.1164/rccm.201103-0430OC.

Di Stefano, A., Caramori, G., Barczyk, A., Vicari, C., Brun, P., Zanini, A., Cappello, F., Garofano, E., Padovani, A., Contoli, M., Casolari, P., Durham, A. L., Chung, K. F., Barnes, P. J., Papi, A., Adcock, I., and Balbi, B., (2014), Innate immunity but not NLRP3 inflammasome activation correlates with severity of stable COPD, *Thorax*, **69**, 516-24. doi: 10.1136/thoraxjnl-2012-203062.

Donaldson, K., Stone, V., Clouter, A., Renwick, L., and MacNee, W., (2001), Ultrafine particles, *Occup Environ Med*, **58** (3), 211-6, 199. DOI: 10.1136/oem.58.3.211.

Donaldson, K., Tran, L., Jimenez, L. A., Duffin, R., Newby, D. E., Mills, N., MacNee, W., and Stone, V., (2005), Combustion-derived nanoparticles: a review of their toxicology following inhalation exposure, *Part Fibre Toxicol*, **2**, 10. DOI: 10.1186/1743-8977-2-10.

Durham, A. I., and Adcock, I. M., (2015), The relationship between COPD and lung cancer, *Lung Cancer*, **90**, 121-127. doi: 10.1016/j.lungcan.2015.08.017.

Eisner, M. D., Anthonisen, N., Coultas, D., Kuenzli, N., Perez-Padilla, R., Postma, D., Romieu, I., Silverman, E. K., and Balmes, J. R., (2010), Novel Risk Factors and the Global Burden of Chronic Obstructive Pulmonary Disease, *Am J Respir Crit Care Med*; **182** (5), 693–718. https://doi.org/10.1164/rccm.200811-1757ST.

Eltom,S., Belvisi, M. G, Stevenson, C. S., Maher, S. A., Dubuis, E., Fitzgerald, K. A., and Birrell, M. A., (2014), Role of the inflammasome caspase1/11-IL-1/18 axis in cigarette smoke driven airway inflammation: an insight into the pathogenesis of COPD, *PLoS One*, **9** (11), e112829. doi: 10.1371/journal.pone.0112829.

Eric, A., (2011). Inaugural article: estrogen induces apoptosis in estrogen deprivation-resistant breast cancer through stress responses as identified by global gene expression across time, *Proc. Natl. Acad. Sci. U.S.A.*, **108**, 18879–18886. 10.1073/pnas.1115188108

Faner, R., Sobradillo, P., Noguera, A., Gomez, C., Cruz, T., Lopez-Giraldo, A., Ballester, E., Soler, N., Arostegui, J. I., Pelegrin, P., Rodriguez-Roisin, R., Yagüe, J., Cosio, B. G., Juan, M., and Agustí, A., (2016), The inflammasome pathway in stable COPD and acute exacerbations, *ERJ Open Res*, **2** (3), 00002-2016. doi:10.1183/23120541.0000-2016.

Franklin, B. S., Bossaller, L., De Nardo, D., Ratter, J. M., Stutz, A., Engels, G., Brenker, C., Nordhoff, M., Mirandola, S. R., Amoudi, A., Mangan, M. S., Zimmer, S., Monks, B. G., Fricke, M., Schmidt, R. E., Espevik, T., Jones, B., Jarnicki, A. G., Hansbro, P. M., Busto, P., Marshak-Rothstein, A., Hornemann, S., Aguzzi, A., Kastenmüller, W., and Latz, E., (2014), The adaptor ASC has extracellular and 'prionoid' activities that propagate inflammation. *Nat Immunol*, **15**, 727–37. doi: 10.1038/ni.2913.

Freire, J., Ajona, D., de Biurrun, G., Agorreta, J., Segura, V., Guruceaga, E., Bleau, A., Pio, R., Blanco, D., and Montuenga, L. M., (2013), Silica-induced Chronic Inflammation Promotes Lung Carcinogenesis in the Context of an Immunosuppressive Microenvironment, *Neoplasia*, **15** (8), 913–924. doi: 10.1593/neo.13310.

Fricker, M., Deane, A., and Hansbro, P. M., (2014), Animal models of chronic obstructive pulmonary disease, *Expert Opin Drug Discov*, **9** (6), 629-45. doi: 10.1517/17460441.2014.909805.

Gaidt, M. M., Ebert, T. S., Chauhan, D., Schmidt, T., Schmid-Burgk, J. L., Rapino, F., Robertson, A. A., Cooper, M. A., Graf, T., and Hornung, V., (2016), Human Monocytes Engage an Alternative Inflammasome Pathway, *Immunity*, **44**, 833-46. doi: 10.1016/j.immuni.2016.01.012.

GBD 2015 Chronic Respiratory Disease Collaborators. (2017), Global, regional, and national deaths, prevalence, disability-adjusted life years, and years lived with disability for chronic obstructive pulmonary disease and asthma, 1990–2015: a systematic analysis for the Global Burden of Disease Study 2015, *Lancet Respir Med*, **5** (9), 691–706. http://dx.doi.org/10.1016/S2213-2600(17)30293-X

Gross, O., Thomas, C. J., Guarda, G., and Tschopp, J., (2011), The inflammasome: an integrated view. *Immunological Reviews*, **243**, 136–151. doi: 10.1111/j.1600-065X.2011.01046.x.

Gross, O., Yazdi, A.S., Thomas, C.J., Masin, M., Heinz, L.X., Guarda, G., Quadroni, M., Drexler, S.K., and Tschopp, J., (2012), Inflammasome activators induce interleukin-1α secretion via distinct pathways with differential requirement for the protease function of caspase-1. *Immunity*, **36** (3), 388–400. doi: 10.1016/j.immuni.2012.01.018.

Heng, T. S., and Painter, M. W., (2008), The Immunological Genome Project: networks of gene expression in immune cells, *Nat Immunol*, **9**, 1091-1094. doi: 10.1038/ni1008-1091.

Hirota, J., Hirota, S., Warner, S., Stefanowicz, D., Shaheen, F., Beck, P. L., Macdonald, J. A., Hackett, T. L., Sin, D. D., Van Eeden, S., and Knight, D. A., (2012), The airway epithelium nucleotide-binding domain and leucine-rich repeat protein 3 inflammasome is active by urban particulate matter, *J Allergy Clin Immunol*, **129** (4), 1116-1125.e6. doi: 10.1016/j.jaci.2011.11.033.

Hoesel, B., and Schmid, J. A., (2013), The complexity of NF-κB signaling in inflammation and cancer, *Mol. Cancer*, **12**, 86. doi: 10.1186/1476-4598-12-86.

Horvat, J. C., Starkey, M. R., Kim, R. Y., Phipps, S., Gibson, P. G., Beagley, K. W., Foster, P. S., and Hansbro, P. M., (2010), Early-life chlamydial lung infection enhances allergic airways disease through age-dependent differences in immunopathology, *J Allergy Clin Immunol*, **125** (3), 617-25, 625.e1-625.e6. doi: 10.1016/j.jaci.2009.10.018.

Hwu, P., Du, M. X., Lapointe, R., Do, M., Taylor, M. W., and Young, H. A., (2000), Indoleamine 2,3-dioxygenase production by human dendritic cells results in the inhibition of t cell proliferation, *J Immunol*, **164** (7), 3596–3599.

Jiang, X. Q., Mei, X. D., and Feng, D., (2016), Air pollution and chronic airway diseases: what should people know and do? *J Thorac Dis*, **8** (1), E31-40. doi: 10.3978/j.issn.2072-1439.2015.11.50.

John-Schuster, G., Hager, K., Conlon, T. M., Irmler, M., Beckers, J., Eickelberg, O., and Yildirim, A. Ö., (2014), Cigarette smoke-induced iBALT mediates macrophage activation in a B cell-dependent manner in COPD, *Am J Physiol Lung Cell Mol Physiol*, **307** (9), L692-706. doi: 10.1152/ajplung.00092.2014.

Justo, O. R., Simioni, P. U., Gabriel, D. L., Tamashiro, W. M., Rosa Pde, T., and Moraes, Â. M., (2015), Evaluation of in vitro anti-inflammatory effects of crude ginger and rosemary extracts obtained through supercritical CO_2 extraction on macrophage and tumor cell line: the influence of vehicle type, *BMC Complement Altern Med*, **15**, 390. doi: 10.1186/s12906-015-0896-9.

Kaku, Y., Imaoka, H., Morimatsu, Y., Komohara, Y., Ohnishi, K., Oda, H., Takenaka, S., Matsuoka, M., Kawayama, T., Takeya, M., and Hoshino, T., (2014), Overexpression of CD163, CD204 and CD206 on alveolar macrophages in the lungs of patients with severe chronic obstructive pulmonary disease, *PLoS One*, **9** (1),e87400. doi: 10.1371/journal.pone.0087400.

Kearley, J., Silver, J. S., Sanden, C., Liu, Z., Berlin, A. A., White, N., Mori, M., Pham, T. H., Ward, C. K., Criner, G. J., Marchetti, N., Mustelin, T., Erjefalt, J. S., Kolbeck, R., and Humbles, A. A., (2015), Cigarette smoke silences innate lymphoid cell function and facilitates an exacerbated type I interleukin-33-dependent response to infection, *Immunity*, **42**, 566–579.

Kim, R. Y., Pinkerton, J. W., Gibson, P. G., Cooper, M. A., Horvat, J. C., and Hansbro, P. M., (2015), Inflammasomes in COPD and neutrophilic asthma, *Thorax*, **70**, 1199-1201. doi: 10.1136/thoraxjnl-2014-206736.

Knüppel, L., Ishikawa, Y., Aichler, M., Heinzelmann, K., Hatz, R., Behr, J., Walch, A., Bächinger, H. P., Eickelberg, O., and Staab-Weijnitz, C. A., (2017), A Novel Antifibrotic Mechanism of Nintedanib and Pirfenidone. Inhibition of collagen fibril assembly, *Am. J. Respir. Cell Mol. Biol*, **57** (1), 77–90. doi: 10.1165/rcmb.2016-0217OC.

Lasithiotaki, I., Tsitoura, E., Samara, K. D., Trachalaki, A., Charalambous, I., Tzanakis, N., and Antoniou, K. M., (2018), NLRP3/Caspase-1 inflammasome activation is decreased in alveolar macrophages in patients with lung cancer, *PLoS One*, **13** (10):e0205242. doi: 10.1371/journal.pone.0205242. eCollection 2018.

Lee, S., Suh, G. Y., Ryter, S. W., Choi, and A. M. K., (2016), Regulation and Function of the Nucleotide Binding Domain Leucine-Rich Repeat-Containing Receptor, Pyrin Domain-Containing-3 Inflammasome in Lung Disease, *Am J Respir Cell Mol* Biol, **54** (2), 151-160. DOI: 10.1165/rcmb.2015-0231TR.

Li, C., Zhihong, H., Wenlong, L., Xiaoyan, L., Qing, C., Wenzhi, L., Siming, X., and Shengming, L., (2016), The Nucleotide-Binding Oligomerization Domain-Like Receptor Family Pyrin Domain-Containing 3 Inflammasome Regulates Bronchial Epithelial Cell Injury and Proapoptosis after Exposure to Biomass Fuel Smoke, *Am J Respir Cell Mol Biol*, **55** (6), 815-824. DOI: 10.1165/rcmb.2016-0051OC.

Li, J., Li, W. X., Bai, C., and Song, Y., (2017), Particulate matter-induced epigenetic changes and lung cancer, *Clin Respir J*, **11** (5), 539-546. doi: 10.1111/crj.12389.

Li, N., Ragheb, K., Lawler, G., Sturgis, J., Rajwa, B., Melendez, J. A., and Robinson, J.P., (2003), Mitochondrial complex I inhibitor rotenone induces apoptosis through enhancing mitochondrial reactive oxygen species production, *J Biol Chem*, **278** (10), 8516–25.10.1074/jbc.M210432200.

Lodovici, M., and Bigagli, E., (2011), Oxidative Stress and Air Pollution Exposure, *Journal of Toxicology*, **2011**, 484074. doi: 10.1155/2011/487074.

Loke, M. S. J., Mann, L., Lewis, G. R., and Thomas, P. S., (2014), Oxidative Stress in Lung Cancer, *Cancer Oxidative Stress and Dietary Antioxidants*, **3**, 23-32. https://doi.org/10.1016/B978-0-12-405205-5.00003-9.

Lommatzsch, M., Cicko, S., Muller, T., Lucattelli, M., Bratke, K., Stoll, P., Grimm, M., Dürk, T., Zissel, G., Ferrari, D., Di Virgilio, F., Sorichter, S., Lungarella, G., Virchow, J. C., and Idzko, M., (2010), Extracellular adenosine triphosphate and chronic obstructive pulmonary disease, *Am J Respir Crit Care Med*, **181** (9), 928–934. doi: 10.1164/rccm.200910-1506OC.

Loomis, D., Grosse, Y., Lauby-Secretan, B., El Ghissassi, F., Bouvard, V., Benbrahim-Tallaa, L., Guha, N., Baan, R., Mattock, H., and Straif, K., (2013), The carcinogenicity of outdoor air pollution. *Lancet Oncol*, **14** (13), 1262-1263. DOI: 10.1016/s1470-2045(13)70487-x.

Lu, Y., Xu, W., Gu, Y., Chang, X., Wei, G., Rong, Z., Qin, L., Chen, X., and Zhou, F., (2019), Non-small Cell Lung Cancer Cells Modulate the Development of Human CD1c+ Conventional Dendritic Cell Subsets Mediated by CD103 and CD205, *Front Immunol*, **10**, 2829. doi: 10.3389/fimmu.2019.02829.

Ma, J., Liu, L., Che, G., Yu, N., Dai, F., and You, Z., (2010), The M1 form of tumor-associated macrophages in non-small cell lung cancer is positively associated with survival time. *BMC Cancer*, **10** (1), 112. doi: 10.1186/1471-2407-10-112.

Mannino, D. M., Aguayo, S. M., Petty, T. L., and Redd, S. C., (2003), Low lung function and incident lung cancer in the United States: data From the First National Health and Nutrition Examination Survey follow-up, *Arch Intern Med*, **163** (12), 1475-80. DOI: 10.1001/archinte.163.12.1475

McLoed, A. G., Sherrill, T. P., Cheng, D. S., Han, W., Saxon, J. A., Gleaves, L. A., Wu, P., Polosukhin, V. V., Karin, M., Yull, F. E., Stathopoulos, G. T., Georgoulias, V., Zaynagetdinov, R., and Blackwell, T. S., (2016), Neutrophil-Derived IL-1β Impairs the Efficacy of NF-κB Inhibitors against Lung Cancer, *Cell Rep*, **16** (1), 120-132. doi: 10.1016/j.celrep.2016.05.085.

Mittal, D., Gubin, M. M., Schreiber, R. D., and Smyth, M. J., (2014), New insights into cancer immunoediting and its three component phases--elimination, equilibrium and escape, *Curr Opin Immunol*, **27**, 16-25. doi: 10.1016/j.coi.2014.01.004.

Mittal, S. K., Cho, K. J., Ishido, S. and Roche P. A., (2015), Interleukin 10 (IL-10)-mediated Immunosuppression: March-i induction regulates antigen presentation by macrophages but not dendritic cells, *J. Biol. Chem*, **290** (45), 27158–27167. doi: 10.1074/jbc.M115.682708.

Moossavi, M., Parsamanesh, N., Bahrami, A., Atkin, S. L., and Sahebkar, A., (2018), Role of the NLRP3 inflammasome in cancer, *Mol Cancer*, **17** (1), 158. doi: 10.1186/s12943-018-0900-3.

Müller, T., Vieira, R. P., Grimm, M., Dürk, T., Cicko, S., Zeiser, R., Jakob, T., Martin, S. F., Blumenthal, B., Sorichter, S., Ferrari, D., Di Virgillio, F., and Idzko, M., (2011), A potential

role for P2X7R in allergic airway inflammation in mice and humans, *Am J Respir Cell Mol Biol*, **44** (4), 456-464. doi: 10.1165/rcmb.2010-0129OC.

Nakanishi, K., Yoshimoto, T., Tsutsui, H., and Okamura, H., (2001), Interleukin-18 regulates both Th1 and Th2 responses, *Annu Rev Immunol*,**19**, 423-74.

Nam. S. J., Go, H., Paik, J. H., Kim, T. M., Heo, D. S., Kim, C. W., Jeon,Y. K., (2014), An increase of M2 macrophages predicts poor prognosis in patients with diffuse large B-cell lymphoma treated with rituximab, cyclophosphamide, doxorubicin, vincristine and prednisone, *Leuk Lymphoma*, **55** (11), 2466–2476. doi: 10.3109/10428194.2013.879713.

Oberdorster, G., Oberdorster, E., and Oberdorster, J., (2005), Nanotoxicology: an emerging discipline evolving from studies of ultrafine particles, *Environ Health Perspect*, 113 (7), 823–39. DOI: 10.1289/ehp.7339.

Perez-Padilla, R., Schilmann, A., and Riojas-Rodriguez, H., (2010), Respiratory health effects of indoor air pollution, *Int J Tuberc Lung Dis*, **14** (9), 1079-86.

Pierdominici, M., Maselli, A., Cecchetti, S., Tinari, A., Mastrofrancesco, A., Alfè, M., Gargiulo, V., Beatrice, C., Di Blasio, G., Carpinelli, G., Ortona, E., Giovannetti, A., and Fiorito, S., (2014), Diesel exhaust particle exposure in vitro impacts T lymphocyte phenotype and function, *Part Fibre Toxicol*, **11**, 74. doi: 10.1186/s12989-014-0074-0.

Powell, H. A., Iyen-Omofoman, B., Baldwin, D. R., Hubbard, R. B., and Tata, L.J., (2013), Chronic obstructive pulmonary disease and risk of lung cancer: the importance of smoking and timing of diagnosis, *J Thorac Oncol*, **8** (1), 6-11. doi: 10.1097/JTO.0b013e318274a7dc.

Provoost, S., Maes, T., Willart, M. A., Joos, G.F., Lambrecht, B. N., and Tournoy, K. G, (2010), Diesel exhaust particles stimulate adaptive immunity by acting on pulmonary dendritic cells, *J. Immunol*, **184** (1), 426–432. doi: 10.4049/jimmunol.0902564.

Punturieri, A., Szabo, E., Croxton, T. L., Shapiro, S. D., and Dubinett, S. M., (2009), Lung cancer and chronic obstructive pulmonary disease: needs and opportunities for integrated research, *J Natl Cancer Inst*, **101** (8), 554-9. doi: 10.1093/jnci/djp023.

Quatromoni, J. G., and Eruslanov, E., (2012), Tumor-associated macrophages: function, phenotype, and link to prognosis in human lung cancer, *Am J Transl Res*, **4** (4), 376-89.

Rogliani, P., Calzetta, L., Ora, J., and Matera, M. G., (2015), Canakinumab for the treatment of chronic obstructive pulmonary disease, *Pulm Parmacol Ther*, **31**, 15–27. doi: 10.1016/j.pupt.2015.01.005.

Sayan, M., and Mossman, B. T., (2016), The NLRP3 inflammasome in pathogenic particle and fibre-associated lung inflammation and diseases, *Part Fibre Toxicol*, **13** (1), 51-65. doi: 10.1186/s12989-016-0162-4.

Shaw, C. A., Mortimer, G. M., Deng, Z. J., Carter, E. S., Connell, S. P., Miller, M. R., Duffin, R., Newby, D. E., Hadoke, P. W., and Minchin, R. F., (2016), Protein corona formation in bronchoalveolar fluid enhances diesel exhaust nanoparticle uptake and pro-inflammatory responses in macrophages, *Nanotoxicology*, **10** (7), 981–91. doi: 10.3109/17435390.2016.1155672.

Shimada, K., Crother, T. R., Karlin, J., Dagvadorj, J., Chiba, N., Chen, S., Ramanujan, V. K., Wolf, A. J., Vergnes, L., Ojcius, D. M., Rentsendorj, A., Vargas, M., Guerrero, C., Wang, Y., Fitzgerald, K. A., Underhill, D. M., Town, T., and Arditi, M., (2012), Oxidized mitochondrial DNA activates the NLRP3 inflammasome during apoptosis, *Immunity*, **36** (3), 401–14. doi:10.1016/j.immuni.2012.01.009.

Skillrud, D. M., Offord, K. P., and Miller, R. D., (1986), Higher risk of lung cancer in chronic obstructive pulmonary disease. A prospective, matched, controlled study, *Ann Intern Med*, **105** (4), 503-7. 10.7326/0003-4819-105-4-503.

Sollberger, G., Strittmatter, G. E., Kistowska, M., French, L. E., and Beer, H. D., (2012), Caspase-4 is required for activation of inflammasomes, *J. Immunol*, **188** (4), 1992–2000. doi: 10.4049/jimmunol.1101620.

Song, Q., Christiani, D. C., XiaorongWang, and Ren, J., (2014), The global contribution of outdoor air pollution to the incidence, prevalence, mortality and hospital admission for chronic obstructive pulmonary disease: a systematic review and meta-analysis. *Int J Environ Res Public Health*, **11** (11), 11822-32. doi: 10.3390/ijerph111111822.

Sorrentino, R., Bertolino, A., Terlizzi, M., Iacono, V. M., Maiolino, P., Cirino, G., Roviezzo, F., and Pinto, A., (2015), B cell depletion increases sphingosine-1-phosphate-dependent airway inflammation in mice, *Am J Respir Cell Mol Biol*, **52** (5), 571–83. doi: 10.1165/rcmb.2014-0207OC.

Sorrentino, R., Terlizzi, M., Di Crescenzo, V. G., Popolo, A., Pecoraro, M., Perillo, G., Galderisi, A., and Pinto, A., (2015b), Human lung cancer-derived immunosuppressive plasmacytoid dendritic cells release IL-1α in an AIM2 inflammasome-dependent manner. *Am J Pathol*, **185** (11), 3115-24. doi: 10.1016/j.ajpath.2015.07.009.

Steggerda, S. M., Bennett, M. K., Chen, J., Emberley, E., Huang, T., Janes, J. R., Li, W., MacKinnon, A. L., Makkouk, A., Marguier, G., Murray, P. J., Neou, S., Pan, A., Parlati, F., Rodriguez, M. L. M., Van de Velde, L. A., Wang, T,, Works, M., Zhang, J., Zhang, W., and Gross, M. I., (2017), Inhibition of arginase by CB-1158 blocks myeloid cell-mediated immune suppression in the tumor microenvironment, *J Immunother Cancer*, **5** (1), 101. doi: 10.1186/s40425-017-0308-4.

Sugimoto, M. A., Sousa, L. P., Pinho, V., Perretti, M., and Teixeira, M. M., (2016), Resolution of Inflammation: What Controls Its Onset? *Frontiers of Immunology*, **7**, 160. doi: 10.3389/fimmu.2016.00160.

Talikka, M., Sierro, N., Ivanov, N. V., Chaudhary, N., Peck, M. J., Hoeng, J., Coggins, C. R., and Peitsch, M. C., (2012), Genomic impact of cigarette smoke, with application to three smoking-related diseases, *Crit Rev Toxicol*, **42** (10), 877-89. doi: 10.3109/10408444.2012.725244.

Terlizzi, M., Casolaro, V., Pinto, A., and Sorrentino, R., (2014), Inflammasome: Cancer's friend or foe? *Pharmacology & Therapeutics*, **143**, 24-33. DOI: 10.1016/j.pharmthera.2014.02.002.

Terlizzi, M., Colarusso, C., Popolo, A., Pinto, A., and Sorrentino, R., (2016), IL-1α and IL-1β-producing macrophages populate lung tumor lesions in mice, *Oncotarget*, **7** (36), 58181-58192. doi: 10.18632/oncotarget.11276.

Terlizzi, M., Di Crescenzo, V. G., Perillo, G., Galderisi, A., Pinto, A., and Sorrentino, R., (2015), Pharmacological inhibition of caspase-8 limits lung tumour outgrowth. *Br J Pharmacol*, **172** (15), 3917-28. doi: 10.1111/bph.13176.

Terlizzi, M., Molino, A., Colarusso, C., Donovan, C., Imitazione, P., Somma, P., Aquino, R. P., Hansbro, P. M., Pinto, A., and Sorrentino, R., (2018), Activation of the absent in melanoma 2 inflammasome in peripheral blood mononuclear cells from idiopathic pulmonary fibrosis patients leads to the release of pro-fibrotic mediators, *Front. Immunol*, **9**, 670. doi: 10.3389/fimmu.2018.00670.

Terzano, C., Di Stefano, F., Conti, V., Graziani, E., and Petroianni, A., (2010), Air pollution ultrafine particles: toxicity beyond the lung, *Eur Rev Med Pharmacol Sci*, **14**, 809–21.

Totlandsdal, A. I., Cassee, F. R., Schwarze, P., Refsnes, M. and Låg, M., (2010), Diesel exhaust particles induce CYP1A1 and pro-inflammatory responses via differential pathways in human bronchial epithelial cells, *Part Fibre Toxicol*, **7**, 41. doi: 10.1186/1743-8977-7-41.

Tsoumakidou, M., Tousa, S., Semitekolou, M., Panagiotou, P., Panagiotou, A., Morianos, I., Litsiou, E., Trochoutsou, A. I., Konstantinou, M., Potaris, K., Footitt, J., Mallia, P., Zakynthinos, S., Johnston, S. L., and Xanthou, G., (2014),Tolerogenic signaling by pulmonary CD1c+ dendritic cells induces regulatory T cells in patients with chronic obstructive pulmonary disease by IL-27/IL-10/inducible costimulator ligand, *J Allergy Clin Immunol*, **134** (4), 944-954.e8. doi: 10.1016/j.jaci.2014.05.045.

Tumurkhuu, G., Shimada, K., Dagvadorj, J., Crother, T. R., Zhang, W., Luthringer, D., Gottlieb, R. A., Chen, S., and Arditi, M., (2016), Ogg1-dependent DNA repair regulates NLRP3 inflammasome and prevents atherosclerosis, *Circ Res*, **119** (6), e76–90. doi:10.1161/CIRCRESAHA.116.308362.

Turner, M. C., Chen, Y., Krewski, D., Calle, E. E., and Thun, M. J., (2007), Chronic obstructive pulmonary disease is associated with lung cancer mortality in a prospective study of never smokers, *Am J Respir Crit Care Med*, **176** (3), 285-90. DOI: 10.1164/rccm.200612-1792OC.

U.S. Department of Health and Human Services, (2014), *The Health Consequences of Smoking: 50 Years of Progress. A Report of the Surgeon General*, Centers for Disease Control and Prevention, National Center for Chronic Disease Prevention and Health Promotion, Office on Smoking and Health, Atlanta, GA

Valavanidis, A., Vlachogianni, T., and Fiotakis, C., (2009), 8-hydroxy-2' -deoxyguanosine (8-OHdG): a critical biomarker of oxidative stress and carcinogenesis, *J Environ Sci Health C Environ Carcinog Ecotoxicol Rev*, **27** (2),120–39. doi:10.1080/10590500902885684.

Valavanidis, A., Vlachogianni, T., Fiotakis, K., and Loridas, S., (2013), Pulmonary oxidative stress, inflammation and cancer: respirable particulate matter, fibrous dusts and ozone as major causes of lung carcinogenesis through reactive oxygen species mechanisms, *Int J Environ Res Public Health*, **10** (9), 3886-907. doi: 10.3390/ijerph10093886.

Vestbo, J., Hurd, S. S., Agustı, A. G., Jones, P. W., Vogelmeier, C., Anzueto, A., Barnes, P. J., Fabbri, L. M., Martinez, F. J., Nishimura. M., Stockley, R. A., Sin, D. D., and Rodriguez-Roisin, R., (2013), Global Strategy for the Diagnosis, Management, and Prevention of Chronic Obstructive Pulmonary Disease: GOLD Executive Summary, *Am J Respir Crit Care Med*, **187** (4), 347–365. DOI: 10.1164/rccm.201204-0596PP.

Vesterdal, L. K., Jantzen, K., Sheykhzade, M., Roursgaard, M., Folkmann, J. K., Loft, S., and Møller, P., (2014), Pulmonary exposure to particles from diesel exhaust, urban dust or single-walled carbon nanotubes and oxidatively damaged DNA and vascular function in apoE(-/-) mice, *Nanotoxicology*, **8** (1), 61-71. doi: 10.3109/17435390.2012.750385.

Wang, J., Liu, X., Xie, M., Xie, J., Xiong, W., and Xu, Y., (2012), Increased expression of interleukin-18 and its receptor in peripheral blood of patients with chronic obstructive pulmonary disease, *COPD*, **9**, 375–381. DOI: 10.3109/15412555.2012.670330.

Wang, W., Dou, S., Dong, W., Xie, M., Cui, L., Zheng, C., and Xiao, W., (2018), Impact of COPD on prognosis of lung cancer: from a perspective on disease heterogeneity, *Int J Chron Obstruct Pulmon Dis*, **13**, 3767-3776. doi: 10.2147/COPD.S168048.

Wang, W., Xie, M., Dou, S., Cui, L., Zheng, C., and Xiao, W., (2018b), The link between chronic obstructive pulmonary disease phenotypes and histological subtypes of lung cancer: a case-control study. *Int J Chron Obstruct Pulmon Dis*, **13**, 1167-1175. doi: 10.2147/COPD.S158818.

Wasswa-Kintu, S., Gan, W. Q., Man, S. F., Pare, P. D., and Sin, D. D., (2005), Relationship between reduced forced expiratory volume in one second and the risk of lung cancer: a systematic review and meta-analysis, *Thorax*, **60** (7), 570-5. DOI: 10.1136/thx.2004.037135.

Xia, T., Zhu, Y., Mu, L., Zhang, Z. F., and Liu, S., (2016), Pulmonary diseases induced by ambient ultrafine and engineered nanoparticles in twenty-first century, *Natl Sci Rev*, **3** (4), 416-429. doi: 10.1093/nsr/nww064.

Yasuda, K., Muto, T., Kawagoe, T., Matsumoto, M., Sasaki, Y., Matsushita, K., Taki, Y., Futatsugi-Yumikura, S., Tsutsui, H., Ishii, K. J., Yoshimoto, T., Akira, S., and Nakanishi K., (2012), Contribution of IL-33-activated type II innate lymphoid cells to pulmonary eosinophilia in intestinal nematode-infected mice, *Proc Natl Acad Sci U S A*, **109**, 3451–3456.

Young, R. P., Hopkins, R. J., Christmas, T., Black, P. N., Metcalf, P., and Gamble, G. D., (2009), COPD prevalence is increased in lung cancer, independent of age, sex and smoking history, *Eur Respir J*, **34** (2), 380-6. doi: 10.1183/09031936.00144208.

Zamarrón, E., Prats, E., Tejero, E., Pardo, P., Galera, R., Casitas, R., Martínez-Cerón, E., Romera, D., Jaureguizar, A., and García-Río, F., (2019), Static lung hyperinflation is an independent risk factor for lung cancer in patients with chronic obstructive pulmonary disease, *Lung Cancer*, **128**, 40-46. doi: 10.1016/j.lungcan.2018.12.012.

Zhang, F., Wang, L., Wang, J., Luo, P., Wang, X., Xia, Z. F., (2016), The caspase-1 inhibitor AC-YVAD-CMK attenuates acute gastric injury in mice: involvement of silencing NLRP3 inflammasome activities, *Sci Rep*, **6**, 24166. doi: 10.1038/srep24166.

Zhou, R., Yazdi, A. S., Menu, P., and Tschopp, J., (2011) A role for mitochondria in NLRP3 inflammasome activation, *Nature*, **469**, 221-5221–225. doi: 10.1038/nature09663.

Zitvogel, L., Tesniere, A. and Kroemer, G., (2006), Cancer despite immunosurveillance: immunoselection and immunosubversion, *Nat. Rev. Immunol*, **6** (10), 715–727. DOI: 10.1038/nri1936.

Zuo, L., He, F., Sergakis, G. G.0, Koozehchian, M. S., Stimpfl, J. N., Rong, Y., Diaz, P. T., and Best, T. M., (2014), Interrelated role of cigarette smoking, oxidative stress, and immune response in COPD and corresponding treatments, *Am J Physiol Lung Cell Mol Physiol*, **307** (3), L205-18. doi: 10.1152/ajplung.00330.2013.

SITOGRAPHY

Air pollution composition: https://www.eea.europa.eu/publications/air-quality-in-europe-2018

Air pollution-related deaths: https://www.who.int/health-topics/air-pollution#tab=tab_1

Association between lung diseases and air pollution: https://www.who.int/news-room/fact-sheets/detail/ambient-(outdoor)-air-quality-and-health

Clinical trial targeting IL-1R in COPD patients: https://clinicaltrials.gov/ct2/show/NCT01448850

Clinical trial targeting IL-1β in COPD patients: https://clinicaltrials.gov/ct2/show/NCT00581945

COPD diagnosis, management and prevention: https://goldcopd.org/wp-content/uploads/2018/11/GOLD-2019-POCKET-GUIDE-FINAL_WMS.pdf

Key fact about COPD: https://www.who.int

Key statistic about lung cancer: https://www.cancer.org/cancer/non-small-cell-lung-cancer/about/key-statistics.html

Risk factors in COPD and lung cancer: https://www.who.int/gard/publications/Risk%20factors.pdf

UNIONE EUROPEA
Fondo Sociale Europeo

Ministero dell'Istruzione,
dell'Università e della Ricerca

PON
RICERCA
E INNOVAZIONE